

ISSN : 2165-4069(Online)

ISSN : 2165-4050(Print)



IJARAI

International Journal of
Advanced Research in Artificial Intelligence

Volume 2 Issue 6

www.ijarai.thesai.org

A Publication of
The Science and Information Organization



INTERNATIONAL JOURNAL OF
ADVANCED RESEARCH IN ARTIFICIAL INTELLIGENCE



THE SCIENCE AND INFORMATION ORGANIZATION

www.thesai.org | info@thesai.org



Editorial Preface

From the Desk of Managing Editor...

"The question of whether computers can think is like the question of whether submarines can swim." — Edsger W. Dijkstra, the quote explains the power of Artificial Intelligence in computers with the changing landscape. The renaissance stimulated by the field of Artificial Intelligence is generating multiple formats and channels of creativity and innovation.

This journal is a special track on Artificial Intelligence by The Science and Information Organization and aims to be a leading forum for engineers, researchers and practitioners throughout the world.

The journal reports results achieved; proposals for new ways of looking at AI problems and include demonstrations of effectiveness. Papers describing existing technologies or algorithms integrating multiple systems are welcomed. IJARAI also invites papers on real life applications, which should describe the current scenarios, proposed solution, emphasize its novelty, and present an in-depth evaluation of the AI techniques being exploited. IJARAI focusses on quality and relevance in its publications.

In addition, IJARAI recognizes the importance of international influences on Artificial Intelligence and seeks international input in all aspects of the journal, including content, authorship of papers, readership, paper reviewers, and Editorial Board membership.

The success of authors and the journal is interdependent. While the Journal is in its initial phase, it is not only the Editor whose work is crucial to producing the journal. The editorial board members, the peer reviewers, scholars around the world who assess submissions, students, and institutions who generously give their expertise in factors small and large— their constant encouragement has helped a lot in the progress of the journal and shall help in future to earn credibility amongst all the reader members.

I add a personal thanks to the whole team that has catalysed so much, and I wish everyone who has been connected with the Journal the very best for the future.

Thank you for Sharing Wisdom!

Managing Editor
IJARAI
Volume 2 Issue 6 June 2013
ISSN: 2165-4069(Online)
ISSN: 2165-4050(Print)
©2013 The Science and Information (SAI) Organization

Associate Editors

Dr.T. V. Prasad

Dean (R&D), Lingaya's University, India

Domain of Research: Bioinformatics, Natural Language Processing, Image Processing, Robotics, Knowledge Representation

Dr.Wichian Sittiprapaporn

Senior Lecturer, Maharakham University, Thailand

Domain of Research: Cognitive Neuroscience; Cognitive Science

Prof.Alaa Sheta

Professor of Computer Science and Engineering, WISE University, Jordan

Domain of Research: Artificial Neural Networks, Genetic Algorithm, Fuzzy Logic Theory, Neuro-Fuzzy Systems, Evolutionary Algorithms, Swarm Intelligence, Robotics

Dr.Yaxin Bi

Lecturer, University of Ulster, United Kingdom

Domain of Research: Ensemble Learning/Machine Learning, Multiple Classification System, Evidence Theory, Text Analytics and Sentiment Analysis

Mr.David M W Powers

Flinders University, Australia

Domain of Research: Language Learning, Cognitive Science and Evolutionary Robotics, Unsupervised Learning, Evaluation, Human Factors, Natural Language Learning, Computational Psycholinguistics, Cognitive Neuroscience, Brain Computer Interface, Sensor Fusion, Model Fusion, Ensembles and Stacking, Self-organization of Ontologies, Sensory-Motor Perception and Reactivity, Feature Selection, Dimension Reduction, Information Retrieval, Information Visualization, Embodied Conversational Agents

Dr.Antonio Dourado

University of Coimbra, France

Domain of Research: Computational Intelligence, Signal Processing, data mining for medical and industrial applications, and intelligent control.

Reviewer Board Members

- **Alaa Sheta**
Electronics Research Institute (ERI)
- **Albert Alexander**
Kongu Engineering College
- **Amir HAJJAM EL HASSANI**
Université de Technologie de Belfort-Monbéliard
- **Amit Verma**
Department in Rayat & Bahra Engineering College, Mo
- **Antonio Dourado**
University of Coimbra
- **B R SARATH KUMAR**
Lenora College of Engineering
- **Babatunde Opeoluwa Akinkunmi**
University of Ibadan
- **Bestoun S.Ahmed**
Universiti Sains Malaysia
- **Chien-Peng Ho**
Information and Communications Research Laboratories, Industrial Technology Research Institute of Taiwan
- **David M W Powers**
Flinders University
- **Dimitris Chrysostomou**
Democritus University
- **Dr.Dhananjay R Kalbande**
Mumbai University
- **Francesco Perrotta**
University of Macerata
- **Frank Ibikunle**
Covenant University
- **Grigoras Gheorghe**
"Gheorghe Asachi" Technical University of Iasi, Romania
- **Guandong Xu**
Victoria University
- **Haibo Yu**
Shanghai Jiao Tong University
- **Jatinderkumar R. Saini**
S.P.College of Engineering, Gujarat
- **Krishna Prasad Miyapuram**
University of Trento
- **Luke Liming Chen**
University of Ulster
- **Marek Reformat**
University of Alberta
- **Md. Zia Ur Rahman**
Narasaraopeta Engg. College, Narasaraopeta
- **Mokhtar Beldjehem**
University of Ottawa
- **Monji Kherallah**
University of Sfax
- **Nitin S. Choubey**
Mukesh Patel School of Technology Management & Eng
- **Rajesh Kumar**
National University of Singapore
- **Rajesh K Shukla**
Sagar Institute of Research & Technology-Excellence, Bhopal MP
- **Rongrong Ji**
Columbia University
- **Said Ghoniemy**
Taif University
- **Samarjeet Borah**
Dept. of CSE, Sikkim Manipal University
- **Sana'a Wafa Tawfeek Al-Sayegh**
University College of Applied Sciences
- **Saurabh Pal**
VBS Purvanchal University, Jaunpur
- **Shahaboddin Shamshirband**
University of Malaya
- **Shaidah Jusoh**
Zarqa University
- **Shrinivas Deshpande**
- **SUKUMAR SENTHILKUMAR**
Universiti Sains Malaysia
- **T C.Manjunath**
HKBK College of Engg
- **T V Narayana Rao**
Hyderabad Institute of Technology and Management
- **T. V. Prasad**

Lingaya's University

- **Vitus S.W Lam**
Domains of Research
- **VUDA Sreenivasarao**
St. Mary's College of Engineering &
Technology
- **Vishal Goyal**
- **Wei Zhong**
University of south Carolina Upstate
- **Wichian Sittiprapaporn**
Mahasarakham University
- **Yaxin Bi**

University of Ulster

- **Yuval Cohen**
The Open University of Israel
- **Zhao Zhang**
Deptment of EE, City University of Hong
Kong
- **Zne-Jung Lee**
Dept. of Information management, Huafan
University
- **Zhigang Yin**
Institute of Linguistics, Chinese Academy of
Social Sciences

CONTENTS

Paper 1 Enterprise Architecture Model that Enables to Search for Patterns of Statistical Information

Authors: Oleg Chertov

PAGE 1 – 5

Paper 2: Clustering Web Documents based on Efficient Multi-Tire Hashing Algorithm for Mining Frequent Termsets

Authors: Noha Negm, Passent Elkafrawy, Mohamed Amin, Abdel Badeeh M. Salem

PAGE 6 – 14

Paper 3: A Structural Algorithm for Complex Natural Languages Parse Generation

Authors: Enikuomehin, Rahman, Ameen

PAGE 15 – 19

Paper 4: Category Decomposition Method Based on Matched Filter for Un-Mixing of Mixed Pixels Acquired with Spaceborne Based Hyperspectral Radiometers

Authors: Kohei Arai

PAGE 20 – 26

Paper 5: Parallelization of 2-D IADE-DY Scheme on Geranium Cadcam Cluster for Heat Equation

Authors: Simon Uzezi Ewedafe, Rio Hirowati Shariffudin

PAGE 27 – 33

Paper 6: An Efficient Routing Protocol under Noisy Environment for Mobile Ad Hoc Networks using Fuzzy Logic

Authors: Supriya Srivastava, A. K. Daniel

PAGE 34 – 39

Paper 7: Lecturer's e-Table (Server Terminal) Which Allows Monitoring the Location at Where Each Student is Looking During Lessons with e-Learning Contents Through Client Terminals

Authors: Kohei Arai

PAGE 40 – 45

Paper 8: Method for 3D Rendering Based on Intersection Image Display Which Allows Representation of Internal Structure of 3D objects

Authors: Kohei Arai

PAGE 46 – 50

Paper 9: 3D Map Creation Based on Knowledgebase System for Texture Mapping Together with Height Estimation Using Objects' Shadows with High Spatial Resolution Remote Sensing Satellite Imagery Data

Authors: Kohei Arai

PAGE 51 – 55

Paper10: Monte Carlo Ray Tracing Based Adjacency Effect and Nonlinear Mixture Pixel Model for Remote Sensing Satellite Imagery Data Analysis

Authors: Kohei Arai

PAGE 56 – 64

Paper 11: Method for Psychological Status Monitoring with Line of Sight Vector Changes (Human Eye Movements) Detected with Wearing Glass

Authors: Kohei Arai, Kiyoshi Hasegawa

PAGE 65 – 70

Paper 12: Mobile Devices Based 3D Image Display Depending on User's Actions and Movements

Authors: Kohei Arai, Herman Tolle, Akihiro Serita

PAGE 71 – 78

Paper 13: Relative Motion of Formation Flying with Elliptical Reference Orbit

Authors: Hany R Dwidar, Ashraf H. Owis

PAGE 79 – 86

Enterprise Architecture Model that Enables to Search for Patterns of Statistical Information

Oleg Chertov

Applied Mathematics Department
NTUU “Kyiv Polytechnic Institute”
Kyiv, Ukraine

Abstract—Enterprise architecture is the stem from which developing of any departmental information system should grow and around which it should revolve. In the paper, a fragment of an enterprise architecture model is built using ArchiMate language. This fragment enables to search for information in enterprises which do not work in productive industry. Such enterprises include official statistics. The proposed model embraces all three architectural levels of corresponding information systems, namely, OLTP, OLAP, and Data Mining. Particularly, the latter level enables to search for patterns of statistical information.

Keywords—Enterprise Architecture; Pattern Search; Data Mining; Architecture Description Language

I. INTRODUCTION

Architectural issues which arise during developing complex information systems play the role of the same importance as those arising during construction of an original building. Correct architectural decisions considerably lower the risks of the whole project of system developing and maintenance, because they make it possible to efficiently use existent infrastructure and optimally plan its further progress.

At first, the term “architecture” was used in the field of IT only in relation to hardware. Later on, this term was used in relation to information systems as a whole. Only with the lapse of time it became clear that it is necessary to apply systems approach not only to developing the information system, but also to developing the whole enterprise.

As a result, term “enterprise architecture” emerged. For the first time, it was used in the report [1]. This terminology assumes relatively wide treatment of the concept of “enterprise.” In particular, the concept can be applied to the architecture of state organizations and offices.

Among various definitions of enterprise architecture, we will primarily use the one proposed by Global Enterprise Architecture Organization (GEAO): “The way in which an enterprise vision is expressed in the structure and dynamics of an enterprise.

It provides, on various architecture abstraction levels, a coherent set of models, principles, guidelines, and policies, used for the translation, alignment, and evolution of the systems that exist within the scope and context of an Enterprise” [2, p. 7].

In general, when describing enterprise architecture, the following principles are frequently used:

— The level of architecture refinement is being chosen in such a way that the amount of information about a certain component is minimized; anything irrelevant to the interconnection with other architecture components is omitted;

— Architecture definition mustn’t contain descriptions of the components themselves.

Usually, four main layers [3, 4] of enterprise architecture are distinguished. They are presented in Table 1.

TABLE I. MAIN LAYERS OF ENTERPRISE ARCHITECTURE (TOGAF)

| № | Layer’s name | Comments |
|---|--------------------------|--|
| 1 | Business architecture | Defines business processes and organizational structures of an enterprise |
| 2 | Information architecture | Describes logical and physical data structures, authorizing access to them |
| 3 | Application architecture | For applied systems, provides a plan and interfaces of their internal interaction, interaction with external systems, sources, or users of data, defines interrelation between applied systems and enterprise business processes supported by them |
| 4 | Technical architecture | Ensures performance of applied systems at a level described in operational requirements (reliability, scalability, capacity etc.), includes hardware, system software, networks, communication protocols etc. |

Such enterprises as official statistics, i.e. those not working in productive industry, obviously need to have special architectural features. In particular, statistics deals with processing and searching not for physical resources but for information, searching being arguably its main activity.

The aim of this paper is to build enterprise architecture for enabling searching for statistical information, including searching for patterns in concealed data distribution features.

The rest of the paper is organized as follows. Section II describes three possible levels of information systems in official statistics. Section III reviews past researches that have been done in the area of Architecture Description Languages for enterprise architecture. Section IV details on the proposed architecture and its considerations for, particularly, searching for patterns of statistical information. Section V concludes the work.

II. THREE LEVELS OF INFORMATION SYSTEMS IN STATISTICS

From the developing a classification of applications for processing data in statistical information systems point of view, three principally different types (levels) may be distinguished.

1) *Online Transaction Processing (OLTP) systems* [5] which ensure basic functionality such as entering the data and results of appropriate statistical observations and surveys, their structured (usually by means of DBMS) storage and accounting, primary and aggregated data control, dissemination of results using various predefined output tables. Examples of such systems are the systems developed and implemented under the direction of the author for processing 2001 All-Ukrainian population census data and 2004 Moldova population census data. OLTP systems allow computing calculation indicators (like living area per one household member), creating predefined output tables and reports, and processing not predefined queries. In other words, representative capacities of such systems are rather limited. Thus, if creating a required output table was not specified at system design phase, obtaining appropriate data becomes practically infeasible, because to get a value of each cell or row of a new table one needs to make separate queries.

2) *Online Analytical Processing (OLAP) systems* [6] which allow creating not predefined tables and carrying out other analytical research of statistical data, including searching for their distribution patterns. Example of such systems is the system developed and implemented under the direction of the author for multidimensional analysis of 2001 All-Ukrainian population census data.

With this OLAP system, the user gained a natural and comprehensive data model arranged in three multidimensional cubes, namely, for the respondents, for the households and for the administrative and territorial units of Ukraine. Cube's dimensions were data features whose intersections enabled to obtain, filter, group, and represent information. For instance, the simplest cube for the administrative and territorial units had such dimensions as area, population size, urban or rural type, center of population type, predominate nationality. The cube for the respondents had 60 dimensions, and the cube for the households had more than 20 dimensions.

A *measure* defines what information is provided by the cube. For instance, a number of respondents can be a measure, and "native language," "marital status," "center of population" etc. can be dimensions. Each cube cell contains a number of respondents with particular features. The user analyzing information from such a cube can "slice" it across different dimensions, obtain aggregated or, on the contrary, detailed findings etc.

3) *Data Mining systems* which perform the most cumbersome and routine analytical operation of searching for concealed patterns that might exist in the analyzed data.

Thus, in contrast to architectural decisions of existent demographic data processing systems (in the US [7], France

[8], Russia etc.) based on utilizing OLTP and OLAP levels only, we propose to add a new level of Data Mining.

Discussed levels differ sufficiently; their comparative analysis is presented in Table 2.

TABLE II. COMPARATIVE FEATURES OF DIFFERENT LEVELS OF STATISTICAL INFORMATION PROCESSING SYSTEMS

| Feature | OLTP | OLAP | Data Mining |
|-------------------|--|---|--|
| Data level | Mainly primary | Mainly consolidated | Primary and consolidated |
| Data variability | High (with each transaction) | Low | Low |
| Typical operation | Data alteration | Data analysis | Searching for patterns |
| Reports | Predefined | Not predefined, but with a certain list of attributes | Not predefined, list of attributes can be dynamically modified |
| Processed data | Only current ones; historical ones are usually stored in archive | Historical and current ones | Historical and current ones |
| Basic structure | Table / primary key | Cube / dimension | Cluster, class, association rule etc. |
| Priority | Efficiency | Flexibility | Intelligence |

III. DISCUSSION ARCHITECTURE DESCRIPTION LANGUAGES

According to the monograph [9], languages used to describe enterprise architecture can be divided into two large groups:

— Universal languages such as language family IDEF [10, 11], BPMN (Business Process Modeling Notation) [12], ARIS (Architecture of Integrated Information Systems) [13], UML (Unified Modeling Language) [14] and others;

— Architecture description languages (ADL).

These two groups are complementary rather than interchangeable. Being inferior to universal modeling languages with respect to detailed description of processes, ADL languages have a natural advantage in describing architectural object features modeled [15].

ISO/IEC/IEEE Standard 42010:2011 [16] provides a rather general definition of an architecture description language as "any form of expression for use in architecture descriptions." It also contains relatively mild criteria of labeling certain modeling languages as architecture description ones. So, nowadays, one term, Architecture Description Language, is being used for modeling languages of different classes:

1) (*Software engineering*) *software architecture description languages* [17], such as ACME [18] and Wright [19] developed at Carnegie Mellon University, Darwin [20], AADL [21] etc.;

2) (*Enterprise activity modeling*) *enterprise architecture description languages*, the most known among them being ArchiMate [9], DEMO [22], ABACUS [23].

When used for describing enterprise architectures, virtually all the modeling languages from the first class have the following disadvantages [9, p. 38]:

Interconnections between different levels (representations) of a model are ill-defined; models created with different representations cannot be easily integrated in future;

— Language semantics is not “transparent;”

— There are restrictions for describing architecture of either business or technological (infrastructure) level of a model.

Thus, to describe enterprise architecture model that enables to search for statistical information and patterns in its distribution, we will use the specialized language ArchiMate which was standardized in 2008 by the Open Group consortium.

IV. PROPOSED ARCHITECTURE

In [24], the concept of on-line analytical mining (OLAM) systems was proposed. Its main idea lies in creating specialized OLAP systems for enabling of optimal searching for certain predefined patterns [25].

Such systems became widely used in criminology (to find out relations between crimes and known delinquents who could potentially commit them [26]), in medicine (to search for correlations between groups of people with a certain missing part of the Y chromosome and clinical presentation of infertility [27]) and so on. However, in a general case discussed in this paper, when the structure and elements of searched-for patterns are not known beforehand, creating OLAM systems is an unacceptable approach.

Therefore, we will build enterprise architecture model assuming that we have all three separate but complementary levels, namely, OLTP, OLAP, and Data Mining.

The model described in ArchiMate consists of three interrelated levels of view, namely, business level, application level, and technological (infrastructure) level.

To build required model at its business level, we will formally describe a process of searching for information. At other two levels, we will represent main software systems and servers used for implementing the described process, respectively (Fig. 1). To simplify notation, we don't show ancillary services like user authentication, backup and restore, contextual access to referenced data, local network support etc. To fit the whole architecture model to one page, detailed description of business functions is presented separately in Fig. 2–4.

In Fig. 1, bold vertical dotted lines additionally distinguish levels of statistical data processing system architecture singled out in Section II. The built model illustrates complementary capacities of OLTP, OLAP, and Data Mining systems when searching for statistical information.

Enterprise architecture model in ArchiMate presented in Fig. 1–4 was built using Archi editor, version 2.2 [28].

V. CONCLUSION

In the paper, enterprise architecture model that enables to search for statistical information is built. In contrast to existent models, the proposed one embraces all three possible architectural levels of corresponding information systems, namely, OLTP, OLAP, and Data Mining. The first level allows searching for required information in output tables, or by means of not predefined queries. The second level allows searching using ad hoc queries. The third level implies preparing microfiles and searching for patterns in concealed data distribution features.

The built model will be used for developing information system for processing data of All-Ukrainian population census to be held in this year.

ACKNOWLEDGMENT

The author would like to thank Mr. Dan Tavrov for his help with the translation of the paper into English.

REFERENCES

- [1] E. N. Fong and A. H. Goldfine, “Information Management Directions: the Integration Challenge,” National Institute of Standards and Technology (NIST), Special Publication 500-167, September 1989.
- [2] K. D. Willett, Information Assurance Architecture. Boca Raton, FL: CRC Press, 2008.
- [3] A. Josey, R. Harrison, P. Homan et al., *Togaf version 9.1 Enterprise Edition: A Pocket Guide*. Wilco, TX : Van Haren Publishing, 2011.
- [4] FEA Consolidated Reference Model Document version 2.3. Retrieved from http://www.whitehouse.gov/omb/assets/fea_docs/FEA_CRM_v23_Final_Oct_2007_Revised.pdf
- [5] G. Weikum and G. Vossen, *Transactional Information Systems: Theory, Algorithms, and the Practice of Concurrency Control and Recovery*. San Diego, CA: Morgan Kaufmann, 2001.
- [6] E. Thomsen, *OLAP Solutions: Building Multidimensional Information Systems*, 2nd ed. N.Y.: John Wiley & Sons, 2002.
- [7] 2010 Decennial response integration system (DRIS) contract. U.S. Census Bureau. Retrieved from
- [8] <http://www.census.gov/procur/www/2010dris/index.html>
- [9] G. Desplanques and G. Rogers, “Strengths and Uncertainties of the French Annual Census Surveys,” *Population*, vol. 63, № 3, pp. 415-439, 2008.
- [10] Marc Lankhorst, *Enterprise Architecture at Work: Modelling, Communication and Analysis*, 3rd ed. Berlin, Heidelberg: Springer-Verlag, 2013.
- [11] *Information Technology — Modeling Languages — Part 1: Syntax and Semantics for IDEF0*, IEEE/ISO/IEC 31320-1-2012. Geneva, New York: IEEE : ISO : IEC, 2012.
- [12] R. J. Mayer, M. K. Painter, and P. S. deWitte, *IDEF Family of Methods for Concurrent Engineering and Business Re-engineering Applications*. Columbus, OH: Knowledge-Based Systems, 1992.
- [13] T. Allweyer, *BPMN 2.0 — Introduction to the Standard for Business Process Modeling*. Norderstedt: BoD, 2010.
- [14] A.-W. Scheer, *ARIS: Business Process Modeling*, 3rd ed. Heidelberg, Berlin: Springer-Verlag, 2000.
- [15] G. Booch, J. Rumbaugh, and I. Jacobson, *The Unified Modeling Language: User Guide*, 2nd ed. Boston: Pearson Education, 2005.
- [16] M. M. Lankhorst and G. I. H. M. Bayens, “A Service-Oriented Reference Architecture for E-government,” in *Advances in Government Enterprise Architecture*, P. Saha ed. Hershey: IGI Global, 2008, pp. 30-55.
- [17] *Systems and Software Engineering — Architecture Description*, ISO/IEC/IEEE 42010:2011. Geneva, New York: ISO : IEC : Institute of Electrical and Electronics Engineers, 2011.

- [18] Richard N. Taylor, Nenad Medvidovic, Eric Dashofy, Software Architecture: Foundations, Theory, and Practice. Trenton, NJ: Wiley, 2009.
- [19] D. Garlan, R. T. Monroe, and D. Wile, "Acme: Architectural Description of Component-Based Systems," in Foundations of Component-Based Systems, G. T. Leavens and M. Sitaraman, Eds. Cambridge: Cambridge University Press, 2000, pp. 47-68.
- [20] R. J. Allen, A Formal Approach to Software Architecture, Ph.D. Thesis. Pittsburgh: Carnegie Mellon University, School of Computer Science, 1997.
- [21] J. Magee, N. Dulay and J. Kramer, "Regis: a Constructive Development Environment for Distributed Programs," IEE/IOP/BCS Distributed Systems Engineering, vol. 1, № 5, pp. 304-312, 1994.
- [22] Peter H. Feiler, David P. Gluch, Model-based Engineering with AADL: an Introduction to the SAE Architecture Analysis & Design Language. — Boston, MA: Addison-Wesley Professional, 2013.
- [23] J. Barjis, "Automatic Business Process Analysis and Simulation Based on DEMO," Enterprise IS, vol. 1, № 4, pp. 365-381, 2007.
- [24] K. Dunsire, T. O'Neill, M. Denford, and J. Leaney, "The ABACUS Architectural Approach to Computer-Based System and Enterprise Evolution," 12th IEEE International Conference and Workshops on the Engineering of Computer-Based Systems, ECBS '05, April 4-7, 2005. N.Y.: IEEE Computer Society Press, 2005, pp. 62-69.
- [25] J. Han, "Towards On-line Analytical Mining in Large Databases," ACM SIGMOD Record, vol. 27, № 1, pp. 97-107, 1998.
- [26] M. Usman and S. Asghar, "An Architecture for Integrated Online Analytical Mining," Journal of Emerging Technologies in Web Intelligence, vol. 3, № 2, pp. 74-99, 2011.
- [27] S. Lin and D. E. Brown, "Outlier-Based Data Association: Combining OLAP and Data Mining," Technical report SIE 020011. Charlottesville: University of Virginia, 2002.
- [28] S. Dzeroski, D. Hristovski and B. Peterlin, "Using Data Mining and OLAP to Discover Patterns in a Database of Patients with Y Chromosome Deletions," AMIA 2000 Annual Symposium, November 4-8, 2000. Los Angeles: AMIA, 2000, pp. 215-219.
- [29] Archi — ArchiMate modelling. Institute of Educational Cybernetics. — Retrieved from <http://archi.cetis.ac.uk/>

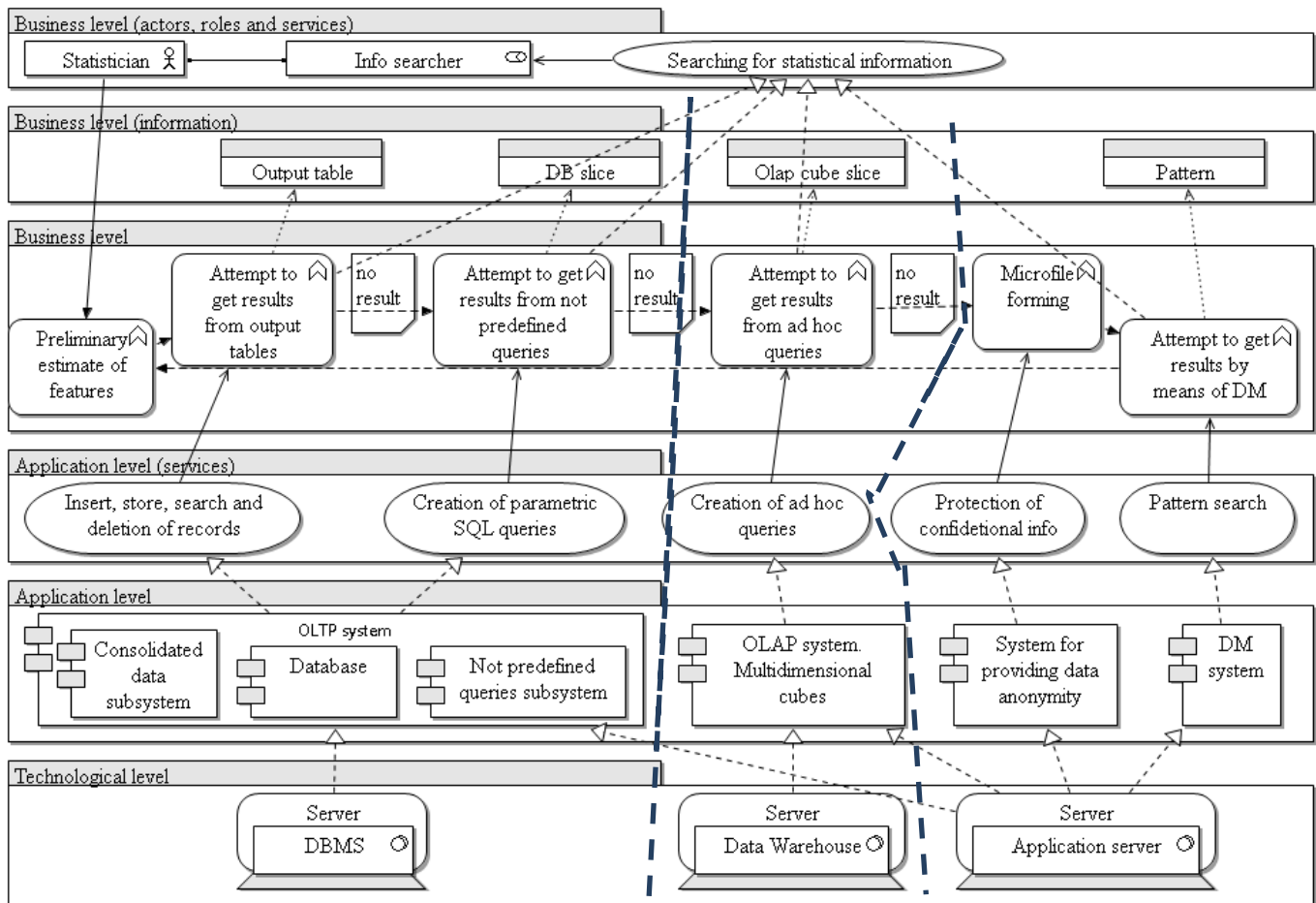


Fig. 1. General architectural model that enables to search for patterns of statistical information.

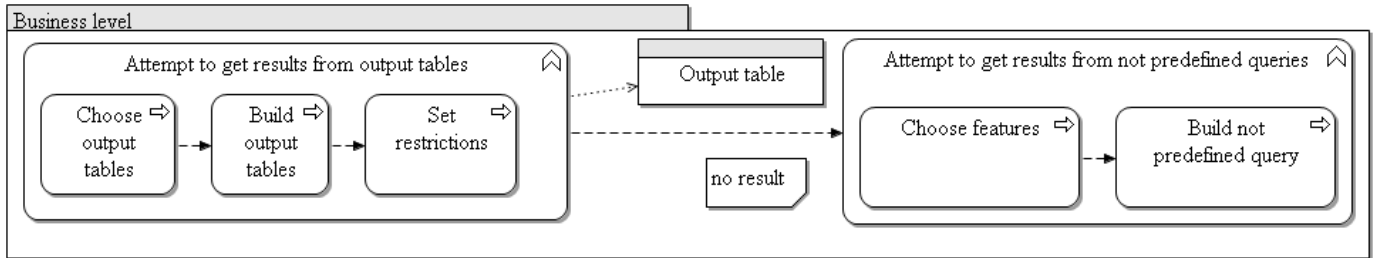


Fig. 2. OLTP business functions for pattern search of statistical information.

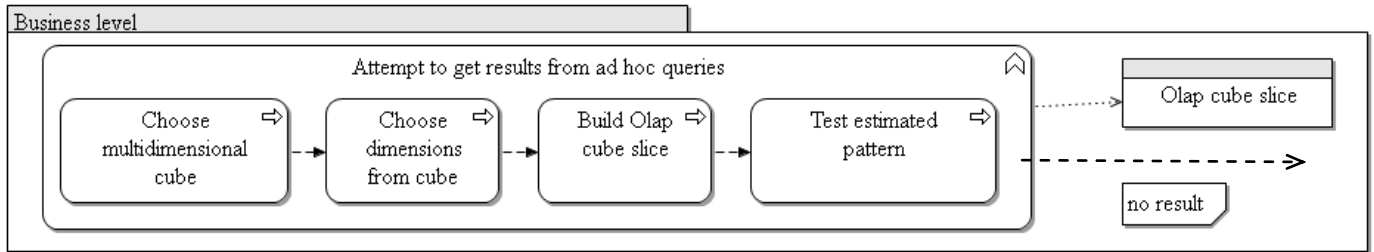


Fig. 3. OLAP business function for pattern search of statistical information.

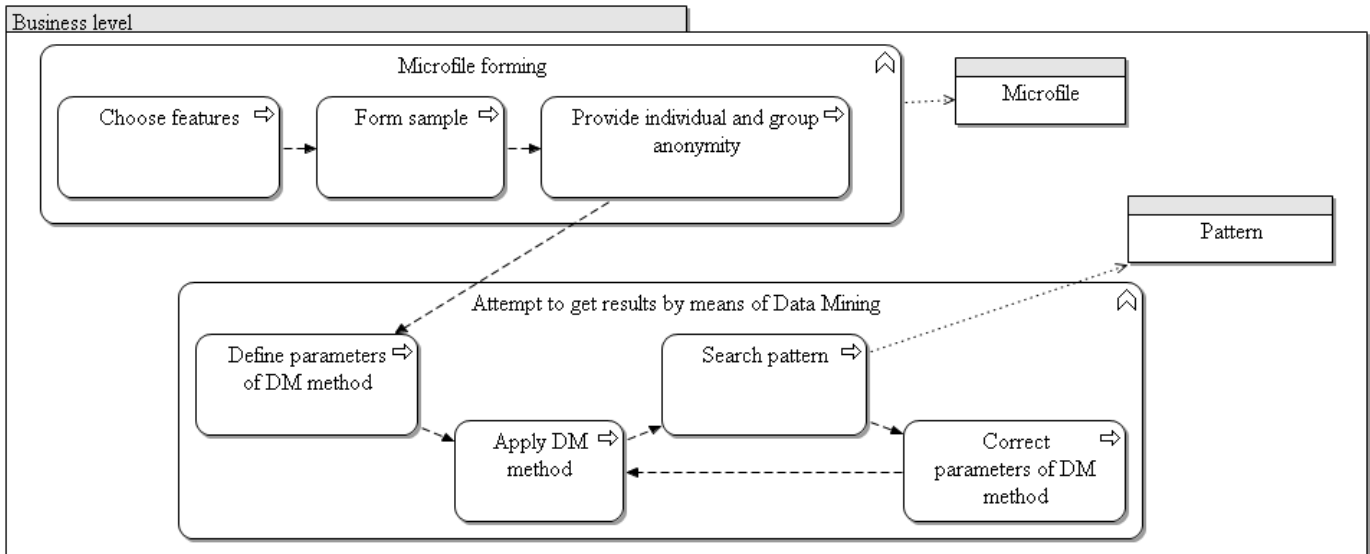


Fig. 4. Data Mining business function for pattern search of statistical information.

Clustering Web Documents based on Efficient Multi-Tire Hashing Algorithm for Mining Frequent Termsets

Noha Negm

Math. and Computer Science Dept.
Faculty of Science, Menoufia University
Shebin El-Kom, EGYPT

Passent Elkafrawy

Math. and Computer Science Dept.
Faculty of Science, Menoufia University
Shebin El-Kom, EGYPT

Mohamed Amin

Math. and Computer Science Dept.
Faculty of Science, Menoufia University
Shebin El-Kom, EGYPT

Abdel Badeeh M. Salem

Computer Science Dept. Faculty of Computers and
Information, Ain Shams University
Cairo, EGYPT

Abstract—Document Clustering is one of the main themes in text mining. It refers to the process of grouping documents with similar contents or topics into clusters to improve both availability and reliability of text mining applications. Some of the recent algorithms address the problem of high dimensionality of the text by using frequent termsets for clustering. Although the drawbacks of the Apriori algorithm, it still the basic algorithm for mining frequent termsets. This paper presents an approach for Clustering Web Documents based on Hashing algorithm for mining Frequent Termsets (CWDHFT). It introduces an efficient Multi-Tire Hashing algorithm for mining Frequent Termsets (MTHFT) instead of Apriori algorithm. The algorithm uses new methodology for generating frequent termsets by building the multi-tire hash table during the scanning process of documents only one time. To avoid hash collision, Multi Tire technique is utilized in this proposed hashing algorithm. Based on the generated frequent termset the documents are partitioned and the clustering occurs by grouping the partitions through the descriptive keywords. By using MTHFT algorithm, the scanning cost and computational cost is improved moreover the performance is considerably increased and increase up the clustering process. The CWDHFT approach improved accuracy, scalability and efficiency when compared with existing clustering algorithms like Bisecting K-means and FIHC.

Keywords—Document Clustering; Knowledge Discovery; Hashing; Frequent termsets; Apriori algorithm; Text Documents; Text Mining; Data Mining

I. INTRODUCTION

This With the recent explosive growth of the amount of content on the Internet, it has become increasingly difficult for users to find and utilize information and for content providers to classify and index documents. Hundreds or thousands of results for a search are often returned by traditional web search engines, which is time consuming for users to browse. On-line libraries, search engines, and other large document repositories are growing so rapidly that it is difficult and costly to categorize every document manually. In order to deal with these problems, researchers look toward automated methods of

working with web documents so that they can be more easily browsed, organized, and indexed with minimal human intervention. To deal with the problem of information overload on the Internet, Clustering and Classification considered the useful and active areas of machine learning research that promise to overcome this problem [1].

Document clustering is known as an unsupervised and automatic organizing text documents into meaningful clusters or group. In other words, the documents in one cluster share the same topic, and the documents in different clusters represent different topics. It is unlike document classification since there is no training stage by using labeled documents. Document clustering has been studied intensively because of its wide applicability in areas such as *Web Mining*, *Search Engines*, *Information Retrieval*, and *Topological Analysis*.

The high dimensionality of the feature space considered a major characteristic of document clustering algorithms, which imposes a big challenge to the performance of clustering algorithms. Next challenge is that not all features are important for document clustering, some of the features may be redundant or irrelevant and some may even misguide the clustering result [2].

Hierarchical and Partitioning methods are categorized as the essentially two algorithms into the clustering technique [3-8]. K-means and its variants are the most well-known partitioning methods that create a flat, non-hierarchical clustering consisting of k clusters. The Bisecting k-means algorithm first selects a cluster to split, and then employs basic k-means to create two sub-clusters, repeating these two steps until the desired number k of clusters is reached [7]. Steinbach in [4] showed that the Bisecting k-means algorithm outperforms basic k-means as well as agglomerative hierarchical clustering in terms of accuracy and efficiency.

A hierarchical clustering method works by grouping data objects into a tree of clusters. These methods can further be classified into agglomerative and divisive hierarchical

clustering depending on whether the hierarchical decomposition is formed in a bottom-up or top down fashion [8]. Steinbach in [9] showed that Unweighted Pair Group Method with Arithmetic Mean (UPGMA) is the most accurate one in agglomerative category.

Both hierarchical and partitioning methods do not really address the problem of high dimensionality in document clustering. Frequent itemset-based clustering method is shown to be a promising approach for high dimensionality clustering in recent literature [10-24]. It reduces the dimension of a vector space by using only frequent itemsets for clustering. The frequent term-based text clustering is based on the following ideas: (1) Frequent terms carry more information about the "cluster" they might belong to; (2) Highly co-related frequent terms probably belong to the same cluster.

Finding frequent itemsets is an important data mining topic, and it was originated from the association rule mining of transaction dataset. The main drawback of frequent itemsets is they are very large in number to compute or store in computer. The very first well known algorithm for frequent itemset generation is Apriori algorithm [10]. It works on the principle of Apriori property, which states that the subset of any frequent itemset is also frequent. Apriori algorithm adopts layer by layer search iteration method to mine association rules. The Apriori algorithm suffers from the following two problems: 1) candidate generation and 2) repeated number of scans.

In this paper, a CWDHFT approach for clustering web documents based on a hashing mining algorithm is proposed. It introduces an efficient Multi-Tire Hashing algorithm (MTHFT) to discover frequent termsets from web text documents. It overcomes the drawbacks of the Apriori algorithm by using new methodology for generating frequent termsets. The multi-tire hash table is building during the scanning process of documents only one time. To avoid hash collision, multi-tire technique is utilized in MTHFT algorithm. The generated set of frequent termsets with varying length is used in the clustering process. Based on the generated frequent termset the documents are partitioned and the clustering occurs by grouping the partitions through the descriptive keywords.

The organization of the paper is as follows. Section 2 discusses the related work to our approach on. In Section 3, we describe the proposed CWDHFT approach and MTHFT algorithm. Section 4 discusses about the results obtained from the comparison of the CWDHFT approach with two other clustering algorithms in this field. Section 5 concludes the work proposed.

II. RELATED WORK

There are many works in the literature that discuss about text clustering algorithms. They address the special characteristics of text documents and use the concept of frequent termsets for the text clustering.

Reference [9], they proposed a new criterion for clustering transactions using frequent itemsets, instead of using a distance function. In principle, this method can also be applied to document clustering by treating a document as a transaction;

however, the method does not create a hierarchy for browsing. The novelty of this approach is that it exploits frequent itemsets (by applying Apriori algorithm) for defining a cluster, organizing the cluster hierarchy, and reducing the dimensionality of document sets.

The FTC and HFTC are proposed in [14]. The basic motivation of FTC is to produce document clusters with overlaps as few as possible. FTC works in a bottom-up fashion. As HFTC greedily picks up the next frequent itemset to minimize the overlapping of the documents that contain both the itemset and some remaining itemsets. The clustering result depends on the order of picking up itemsets, which in turn depends on the greedy heuristic used. The weakness of the HFTC algorithm is that it is not scalable for large document collections.

To measure the cohesiveness of a cluster directly using frequent itemsets, the FIHC algorithm is proposed in [15]. Two kinds of frequent item are defined in FIHC: global frequent item and cluster frequent item. However, FIHC has three disadvantages in practical application: first, it cannot solve cluster conflict when assigning documents to clusters. Second, after a document has been assigned to a cluster, the cluster frequent items were changed and FIHC does not consider this change in afterward overlapping measure. Third, in FIHC, frequent itemsets is used merely in constructing initial clusters.

Frequent Term Set-based Clustering (FTSC) algorithm is introduced in [16]. FTSC algorithm used the frequent feature terms as candidate set and does not cluster document vectors with high dimensions directly. The results of the clustering texts by FTSC algorithm cannot reflect the overlap of text classes. But FTSC and the improvement FTSHC algorithms are comparatively more efficient than K-Means algorithm in the clustering performance.

Clustering based on Frequent Word Sequence (CFWS) is proposed in [17]. CFWS uses frequent word sequence and K-mismatch for document clustering. By using the CFWS there are overlaps in the final clusters. With K-mismatch, frequent sequences of candidate clusters are used to produce final clusters. Document Clustering Based on Maximal Frequent Sequences (CMS) is proposed in [18]. The basic idea of CMS is to use Maximal Frequent Sequences (MFS) of words as features in Vector Space Model (VSM) for document representation and then K-means is employed to group documents into clusters. CMS is rather a method concerning feature selection in document clustering than a specific clustering method. Its performance completely depends on the effectiveness of using MFS for document representation in clustering, and the effectiveness of K-means.

A frequent term based parallel clustering algorithm which could be employed to cluster short documents in very large text database is presented in [22]. A semantic classification method is also employed to enhance the accuracy of clustering. The experimental analysis proved that the algorithm was more precise and efficient than other clustering algorithms when clustering large scale short documents. In addition, the algorithm has good scalability and also could be employed to process huge data.

The document clustering algorithm on the basis of frequent term sets is proposed in [23]. Initially, documents were denoted as per the Vector Space Model and every term is sorted in accordance with their relative frequency. Then frequent term sets can be mined using frequent-pattern growth (FP growth). Lastly, documents were clustered on the basis of these frequent term sets. The approach was efficient for very large databases, and gave a clear explanation of the determined clusters by their frequent term sets. The efficiency and suitability of the proposed algorithm has been demonstrated with the aid of experimental results.

Reference [25] a hierarchical clustering algorithm using closed frequent itemsets that use Wikipedia as an external knowledge to enhance the document representation is presented. Firstly, construct the initial clusters from the generalized closed frequent itemsets. Then used the two methods TF-IDF and Wikipedia as external knowledge, to remove the document duplication and construct the final clusters. The drawback in this approach is that it might not be of great use for datasets which do not have sufficient coverage in Wikipedia.

A Frequent Concept based Document Clustering (FCDC) algorithm is proposed in [26]. It utilizes the semantic relationship between words to create concepts. It exploits the WordNet ontology in turn to create low dimensional feature vector which allows us to develop an efficient clustering algorithm. It used a hierarchical approach to cluster text documents having common concepts. FCDC found more accurate, scalable and effective when compared with existing clustering algorithms like Bisecting K-means, UPGMA and FIHC.

To the best of our knowledge, all the previous researchers depend on the Apriori algorithm and their improvements for generating the frequent termsets from text documents. Moreover they don't address the improvements in the execution time as the major factor in the mining process.

III. CLUSTERING WEB DOCUMENTS BASED ON MINING FREQUENT TERMSETS

The proposed web document clustering approach based on frequent termsets CWDHFT is shown in Fig.1. The main characteristic of the approach is that it introduces a new mining algorithm for generating frequent termsets to overcome the drawbacks of the Apriori algorithm. Moreover it speeds up the mining and clustering process. CWDHFT consists of the four main stages:

- Document Preprocessing
- Mining of Frequent Termsets
- Document Clustering
- Post Processing

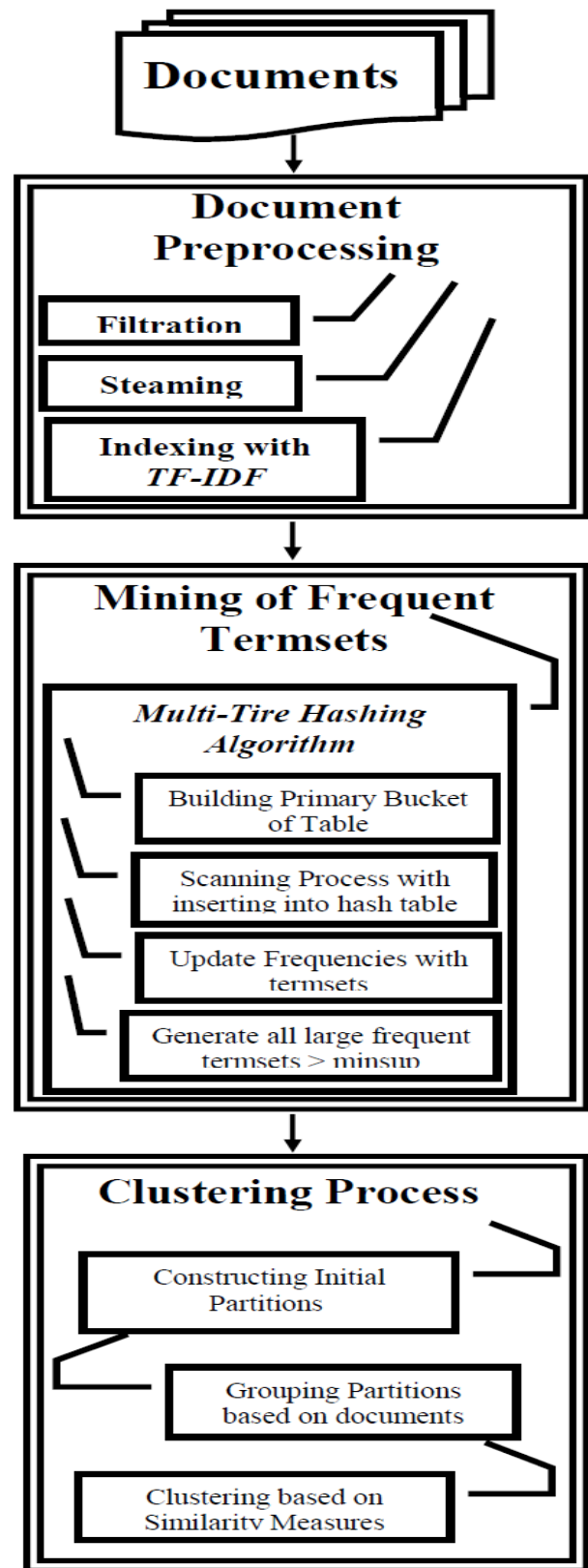


Fig. 1. CWDHFT approach.

A. Document Preprocessing Stage

Our approach employs several preprocessing steps including stop words removal, stemming on the document set and indexing by applying TF*ID:

- **Stop words removal:** Stop-words are words that from non-linguistic view do not carry information such as (a, an, the, this, that, I, you, she, he, again, almost, before, after). Stop-words removing is to remove this non-information bearing words from the documents and reduce noise. One major property of stop-words is that they are extremely common words. The explanation of the sentences still held after these stop-words are removed. To organize large corpus, removing the stop words affords the similar advantages. Firstly it could save huge amount of space. Secondly it helps to deduce the noises and keep the core words, and it will make later processing more effective and efficient.
- **Stemming:** Removes the affixes in the words and produces the root word known as the stem. Typically, the stemming process will be performed so that the words are transformed into their root form. *For example* connected, connecting and connection will be transformed into connect. A good stemmer should be able to convert different syntactic forms of a word into its normalized form, reduce the number of index terms, save memory and storage and may increase the performance of clustering algorithms to some extent; meanwhile it should try stemming. Porter Stemmer [27] is a widely applied method to stem documents. It is compact, simple and relatively accurate. It does not require creating a suffix list before applied. In this paper, we apply Porter Stemmer in our preprocessing.
- **TF*IDF:** In many weighting schemes the weights as in (1) are the product of two factors, the *term frequency* (*tf*) and the *inverse document frequency* (*idf*) [28]:

$$w_{i,j} = tf_{i,j} * idf_i \quad (1)$$

- The term frequency is a function of the number of occurrences of the particular word in the document divided by the number of words in the entire document. A word appearing frequently in the text is thus considered more important to describe the content than a word appearing less often. The inverse document frequency models the distinguishing power of the word in the text set; the fewer documents that contain the word the more information about the text in the text set it gives. There are many variants of the *idf*-measure. A simple example is as in (2):

$$idf_i = \log\left(\frac{N}{Nt_j}\right) \quad (2)$$

where Nt_j denotes the number of documents in collection N in which t_j occurs at least once. Once a weighting scheme has been selected, automated indexing can be performed by simply selecting the top K of words that satisfy the given weight constraints for each document. The major advantage of

an automated indexing procedure is that it reduces the cost of the indexing step.

B. Mining of Frequent Termset Stage

The goal of frequent termset mining is to discover sets of terms that frequently co-occur in the document. The problem is non-trivial in text documents because the documents can be very large, consisting of many distinct terms, and contain interesting termsets of high cardinality. Although the drawbacks of the Apriori algorithm, it still use for generating the frequent termsets that used in the document clustering.

In order to speed up the mining process as well as to address the scalability with different documents regardless of their sizes, we introduce a new algorithm called Multi-Tire Hashing Frequent Termsets algorithm (MTHFT). It is basically different from all the previous algorithms since it overcomes the drawbacks of Apriori algorithm by employing the power of data structure called Multi-Tire Hash Table. Moreover it uses new methodology for generating frequent termsets by building the hash table during the scanning of documents only one time consequently, the number of scanning on documents decreased.

1) *Hash Table:* The hash table is a data structure that speeds up searching for information by a particular aspect of that information, called a key. The idea behind the hash table is to process the key with a function that returns a hash value; that hash value then determines where in the data structure the terms will (or probably will) be stored. The hash tables can provide constant time $O(1)$ lookup on average, regardless of the number of terms in the table. To avoid hash collision, Multi Tire technique is utilized in this proposed hashing algorithm. It consists of two major components: bucket array and hash function.

a) *Bucket Array:* A bucket array for a hash table is an array U of size R , where each cell of U is thought of as a "Bucket" and the integer R defines the capacity of the array. If the keys are integers well distributed in the range $[0, R-1]$, this bucket array is all that is needed. An element e with key v is simply inserted into the bucket $U[v]$.

b) *Hash Function:* The second part of a hash table structure is a function, h , that maps each key v in our dictionary to an integer in the range $[0, R-1]$, where R is the capacity of the bucket array for this table. The main idea of this approach is to use the hash function value, $h(v)$, as an index into our bucket array, U , instead of the key v . That is, we store the item (v, e) in the bucket $U[h(v)]$. The benefit of the hash function is to reduce the range of array indices that need to be handled. The Division Method (The mod function $h(v) = v \bmod R$) used for creating hash function $h(v)$ in hash table.

2) *Multi-Tire Hashing Frequent Termsets Algorithm:* The MTHFT algorithm as shown in Fig. 2 employs the following two main steps:

- Based on the number of the English alphabet letters $R = 26$, a dictionary table constructed as shown in Table 1

and gives each character a unique numeric number from 0 to 25.

MTHFT Algorithm:

T_m : Set of all termsets for each document d
 C_m : Candidate termsets for each document d
 I_k : Frequent termsets of size k .

Input: All Text documents.

Process logic: Building Multi-Tire Hash Table and Finding the frequent termsets.

Output: Generating the frequent termsets.

```

for each document  $d_m \in D$  do begin
     $T_m = \{ t_i : t_i \in d_m, 1 \leq i \leq n \}$ 
    for each term  $t_i \in T_m$  do
         $h(t_i) = t_i \text{ mod } N;$ 
         $t_i.\text{count}++;$ 
        // insert each term in hash table
    end
     $C_k = \text{all combinations of } t_i \in d_m$ 
     $C_m = \text{subset}(C_k, d_m);$ 
    for each candidate  $c_j \in C_m$  do
         $h(c_j) = c_j \text{ mod } N;$ 
         $c_j.\text{count}++;$ 
        // insert each candidate in hash table
    end
end
for given  $s = \text{minsup}$  in hash table do
     $I_1 = \{ t \mid t.\text{count} \geq \text{minsup} \}$ 
     $I_k = \{ c \mid c.\text{count} \geq \text{minsup}, k \geq 2 \}$ 
end
    
```

Fig. 2. The MTHFT algorithm.

- There are also two main processes for a dynamic multi-tire hash table: the building process and the scanning process.

a) *The Building Process:* In the dynamic hash table, a primary bucket is only built at the first. It depends on the number of the English alphabet letter R, not on the number of all terms as shown in Table 2. Their locations in the hash table are determined using the division method of hash function.

TABLE I. THE DICTIONARY TABLE FOR THE ENGLISH ALPHABET LETTERS

| Dictionary Table | |
|------------------|----------|
| Letters | Location |
| A | 0 |
| B | 1 |
| C | 2 |
| D | 3 |
| E | 4 |
| F | 5 |
| | |
| V | 21 |
| W | 22 |
| X | 23 |
| Y | 24 |
| Z | 25 |

TABLE II. THE PRIMARY BUCKET OF MULTI-TIRE HASH TABLE

| | | | | | |
|------|------|------|-------|-------|-------|
| A(0) | B(1) | C(2) | | Y(24) | Z(25) |
|------|------|------|-------|-------|-------|

For example, the alphabet letter E takes the unique numeric number 4 in the dictionary table, and their location is determined by applying the hash function so that its location is also 4 and so on.

b) *The Scanning Process:* After building a primary bucket, each document is scanned only once as follows:

- For first document, select all terms and make all possible combinations of terms after that determine their locations in the dynamic hash table using the hash function $h(v)$. in hash table, insert them in their locations with their frequencies.
- For each document, all terms and termsets are inserted in a hash table and their frequencies are updated, the process continues until there is no document in the collection.
- Save the multi-tire hash table into secondary storage media for further processing.
- Insert different minimum support values and scan the multi-tire hash table to determine the large frequent termsets that satisfy each threshold support value without redoing the mining process again.
- Insert the generated large frequent termsets in the Clustering process.

3) *The advantages of MTHFT Algorithm:* The MTHFT algorithm has many advantages summarized as follows:

- Provides facilities to avoid unnecessary scans to the documents, which minimize the I/O. Where the scanning process occurs on the hash table instead of whole documents compared to Apriori algorithm
- The easy manipulations on hash data structure and directly computing frequent termsets are the added advantages of this algorithm, moreover the fast access and search of data with efficiency.
- MTHFT shows better performance in terms of time taken to generate frequent termsets when compared to Apriori algorithm. Furthermore, it permits the end user to change the threshold support and confidence factor without re-scanning the original documents since the algorithm saves the hash table into secondary storage media
- The main advantage of this algorithm is that, it is scalable with all types of documents regardless of their sizes.
- Depending on the multi-tire technique in building the primary bucket, each bucket can store only a single element then we cannot associate more than one term with a single bucket, which is a problem in the case of collisions.

C. Documents Clustering Stage

Document clustering algorithm based on frequent termsets considered a keyword-based algorithm which picks up the core

words with specific criteria and groups the documents based on these keywords. this approach includes three main steps:

- Picking out all frequent termsets
- Constructing partitions
- Clustering documents

1) *Picking out all Frequent Termsets:* The Multi-Tire Hashing algorithm is used in the previous step to find out the large frequent termsets furthermore to speeding up the mining process. it have ability to determine large frequent termsets at different minimum support threshold values without redoing the mining process again. Therefore, we can pick out different sets of frequent termsets in the clustering process easily. We start with a set of 2-large frequent termsets.

2) *Constructing Partitions:* Constructing partitions include two sub steps: constructing initial partitions and merging non-overlapping partitions.

a) *Constructing initial partitions:* initially, we sort the set of 2-large frequent termsets in descending order in accordance with their support level as in (3):

$$Sup(lf_1) > Sup(lf_2) > Sup(lf_k) \quad (3)$$

Then, the first 2-large frequent termsets from the sorted list is selected. Afterward, an initial partition P1 which contains all the documents including the both termsets is constructed. Next, we take the second 2-large frequent termsets whose support is less than the previous one to form a new partition P2. This partition is formed by the same way of the partition P1 and takes away the documents that are in the initial partition this avoid the overlapping between partitions since each document keeps only within the best initial partition. This procedure is repeated until every 2-large frequent termsets moved into partition P(i).

b) *Merging non-overlapping partitions:* in this step, all partitions that contain the similar documents are merged into one partition. The benefit of this step is reducing the number of resulted partitions.

3) *Clustering Documents:* In this step, we don't require to pre-specified number of clusters we have a set of non-overlapping partitions P(i) and each partition has a number of documents D. We first identify the words that used for constructing each partition P(i) which called labeling Words Ld [W(i)]. The labeling words are obtained from all 2-large frequent termsets that contained in each partition. For each document, Derived keywords Vd [W(i)] are obtained from taking into account the difference words between the top weighted frequent words for each document with the labeling words. Subsequently the total support of each derived word is computed within the partition.

The set of words satisfying the partition threshold (the percentage of the documents in partition P(i) that contains the termset) are formed as Descriptive Words Pw [c(i)] of the partition P(i). Afterward, we compute the similarity of each document in the partitions with respect to the descriptive words. The definition of the similarity measure plays an

importance role in obtaining effective and meaningful clusters. The similarity between two documents Sm is computed as in [8]. Based on the similarity measure, a new cluster is formed from the partitions i.e. each cluster will contain all partitions that have the similar similarity measures.

D. Post processing

Includes the major applications in which the document clustering is used, for example, the recommendation application which uses the results of clustering for recommending news articles to the users.

IV. EXPERIMENTAL RESULTS AND PERFORMANCE EVALUATION

Our experiments have been conducted on a personal computer with a 2.50 GHz CPU and 6.00 GB RAM and we have implemented the proposed clustering approach CWDHFT using C#.net language. To evaluate the effectiveness of proposed MTHFT algorithm in the mining process, this section presents the result comparisons between our MTHFT algorithm and Apriori algorithm. Moreover, several popular hierarchical document clustering algorithms Bisecting K-means and FIHC are compared with our CWDHFT approach for clustering web documents. The rest of this section first describes the characteristics of the datasets, then explains the evaluation measures, and finally presents and analyzes the experiment results.

A. Datasets

We have used the largest datasets Reuters-21578 to exam the efficiency and scalability of our algorithm [29]. The Reuters-21578 collection is distributed in 22 files. Each of the first 21 files (reut2-000.sgm through reut2-020.sgm) contain 1000 documents, while the last (reut2- 021.sgm) contains 578 documents. Documents were marked up with SGML tags. There are 5 categories Exchanges, Organizations, People, Places and Topics in the Reuters dataset and each category has again sub categories in total 672 sub categories. We have collected the TOPIC category sets to form the dataset. The TOPICS category set contains 135 categories. From these documents we collect the valid text data of each category by extracting the text which is in between <BODY> ,</BODY> and placed in a text document and named it according to the topic. From Reuters, we have considered 5000 documents the our datasets.

B. Evaluation Methods

The F-measure, as the commonly used external measurement, is used to evaluate the accuracy of our clustering algorithms. F-measure is an aggregation of Precision and Recall concept of information retrieval. Recall is the ratio of the number of relevant documents retrieved for a query to the total number of relevant documents in the entire collection as in (4):

$$Recall (K_i, C_j) = \frac{n_{ij}}{|K_i|} \quad (4)$$

Precision is the ratio of the number of relevant documents to the total number of documents retrieved for a query as in (5):

$$Precision(K_i, C_j) = \frac{n_{ij}}{|C_j|} \quad (5)$$

While F-measure for cluster C_j and class K_i is calculated as in (6):

$$F(K_i, C_j) = \frac{2 * Recall(K_i, C_j) * Precision(K_i, C_j)}{Recall(K_i, C_j) + Precision(K_i, C_j)} \quad (6)$$

where n_{ij} is the number of members of class K_i in cluster C_j . $|C_j|$ is the number of members of cluster C_j and $|K_i|$ is the number of members of class K_i .

The weighted sum of all maximum F-measures for all natural classes is used to measure the quality of a clustering result C . This measure is called the overall F-measure of C , denoted $F(C)$ is calculated as in (7):

$$F(C) = \sum_{K_i \in K} \frac{|K_i|}{|D|} \max_{C_j \in C} \{F(K_i, C_j)\} \quad (7)$$

where K denotes all natural classes; C denotes all clusters at all levels; $|K_i|$ denotes the number of documents in natural class K_i ; and $|D|$ denotes the total number of documents in the dataset. The range of $F(C)$ is $[0,1]$. A large $F(C)$ value indicates a higher accuracy of clustering.

C. Experimental Results

In this section, we evaluate the performance of our MTHFT algorithm in terms of the efficiency and scalability of finding frequent termsets, moreover the accuracy and efficiency of CWDHFT approach.

1) *Evaluation of MTHFT algorithm for finding frequent termsets:* We evaluated our MTHFT algorithm of finding frequent termsets in terms of its efficiency and scalability. In our experiment, we compared the MTHFT algorithm with Apriori algorithm, which is the most representative frequent itemset mining algorithm although of its drawbacks. As we know, the efficiency of Apriori is sensitive to the minimum support level and the size of documents. When the minimum support is decreased, the runtime of Apriori increases as there are more frequent itemsets. Moreover, when the size of documents become very large, most time is consuming in the multiple scanning on the documents and generating frequent termsets at different minimum support. In MTHFT algorithm, the time is consumed in building a hash table only one time. After saving the hash table there is no time consuming in generating new different frequent termsets at different minimum support threshold.

Fig. 3 shows a comparison of results of Apriori and MTHFT algorithm for various values of minimum support thresholds at the Reuters datasets. Support is taken as X-axis and the execution time taken to find the frequent termsets is taken as Y-axis. We first chose small value of minimum support equals to 30% then compute the execution time for both algorithms.

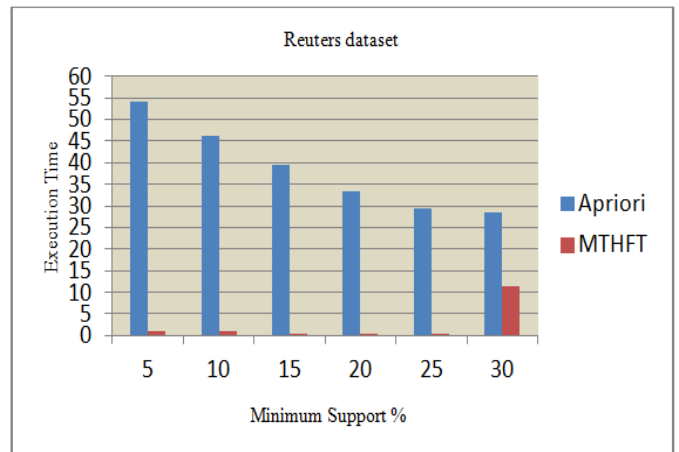


Fig. 3. Time comparison between Apriori and MTHFT algorithms on Reuters dataset.

From the chart, it can be seen that the execution time taken for MTHFT algorithm decreases as the minimum support increased in comparable to Apriori algorithm. At MTHFT algorithm, the whole execution time is consumed in building the hash table the first time. When entering new minimum support, there is no time consumed, however, the time is taken for searching the hash table. We noticed that the execution time decreases as the minimum support increased in comparable to Apriori algorithm. In Apriori algorithm, each time entering a new minimum support it required to redo the mining process from the beginning. We conclude that MTHFT is significantly more efficient than Apriori algorithm in all cases specially for large documents since the complexity of finding the frequent termsets is lower than Apriori.

To examine the scalability of MTHFT algorithm, we create a larger dataset from Reuters. We duplicated the files in Reuters until we get 10000 documents. Fig. 4 illustrates the results of applying MTHFT algorithm and Apriori on different sizes of documents of Reuters at small value of minimum support threshold 15% to ensure that the generated frequent termset in both algorithms is approximately the same. We noticed that MTHFT algorithm is about two to three times faster than Apriori and performs better with large number of documents in contrast Apriori algorithm.

Evaluation of the text clustering algorithm: For a comparison with CWDHFT approach, we also executed Bisecting k-means and FIHC on the same documents. We chose Bisecting k-means because it has been reported to produce a better clustering result consistently compared to k-means and agglomerative hierarchical clustering algorithms. FIHC is also chosen because it uses frequent word sets. For a fair comparison, we did not implement Bisecting k-means and FIHC algorithms by ourselves. We downloaded the CLUTO toolkit [30] to perform Bisecting k-means, and obtained FIHC [31] from their author.

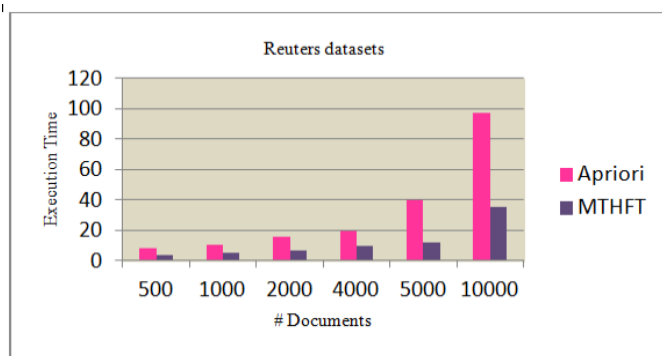


Fig. 4. Time comparison between Apriori and MTHFT algorithms on different sizes of Reuters at MinSup=15%.

Fig. 5 shows the comparison between all the three clustering approaches based on the overall F-measure values with different numbers of clusters. Our CWDHFT approach outperforms all other approaches in terms of accuracy, it has better F-measure because it uses a better model for text documents.

Many experiments were conducted to exam the efficiency of CWDHFT approach. Fig. 6 compares the execution time of CWDHFT approach with FIHC and Bisecting K-means on different sizes of documents of Reuters. The minimum support is set to 15% to ensure that the accuracy of all produced clustering are approximately the same. The number of documents is taken as X-axis and the time taken to find the clusters is taken as Y-axis. CWDHFT approach runs approximately twice faster than the two approaches FIHC and Bisecting K-means. We conclude that CWDHFT is more efficient than other approaches.



Fig. 5. Overall F-measure results comparison with Reuters dataset.

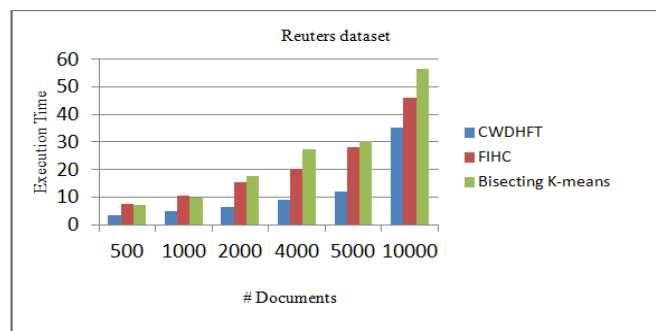


Fig. 6. Efficiency comparison of CWDHFT with FIHC and Bisecting K-means on different sizes of Reuters at minsup=15%.

V. CONCLUSION

In this paper, we presented a novel CWDHFT approach for web document clustering based on hashing algorithm for mining frequent termsets that provides significant dimensionality reduction. The originality of CWDHFT approach is by introducing an efficient MTHFT algorithm for mining frequent termsets. MTHFT algorithm introduced a novel method for mining frequent termsets by building the multi-tire hash table during the scanning process of documents only one time. Furthermore it provided a possibility for mining new frequent termsets at different minimum support threshold without needing to rescan the documents. This is the major factor for speeding up the clustering process.

Experiments are conducted to evaluate MTHFT algorithm in comparison with Apriori algorithm and to evaluate the CWDHFT approach in comparison with Bisecting K-means and FIHC. The largest dataset, Reuters, is chosen to exam the efficiency and scalability of our algorithm. The experimental results show that in mining process, the scanning and computational cost is improved when processing large size of documents. The proposed document clustering, CWDHFT, approach improved accuracy, scalability and efficiency when compared with other clustering algorithms. Moreover, it automatically generates a natural description for the generated clusters by a set of frequent termsets. From all experiments, we conclude that CWDHFT approach has favorable quality in clustering documents using frequent termsets.

VI. FUTURE WORK

The area of document clustering has many issues which need to be solved. In this work, few issues e.g. high dimensionality and accuracy are focused. In future work, we intend to propose a novel technique for clustering web documents based on Association Rules instead of using frequent termsets.

REFERENCES

- [1] S. Sharma, and V. Gupta, Recent developments in text clustering techniques, International Journal of Computer Applications, vol. 37, pp. 14-19, 2012
- [2] S. Fabrizio, "Machine learning in automated text categorization," International Conference on ACM Computing Surveys, vol. 34, pp. 1-47, 2002.
- [3] K. Jain, N. Murty, and J. Flynn, "Data clustering: a review," International Conference on ACM Computing Surveys, vol. 31, pp. 264-323, 1999.
- [4] M. Steinbach, G. Karypis, and V. Kumar, "A comparison of document clustering techniques," KDD Workshop on Text Mining, 2000. Available online : <http://glaros.dtc.umn.edu/gkhome/node/157>
- [5] P. Berkhin, "Survey of clustering data mining techniques," 2004, [Online]. Available: http://www.acrue.com/products/rp_cluster_review.pdf
- [6] R. Xu, "Survey of clustering algorithms," International Conference of IEEE Transactions on Neural Networks, vol.15, pp. 634-678, 2005.
- [7] F. Benjamin, W. Ke, and E. Martin, "Hierarchical document clustering," Simon Fraser University, Canada, pp. 555-559, 2005.
- [8] J. Ashish, J. Nitin, "Hierarchical document clustering: A review," 2nd National Conference on Information and Communication Technology, 2011, Proceedings published in International Journal of Computer Applications.
- [9] B. Fung, K. Wang, and M. Ester, "Hierarchical document clustering using frequent itemsets," International Conference on Data Mining, vol.

- [10] 30, pp. 59-70, 2003.
- [11] R. Agrawal, T. Imielinski, and A. Swami, "Mining association rules between sets of items in large databases," International Conference on Management of Data, vol. 22, pp. 207-216, Washington 1993.
- [12] O. Zaiane and M. Antonie, "Classifying text documents by association terms with text categories," International Conference of Australasian Database, vol. 24, pp. 215-222, 2002.
- [13] B. Liu, W. Hsu and Y. Ma, "Integrating classification and association rule mining," International Conference of ACM SIGKDD on Knowledge Discovery and Data Mining, pp. 80-86, 1998.
- [14] O. Zamir and O. Etzioni, "Web document clustering: A feasibility demonstration," International Conference of ACM SIGIR, pp. 46-54, 1998.
- [15] M. Beil, and X. Xu. "Frequent term-based text clustering," International Conference on Knowledge Discovery and Data Mining, pp. 436- 442, 2002.
- [16] M. Hassan and K. John, "High quality, efficient hierarchical document clustering using closed interesting itemsets," International IEEE Conference on Data Mining, pp. 991-996, 2006.
- [17] L. Xiangwei, H. Pilian, "A study on text clustering algorithms based on frequent term sets," Springer-Verlag Berlin Heidelberg, 2005.
- [18] Y.J. Li, S.M. Chung, J.D. Holt, "Text document clustering based on frequent word meaning sequences," Data & Knowledge Engineering, vol. 64, pp. 381-404, 2008.
- [19] H. Edith, A.G. Rene, J.A. Carrasco-Ochoa, and J.F. Martinez-Trinidad, "Document clustering based on maximal frequent sequence," FinTal vol. 4139, pp. 257-267, LNAI 2006.
- [20] Z. Chong, L. Yansheng, Z. Lei and H. Rong, FICW: Frequent itemset based text clustering with window constraint, Wuhan University journal of natural sciences, vol. 11, pp. 1345-1351, 2006.
- [21] L. Wang, L. Tian, Y. Jia and W. Han, "A Hybrid algorithm for web document clustering based on frequent term sets and k-means," Lecture Notes in Computer Science, Springer Berlin, vol. 4537, pp. 198-203, 2010.
- [22] Z. Su, W. Song, M. Lin, and J. Li, "Web text clustering for personalized e-Learning based on maximal frequent itemsets," International Conference on Computer Science and Software Engineering, vol. 06, pp. 452-455, 2008.
- [23] Y. Wang, Y. Jia and S. Yang, "Short documents clustering in very large text databases," Lecture Notes in Computer Science, Springer Berlin, vol. 4256, pp. 38-93, 2006.
- [24] W. Liu and X. Zheng, "Documents clustering based on frequent term sets," Intelligent Systems and Control, 2005.
- [25] H. Anaya, A. Pons and R. Berlanga, "A Document clustering algorithm for discovering and describing topics," Pattern Recognition Letters, vol. 31, pp. 502-510, April 2010.
- [26] R. Kiran, S. Ravi, and p. Vikram, "Frequent itemset based hierarchical document clustering using Wikipedia as external knowledge," Springer-Verlag Berlin Heidelberg, 2010.
- [27] R. Baghel and Dr. R. Dhir, A Frequent concept based document clustering algorithm, International Journal of Computer Applications, vol. 4, pp. 0975 - 8887, 2010.
- [28] <http://tartarus.org/martin/PorterStemmer/>
- [29] M. Berry, "Survey of text mining: clustering, classification, and retrieval," Springer-Verlag New York, Inc., 2004.
- [30] <http://kdd.ics.uci.edu/databases/reuters21578/reuters21578.html>
- [31] <http://glaros.dtc.umn.edu/gkhome/views/cluto>
- [32] http://ddm.cs.sfu.ca/dmssoft/Clustering/fihc_index.html

A Structural Algorithm for Complex Natural Languages Parse Generation

Enikuomihin, A. O.

Dept. of Computer Science,
Lagos State University,
Lagos, Nigeria

Rahman, M. A.

Dept. of Computer Science,
Lagos State University,
Lagos, Nigeria

Ameen A. O.

Dept. of Computer Science,
University of Ilorin,
Ilorin, Nigeria

Abstract— In artificial intelligence, the study of how humans understand natural languages is cognitive based and such science is essential in the development of a modern day embedded robotic systems. Such systems should have the capability to process natural languages and generate meaningful output. As against machines, humans have the ability to understand a natural language sentence due to the in-born facility inherent in them and such is used to process it. Robotics requires appropriate PARSE systems to be developed in order to handle language based operations. In this paper, we present a new method of generating parse structures on complex natural language using algorithmic processes. The paper explores the process of generating meaning via parse structure and improves on the existing results using well established parsing scheme. The resulting algorithm was implemented in Java and a natural language interface for parse generation is presented. The result further shows that tokenizing sentences into their respective units affects the parse structure in the first instance and semantic representation in the larger scale. Efforts were made to limit the rules used in the generation of the grammar since natural language rules are almost infinite depending on the language set.

Keywords—Natural Language; Syntax; Parsing; Meaning Representation

I. INTRODUCTION

Natural languages [1,2] are used in our everyday communication. They are commonly referred to as human languages. Humans are able to process natural languages easily because it is their basic language of communication since birth. The human system has the capability to learn and use such languages and improve on it over time. Recently, there has been renewed effort in developing systems that emulate human due to increased service rendering requirements including several efforts in [3].

A major factor to be considered in such system is that, they must have the capability to act like human. The need includes the ability to process human speech, (Speech Recognition, an area that has had great research attention) in a way that it can receive speech signals, converts it into text, processes the text and provides a response to the user. The user is obviously more comfortable using his or her natural language to present such speech. However, natural language is a very complex language due to the high level of ambiguity existing in it. This is one of many factors, others include the availability of large set of words in several unstructured order. Thus, to make a functional system, these issues must be clearly addressed. Processing natural languages involves the concept of

interpretation and generalization [4]. In Interpretation, the process involves understanding the natural languages while generalization is a next to interpretation handles the representation of the interpreted language. The process of representation will only be functional if the language of presentation is understood by the system. In understanding such languages, several stages of operations are involved. They include morphological analysis (how words are built from morphemes, a morpheme is the smallest meaningful unit in the grammar of a language), chunking (breaking down sentences into words known as tokens, a token is a symbol regarded as an individual concrete mark, not as a class of identical symbols, *it* is a popular alternative to full parsing), syntactic analysis (analyzing the sentences to determine if they are syntactically correct) and semantic analysis (looking into the meanings). One can consider the importance related to the representation in morphemes as stated above, using the following example, Consider the word "Unladylike" This word consists of three morphemes and four syllables. The Morpheme breaks into: un- 'not', lady '(well behaved) female adult human', like 'having the characteristics of'. None of these morphemes can be broken up any more without losing all the meaning the word is trying to convey. *Lady* cannot be broken up into "la" and "dy," even though "la" and "dy" are separate syllables. Note that each syllable has no meaning on its own.

Thus, our representational framework can be determined by the morphology existing in any given word. This process can be manually interpreted but as the set of terms to be considered increases, the manual interpretation has greater tendencies to fail. Thus an appropriate scheme is to introduce algorithms that can handle such complex representation of natural language in a way that appropriate parse needed for machine translation of natural language can be generated. Such algorithm will generate syntactic structures for natural language sentences by producing a syntactic analysis of any given sentence correctly whose output is the syntactic structure represented by a syntax tree. The syntax tree shows how words build up to form correct sentences. Children learn language by discovering patterns and templates. We learn how to express plural or singular and how to match those forms in verbs and nouns. We learn how to put together a sentence, a question, or a command. Natural Language Processing assumes that if we can define those patterns and describe them to a computer then we can teach a machine something of how we speak and understand each other. Much of this work is

based on research in linguistics and cognitive science. A sentence then has to be parsed for syntactic analysis. Thus, the need for the appropriate algorithm that can handle the parsing of complex natural language sentences.

In this paper, the discussions above were considered and we present an algorithm using the UML (unified modelling language) to parse natural language sentences. This model depicts various aspects of the algorithm which includes:

- An association diagram that shows the major components in our system and how they associate with one another.
- A dependency diagram that shows how each component depends on the other in order to be able to carry out its own work.
- A class diagram that depicts each component in terms of classes showing its members and methods.
- A pseudo code to show the major steps involved in each component.

A scalable interface showing the implementation of the algorithm was developed and tested to determine the level of correctness of the output.

II. BACKGROUND AND EARLIER WORK

Natural Language Processing (NLP) is the capacity of a computer to "understand" natural language text at a level that allows meaningful interaction between the computer and a person working in a particular application domain [5]. The natural language processing concepts involves the use of many tools which are essentials of developing a man-like machine. This tools includes some programming languages such as Prolog, Ale, Lisp/Scheme, and C/C++. The tools are formulated appropriately within some defined concepts using Statistical Methods - Markov models, probabilistic grammars, text-based analysis and also Abstract Models such as Context-free grammars (BNF), Attribute grammars, Predicate calculus and other semantic models, Knowledge-based and ontological methods [6].

In this paper, we focus on the generation of appropriate parse structure for any natural language sentence. This step is considered as a major step in the natural language research domain. Syntactic analysis majorly involve the structure of a given natural language sentence presented by retrieving it in a structural manner with the rules of forming the sentences, and the words that make up those sentences. This is also includes the grammar and lexicon. It involves morphology that is the formation of words from stems, prefixes, and suffixes. Syntactic analysis shows the legal combination of words in a sentence. Generating syntactic structure involves the use of grammar, that is, the rules for forming correct sentences. Natural languages have to be parsed to obtain the syntactic information encoded in them. But natural language is ambiguous which necessitated the intervention of the use of an algorithm. This structure will present the analysis of a sentence by showing how words combine correctly to form valid phrases and how this phrase legally build up sentences. A parsing algorithm operates based on some set of rules known as grammar that tells the parser valid phrases and words in a sentence. The ambiguity of natural languages leads

to a complex analysis of it, so it is more suitable to use a parsing algorithm in situations where the natural language sentence is complex. In such cases, a sentence generates multiple parse trees for the same natural language. As natural language understanding improves, computers will be able to learn from the information online and apply what they learned in the real world. Combined with natural language generation, computers will become more and more capable of receiving and giving instructions. Ambiguities are a problem because they can lead to two or more different interpretations of the same word. They are often part of the subconscious knowledge, so requirements writers will not necessarily recognize these potential sources of misunderstandings. There are different kinds of ambiguity. *Lexical ambiguity* refers to single expressions that may be reasonably interpreted in more than one way.

The study of natural language processing also incorporates other fields such as linguistics and statistics. The knowledge of linguistics provides the grammars and vocabularies needed and the knowledge of statistics provide mathematical models that the algorithm for processing natural languages uses. Various algorithms had been developed in time past for natural language processing and more algorithms are currently under development to solve more of natural language processing problems. In 1950, Alan Turing [7] proposed "Turing Test" in his famous article "Computing Machinery Intelligence". Turing test is a test that is used to know the ability of computer systems to impersonate humans. In 1954, the George Town experiment came up which involved a full automatic translation of more than sixty Russian sentences into English. In addition, in 1960s, some successful natural language processing systems were developed. These systems majorly include: ELIZA, [8,9]. SHRDLU [10]., a system that works in restricted blocks with restricted vocabularies that can be used to control robotic arms. Many programmers began to write conceptual ontologies in 1970, they are structured to appropriate real-world information into computer system. Up to the 1980s, most natural language processing systems were based on complex sets of hand-written rules.

Furthermore, in 1980s [4], the first "statistical machine translation systems" was developed. At this time, there was a great revolution in natural language processing with the introduction of "machine learning algorithms" for language processing. This is as a result of the increase in computational power resulting from the application of Moore's law [11]. Natural Language Processing (NLP) is an area of research and application that explores how computers can be used to understand and manipulate natural language text or speech to do useful things. NLP researchers aim to gather knowledge on how human beings understand and use language so that appropriate tools and techniques can be developed to make computer systems understand and manipulate natural languages to perform the desired tasks. Statistical methods are used in NLP for a number of purposes, e.g., for word sense disambiguation, for generating grammars and parsing. At the core of any NLP task there is the important issue of natural language understanding. The process of building computer programs that understand natural language involves three major problems: the first one relates to the thought process,

the second one to the representation and meaning of the linguistic input, and the third one to the world knowledge. Thus, an NLP system may begin at the word level – to determine the morphological structure, nature (such as part-of-speech, meaning etc.) of the word – and then may move on to the sentence level – to determine the word order, grammar, meaning of the entire sentence, etc.— and then to the context and the overall environment or domain. A given word or a sentence may have a specific meaning or connotation in a given context or domain, and may be related to many other words and/or sentences in the given context. Automatic text processing systems generally take some form of text input and transform it into an output of some different form. The central task for natural language text processing systems is the translation of potentially ambiguous natural language queries and texts into unambiguous internal representations in which matching and retrieval can take place. Masaru Tornita (1984) [3],” proposed that “When a parser encounters an ambiguous input sentence, it can deal with that sentence in one of two ways. One way is to produce a single parse which is the most preferable. Such parsers are called one-path parsers. On the other hand, parsers that produce all possible parses of the ambiguous sentence are called all-paths parsers”. A suitable parser for parsing natural languages is one that generates several parses or parses trees for a natural language sentence because a sentence can have a syntax and different meaning. NLP systems, in their fullest implementation, make elegant use of this kind of structural information. They may store a representation of either of these sentences, which retains the fact that Chelsea won Benfica or vice versa. They may also store, not only the fact that a word is a verb, but the kind of verb it is.

One-path parsers are, naturally, much faster than all-paths parsers because they look for only one parse. There are, however, situations where all-paths parsers should be used. MLR is an extension of LR. The LR parsing algorithm, however, has seldom been used for natural language processing, because the LR parsing algorithm is applicable only to a small subset of context-free grammars, and usually it cannot apply to natural languages. Though the efficiency of a LR parsing algorithm is preserved, MLR parsing algorithm can apply to arbitrary context-free grammars, and is therefore applicable to natural languages. We cannot directly adopt the LR parsing technique for natural languages because not all context-free phrase structure grammars (CFPSG's) can have an LR parsing table. Only a small subset of CFPSG's called LR grammar can have such an LR parsing table. Every ambiguous grammar is not LR, and since natural language grammars are almost always ambiguous, they are not LR therefore we cannot have an LR parsing table for natural language grammars. Liddy (1998) and Feldman (1999) [5] suggest that in order to understand natural languages, it is important to be able to distinguish among the following seven interdependent levels, that people use to extract meaning from text or spoken languages:

- Phonetic or phonological level that deals with pronunciation

- Morphological level that deals with the smallest parts of words, that carry a meaning, and suffixes and prefixes
- Lexical level that deals with lexical meaning of words and parts of speech analyses
- Syntactic level that deals with grammar and structure of sentences
- Semantic level that deals with the meaning of words and sentences
- Discourse level that deals with the structure of different kinds of text using document structures and
- Pragmatic level that deals with the knowledge that comes from the outside world, i.e., from outside the contents of the document.

The above justification seems sufficient for the development of an appropriate model for implementing an algorithm for parse generation of natural language sentences.

III. MODEL

We present a model to show the major components in our algorithm and how they interact in order to generate effective parse results for complex natural language sentences. To parse a natural language sentence (syntactic analysis), the most important things to consider are:

- The parser (the algorithm)
- Set of grammars for the language (the rules of correct syntax)

Based on our model, the major components used are: Tokenizer - which breaks down a given sentence into words usually known as tokens, Part of speech tagger - represented as those whose function is to tag each word to their respective part of speech. Parse- which analyses the sentence to check if it conforms to some sets of grammar (English grammar) for the language of the input sentence and finally the ParseTree, The parse tree represents the graphical nature of the natural language. The UML Association diagram is necessary to visualize the association between the classes. The UML Class diagram is used to visually describe the problem domain in terms of types of object (classes) related to each other in different ways. There are three primary inter-object relationships: *association*, *aggregation*, and *composition*. Using the **right** relationship line is important for placing implicit restrictions on the visibility and propagation of changes to the related classes.

Following from above, the formulated PSEUDOCODE is then presented as:

```
Class Tokenizer
//variable declaration
String sentence
Int i,tokenLength // i is a counter

Sentence=get sentence from user
Break sentence to tokens//break sentence to words
tokenLength=get number of words in sentence
```

```
//create two arrays to store the words and their part of  
speech  
New tokenArray(tokenLength)  
New posArray(tokenLength)  
tokenArray=tokens//store tokens in array  
  
//tag words to their part of speech  
For(i=0; i<tokenLength; i++)  
{ posArray[i]=posTagger.tagWord(tokenArray[i])  
}  
  
//parse sentence and get parse tree  
parseTree=parser.parseSentence(tokenArray,posArray)  
  
display parseTree  
  
Class POSTagger  
//Variable declaration  
String pos  
  
//create an array of words and their part of speech  
New dictionary(l)//where l is number of words in  
dictionary  
New partOfSpeech(l)  
  
Function tagWord(String word)  
{  
  For(i=0; i<l; i++)  
  {  
    If(dictionary[i]=word)  
    {  
      Pos=partOfSpeech[i]  
      Return pos  
    }  
  }  
}
```

Class parser

```
//variable declaration  
int number of words
```

```
function parseSentence(String[] words, String[] pos)  
{  
  numberOfWords=words.getNumberofWord  
  
  if(numberOfWords=3)  
  {  
    If(words follow grammer 1)  
      Draw parse tree 1  
    Else if(words follow grammer 2)  
      Draw parse tree 2  
    |  
    |  
    Else if(words follow grammer n)  
      Draw parse tree n  
  }  
}
```

```
Else if(numberOfWords=4)  
{  
  If(words follow grammer 1)  
    Draw parse tree 1  
  Else if(words follow grammer 2)  
    Draw parse tree 2  
  |  
  |  
  Else if(words follow grammer n)  
    Draw parse tree n  
}  
|  
|  
Else if(numberOfWords=n)  
{  
  If(words follow grammer n)  
    Draw parse tree n  
}  
}
```

IV. IMPLEMENTATION AND RESULT

The model is implemented as a stand-alone application using the java programming language. The application was designed such that only an input sentence of a maximally defined number of terms can be accommodated. When a user enters a sentence within the specified limit, the system verifies the correctness of the sentence and then outputs a graphical display of the parse tree for the sentence. The resulting output is shown in figure 1.

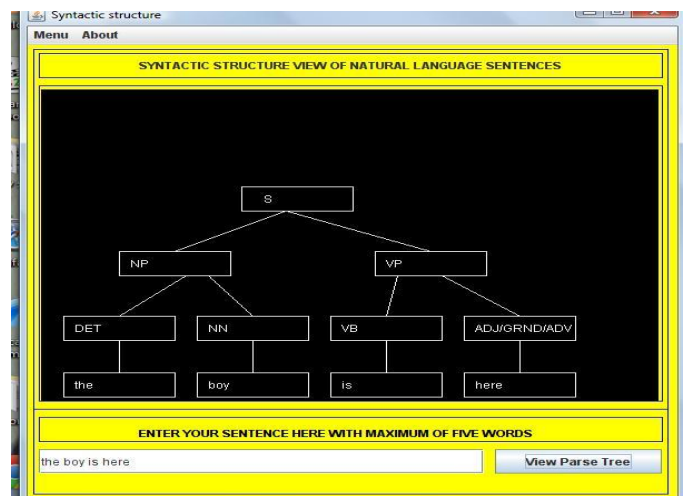


Fig.1. Simple java based parser

Figure 1.6 shows the parsing of a natural language sentence based on codes developed in java. The generation is extended by implementing an internal scheme based on a dictionary such that when a word is not present in the application's dictionary, the structure of the surrounding words can be used to tell the possible part of speech the word will belong to. For example, the word "here" shown in figure 1.6 is not in the application's dictionary yet it was tagged as either adjective or gerund or adverb, this is because only these categories of words can occupy that position once the preceding words follows the order "determinant noun verb".

Figure 2 shows another generation of the parser interface where the rule implements the sentence format “noun verb gerund”.

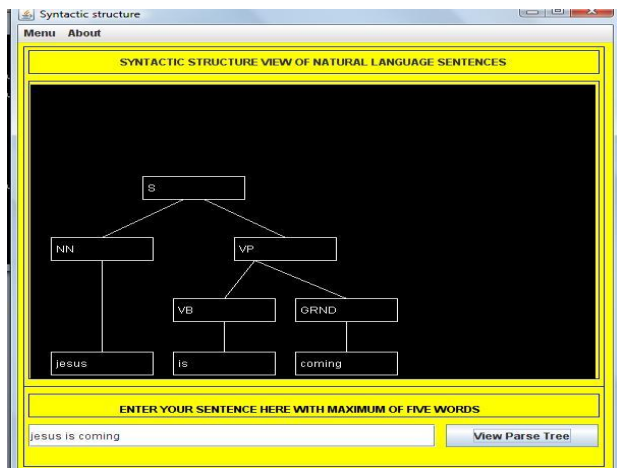


Fig.2. Noun Gerund parse

If a user enters an invalid sentence or a sentence whose grammar is not present in our list of grammars, the system will output the following:

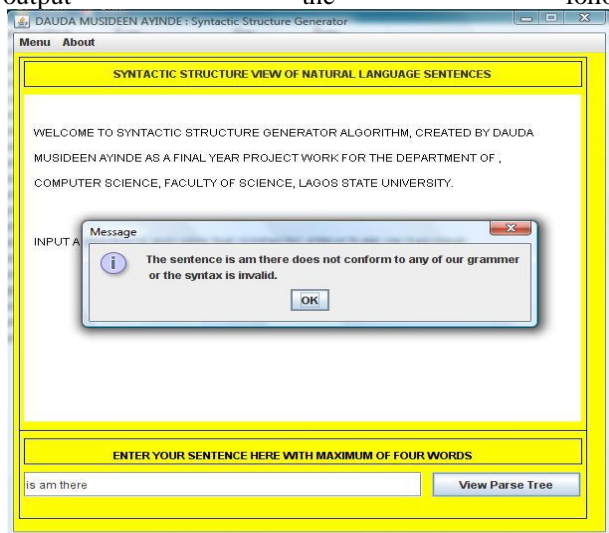


Fig.3. Parsing non defined sentence grammar

V. CONCLUSION

The algorithm presented in this paper can be extended based on the required complexity of the system. The defined process for tokenization and the use of a natural language interface in solving parse generation has shown the effectiveness of a well posted algorithm in solving the natural language parse generation problem. An extension of this work is in its ability to generate one parses tree even when the observed ambiguity is high. Parsing natural language is a complex task, an efficient algorithm for parsing natural language has been shown in this work as a necessary tool even within the inherent complexity observed.

An extended form of the LR parsing algorithm though not discussed in this paper will also be an efficient algorithm as it will generate multiple parses for natural language sentences. Such is similar to multiple application of the algorithm presented in this paper and can be called the MLR parsing algorithm.

REFERENCES

- [1] J. S. Amberg, Introduction: what is language”, The American journal of English, history, structure and usage, page 1-10. (1987)
- [2] J. Lyons, Natural language and Universal Grammar. New York: Cambridge University Press. pp. 68–70. ISBN 978-0521246965. (1991).
- [3] P.Pantel, T. Lin, and M.I Gamon, Mining Entity Types from Query Logs via User Intent Modeling, Association for Computational Linguistics, July 2012
- [4] G,G. Chowdhury, Natural language processing”, The journal of department of computer and information science, university of strathclyde, page1-22. ,(1991)”
- [5] F. S. Liddy, Natural language processing”, The journal of department of information science, Page 1-20. (1999)”
- [6] T. Masaru,”An Efficient All-paths Parsing Algorithm for Natural Languages”, The journal of Computer Science Department, Carnegie-Mellon University, Pittsburgh, PA 15213, 25, page 1-36. (1984),
- [7] J. Agar, The government machine: a revolutionary history of the computer. Cambridge, Massachusetts: MIT Press. ISBN 978-0-262-01202-7. (2003).
- [8] P. McCorduck, Machines Who Think (2nd ed.), Natick, MA: A. K. Peters, Ltd., ISBN 1-56881-205-1(2004),
- [9] J. Weizenbaum, "ELIZA—A Computer Program For the Study of Natural Language Communication Between Man And Machine", Communications of the ACM 9 (1): 36–45, (January 1966) doi:10.1145/365153.365168
- [10] T. Winograd, "Procedures as a Representation for Data in a Computer Program for Understanding Natural Language", MIT AI Technical Report 235, February 1971
- [11] La Fontaine, B., "Lasers and Moore's Law", SPIE Professional, Oct. 2010, p. 20; <http://spie.org/x42152.xm>

Category Decomposition Method Based on Matched Filter for Un-Mixing of Mixed Pixels Acquired with Spaceborne Based Hyperspectral Radiometers

Kohei Arai¹

Graduate School of Science and Engineering
Saga University
Saga City, Japan

Abstract—Category decomposition method based on matched filter for un-mixing of mixed pixels: mixels which are acquired with spaceborne based hyperspectral radiometers is proposed. Through simulation studies with simulated mixed pixels which are created with spectral reflectance data derived from USGS spectral library as well as actual airborne based hyperspectral radiometer imagery data, it is found that the proposed method works well with acceptable decomposition accuracy.

Keywords—category decomposition; hyperspectral radiometer; mixed pixel; un-mixing; matched filter;

I. INTRODUCTION

Hyperspectrometer in the visible to near infrared wavelength regions are developed and used for general purposes of earth observation missions such as Agriculture, Mineralogy, Surveillance, Physics, Chemical Imaging, Environment, in particular, for mineral resources explorations and agricultural monitoring [1]-[15]. Hyperspectrometer allows estimate atmospheric constituents by using absorption characteristics of the atmospheric constituents because spectral bandwidth of the hyperspectrometer is quite narrow like an atmospheric sounder onboard earth observation satellites [16].

Remote sensing is the practice of deriving information about the earth land and water surfaces using images acquired from an overhead perspective, using electromagnetic radiation in one or more regions of the electromagnetic spectrum, reflected or emitted from the earth surface. In particular, hyperspectral sensor (for instance, T.Lillesand et al., 1994 [17]) that covers from visible to short wave infrared wavelength region has many continuation spectrum bands (G.Vane, et al., 1993 [18], J.B.Adams, et al., 1986 [19]). Not only one single ground cover target but also two or more targets (category) are contained in the instantaneous field of view of the sensor. It is generally called as mixed pixel (Mixel) (K.Arai, 1991 [20]).

Un-mixing is the technique of presuming the category kind that constitutes the mixel, and its mixing ratio (N.Keshava, et al., 2002 [21]). There are two models for the Mixel, a linear and a nonlinear model (S.Liangprocapart et al., 1998 [22], K. Arai et al., 1992 [23]). The spectrum feature of the pixel that consists of one category is called a pure pixel (also it is called an end-member). Un-mixing is performed based on the linear or the nonlinear models (C.C.Borel et al., 1994 [24]). It is as

which a linear model disregards the interaction between end-members, and a nonlinear model considers the multiple reflection and scattering which depends on the geometric relations among the sun, a ground cover target, and a sensor (K.Arai et al., 2002 [25]). There are linear model based un-mixing methods that based on (1) a maximum likelihood method (J.J.Settle, 1996 [26], M.Matsumoto, et al., 1991 [27]), (2) a least square method with constraints (C.I.Chang, 2003 [28], K.Arai et al., 1995 [29]), (3) a spectrum feature matching (A.S.Mazer, 1988 [30]), (4) a partial space projective technique (C.Chang, et al., 1998 [31], K.Arai et al., 2002 [32]), (5) a rectangular partial space method (J.C.Harsanyi et al., 1994 [33]), etc. The least square method with a constraint presumes a mixing ratio vector based on an end-member's spectrum feature vector by the generalized inverse matrix or the least-squares method which makes convex combination conditions a constraint. The spectrum feature matching searches and selects two or more spectrum features out of a plenty of spectrum features in a spectral database. It is the spectral feature matching method in consideration of those mixing ratios, and the spectrum feature of the Mixel in concern.

Further studies are required for appropriate end-member determination, improvement of accuracy, reduction of processing time, etc. for un-mixing methods. This paper mainly focuses on improvement of un-mixing accuracy, estimation accuracy of mixing ratio. The methods based on a partial space projective technique (C.Chang, et al., 1998 [31], K.Arai et al., 2002 [34]), and a rectangular partial space method (J.C.Harsanyi et al., 1994 [33]) may make the spectrum feature of a desirable category conspicuous, they map and combine the spectrum feature of the Mixel with subspace which is made to intersect perpendicularly with the other spectrum feature. It also can perform dimensionality reduction. Moreover, the un-mixing technique based on an orthogonal subspace method has comparatively good un-mixing accuracy, and is used abundantly. Furthermore, it is equivalent to the un-mixing based on a maximum likelihood method, and this is also equivalent to the method of least square. An independent component analysis method (ICA) decomposes given Mixel into a highly independent component in the spectrum feature space in alignment (L.Parra, et al., 2000 [35]). Namely, it is determined that a mixing ratio can express the spectrum feature of Mixel by taking into

consideration an end-member's spectrum feature and its variation. The statistic model about a component is considered and presumption of a statistic model and the ratio of each component are presumed by unsupervised learning. Therefore, it is the method of using the independent component analysis with constraints. Moreover, since the orthogonal subspace method becomes ideally independent in the spectrum feature after projection, it is also equivalent to ICA. From the above reason, this paper shall examine the un-mixing based on the orthogonal subspace method. The subspace method with learning process is already proposed as the image classification technique (Oja Erkki, 1983 [36]). The basic idea for that is the following. If the axis of coordinates of the subspace in the orthogonal subspace method is rotated, then classification accuracy will be improved to find an appropriate angle for a high classification performance, and then the spectrum feature of a pixel is mapped and classified into the orthogonal subspace of this optimal axis-of-coordinates angle.

The following section describes the proposed category decomposition with matched filter method followed by some experiments. Then conclusion is described together with some discussions.

II. PROPOSED METHOD

A. Conventional Un-Mixing Method

Hyper-spectral data represented by vector Y can be expressed as follows:

$$Y = \begin{bmatrix} y_1 \\ y_2 \\ \vdots \\ y_n \end{bmatrix} = \begin{bmatrix} m_1 \\ m_2 \\ \vdots \\ m_m \end{bmatrix} \begin{bmatrix} z_{11} & z_{12} & \dots & z_{1n} \\ z_{21} & \dots & \dots & z_{2n} \\ \vdots & \vdots & \vdots & \vdots \\ z_{m1} & \dots & \dots & z_{mn} \end{bmatrix} = mZ \quad (1)$$

where m denotes mixing ratio vector of each ground cover target no.1 to m , while Z denotes the spectral characteristics of the ground cover target such that if the inverse matrix of Z is existing then the mixing ratio vector can be estimated as follows,

$$m = YZ^{-1} \quad (2)$$

It is, however, not always true that the inverse matrix exists. In order to solve this problem, regularization techniques with constraints, a prior information, etc., have been proposed. One of those is the generalized inverse matrix, or so called "Moore-Penrose" inverse matrix that is derived from Singular Value Decomposition (SVD). If Y is expressed with SVD as follows:

$$X = u^t Y v \quad (3)$$

where u and v are orthogonal vectors, then the Moore-Penrose generalized inverse matrix Y^+ is expressed by the following equation:

$$Y^+ = v^t Y u \quad (4)$$

Therefore, if u and v can be calculated then the generalized inverse matrix can also be calculated. This method is referred to the conventional SVD based method hereafter.

However, the number of spectral bands, n is more than 200 for hyperspectral imaging sensors, so that a time-consuming matrix calculation is required. In order to overcome this situation, the subspace method (SSM) is introduced.

If an n -dimensional observation data Y is mapped into an n -dimensional feature space of X , in general, then the square of the norm of Y is mapped to that of X as follows:

$$\|p_i X\|^2 = X^t p_i p_i X = X^t p_i X \quad (5)$$

where p_i denotes the orthogonal mapping matrix so that $p_i X$ can be mapped from X to the subspace. Thus the mixing ratio of ground cover target, j , can be estimated with the following equation:

$$\sqrt{X^t p_i X} = \sum_{j=1}^n m_j \sqrt{X_j^t p_j X_j} \quad (6)$$

If the dominant dimensions are selected from the subspace, then SSM can also reduce the dimensionality of the feature space. It may be said that the first three dimensions would cover more than 90% of the whole information, following the subspace method of conversion of orthogonal mapping. This can reduce time-consuming computations for the matrix calculations. By using the probability density function of the mapped observation vector, un-mixing can be done without any time-consuming calculation. The subspace method is closely related to the well known PCA (Principal Component Analysis) analysis which allows convert feature space coordinate into the principal coordinate system using rotation of coordinate system. In this case the original feature space, X , is mapped into the subspace, u . On the other hand, the proposed subspace method adjust the rotation angle to concentrate the information content, the rotation angle is adjusted through an iterative learning process. The most appropriate rotation angle is determined by category by category. Generally, PCA determines an appropriate rotation angle in the sense of average means. On the other hand, the proposed method takes separability between all the combinations of categories

By using the definition of length which is expressed with the equation (5),

$$\begin{aligned} (p_1 X_1)^t p_1 X &= (p_1 X_1)^t (m_1 p_1 X_1 + \dots + m_m p_1 X_m) \\ \dots \\ (p_m X_m)^t p_m X &= (p_m X_m)^t (m_1 p_m X_1 + \dots + m_m p_m X_m) \end{aligned} \quad (7)$$

then,

$$\begin{aligned} \|p_1 X\| \cos \alpha^1 &= m_1 \|p_1 X_1\| \cos \alpha_{1,1}^1 + \dots + m_m \|p_1 X_m\| \cos \alpha_{1,m}^1 \\ \dots \\ \|p_m X\| \cos \alpha^m &= m_m \|p_m X_1\| \cos \alpha_{m,1}^m + \dots + m_m \|p_m X_m\| \cos \alpha_{m,m}^m \end{aligned} \quad (8)$$

where X_i denotes feature vector of category i while X denotes unknown vector which has to be estimated its mixing ratio. Feature vector X_i of category i can be mapped onto subspace $p_i X_i$. The angle between its coordinate, $p_i X_i$ and orthogonal transformation of $p_k X_k$ is $\alpha_{i,k}^i$. Thus mixing ratio, m_i can be estimated.

B. Matched Filter

Hyper-spectral radiometer has more than one hundred spectral channels. Therefore, it requires, in general, a huge computer resources for category decomposition, or un-mixing which is composed with huge element size of matrix calculus. On the other hand, there is a matched filter which allows extract specific object which has a specific spectral feature from mixed spectral characteristics of object. In this section, background theory of matched filter is introduced. If the specific spectral feature is known a prior basis, then the matched filter can be used for category decomposition. In other word, if there is intensive ground cover material, mixing ratio of the material in the mixed pixel in concern can be estimated with the proposed matched filter.

In the time domain, output signal $y[n]$ is expressed as equation (1),

$$y[n] = \sum_{k=-\infty}^{\infty} h[n-k]x[k]. \quad (1)$$

where x and h denotes input signal and impulse response function of the system. Input signal consists of signal and noise as shown in equation (2).

$$x = s + v. \quad (2)$$

where v denotes noise and noise power is expressed as equation (3).

$$R_v = E\{vv^H\} \quad (3)$$

where H denotes complex conjugate. Then output can be represented as equation (4)

$$y = \sum_{k=-\infty}^{\infty} h^*[k]x[k] = h^H x = h^H s + h^H v = y_s + y_v. \quad (4)$$

The signal-to-noise ratio SNR is expressed as equation (5)

$$SNR = \frac{|y_s|^2}{E\{|y_v|^2\}}. \quad (5)$$

Signal component can be expressed as equation (6).

$$|y_s|^2 = y_s^H y_s = h^H s s^H h. \quad (6)$$

Nose component, on the other hand, is expressed with equation (7).

$$E\{|y_v|^2\} = E\{y_v^H y_v\} = E\{h^H v v^H h\} = h^H R_v h. \quad (7)$$

Thus signal-to-noise ratio becomes the following equation,

$$SNR = \frac{h^H s s^H h}{h^H R_v h}. \quad (8)$$

Assuming the following equation,

$$h^H R_v h = 1 \quad (9)$$

Then cost function can be expressed with the following equation using Lagrange multiplier, λ ,

$$\mathcal{L} = h^H s s^H h + \lambda(1 - h^H R_v h) \quad (10)$$

From equation (10), the following equations are derived,

$$\nabla_{h^*} \mathcal{L} = s s^H h - \lambda R_v h = 0 \quad (11)$$

$$(s s^H) h = \lambda R_v h \quad (12)$$

This is well known as a generalized eigen value problem.

$$h^H (s s^H) h = \lambda h^H R_v h. \quad (13)$$

Since $s s^H$ is of unit rank, it has only one nonzero eigen value. Therefore, it can be shown that this eigen value equals

$$\lambda_{\max} = s^H R_v^{-1} s, \quad (14)$$

which is yielding the following optimal matched filter

$$h = \frac{1}{\sqrt{s^H R_v^{-1} s}} R_v^{-1} s. \quad (15)$$

C. Un-Mixing Method

The mixed pixel: Mixel in concern is assumed to be composed with several ground cover materials. Figure 1 shows mathematical model of the Mixel. Namely, the Mixel is composed with more than two spectral characteristics are combine together depending on their mixing ratios. Using spectral characteristic of ground cover material in concern, it is possible to extract same spectral characteristic from the combined spectral characteristics using matched filter.

Two types of noises, colored and white noise are added to the pure pixel of spectral characteristics.

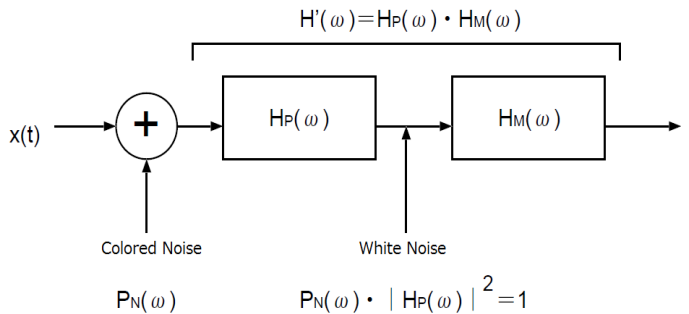
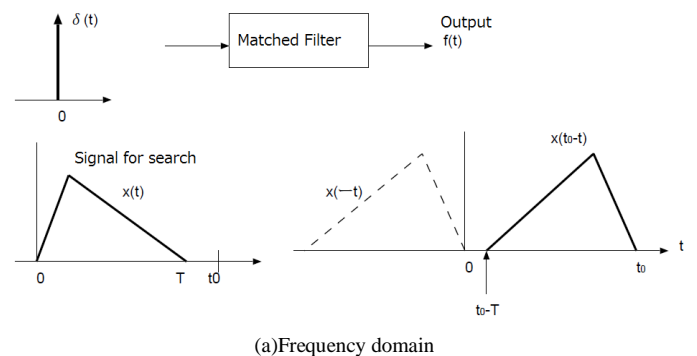


Fig. 1. Spectral characteristic of Mixel model

If the proposed matched filter is applied to the Mixel data with a assumed spectral feature of pure pixel in concern, then mixing ratio can be estimated as shown in Figure 2.



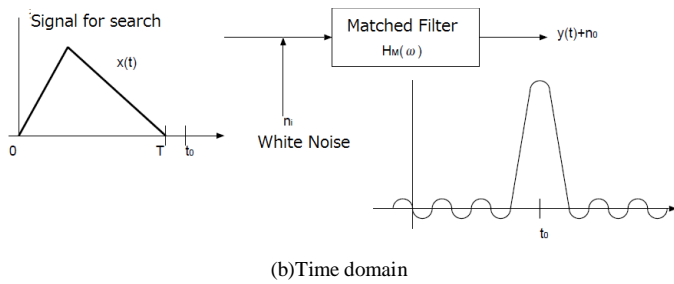


Fig. 2. Mixing ratio estimation from the Mixels by using the specific spectral feature of the assumed ground cover materials in concern

Matched filter can be applied in frequency and time domains. Using Fourier transformation, the proposed un-mixing method based on matched filter can be expressed in both time and frequency domains as shown in Figure 3.

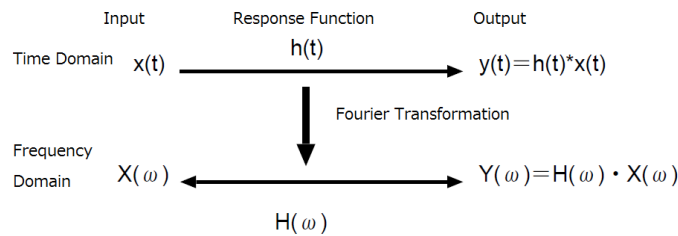


Fig. 3. Proposed un-mixing method based on matched filter which is expressed in both time and frequency domains

III. EXPERIMENTS AND SIMULATIONS

A. Simulation Method

From the Unites State of America Geological Survey: USGS web site so called “Spectral Library”, spectral characteristics (surface reflectance) can be retrieved for huge number of ground cover materials. In the library, two ground cover materials which show a good correlation between both spectral characteristics are chosen. Also two ground cover materials which show a poor correlation between both are selected. Moreover, ground cover materials which show a middle level of correlation are used. These are shown in Figure 4. 437 spectral channels ranged from 500 nm to 2500 nm of wavelength region of spectral characteristics are used.

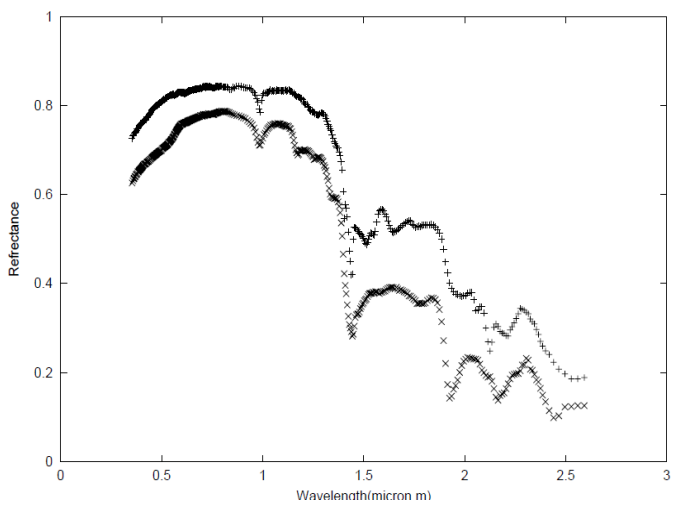
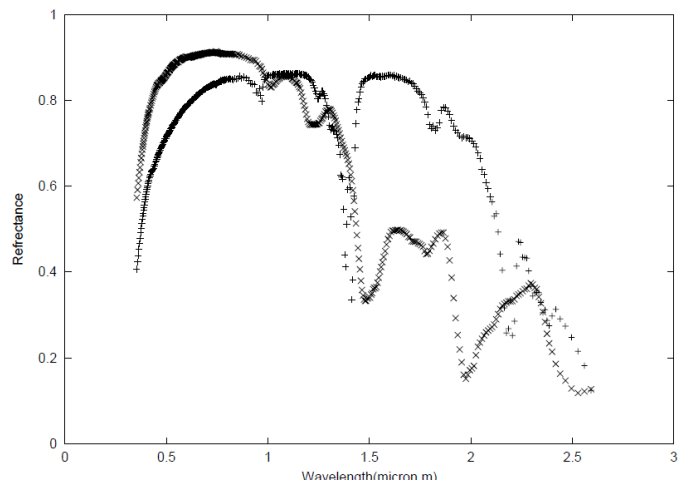
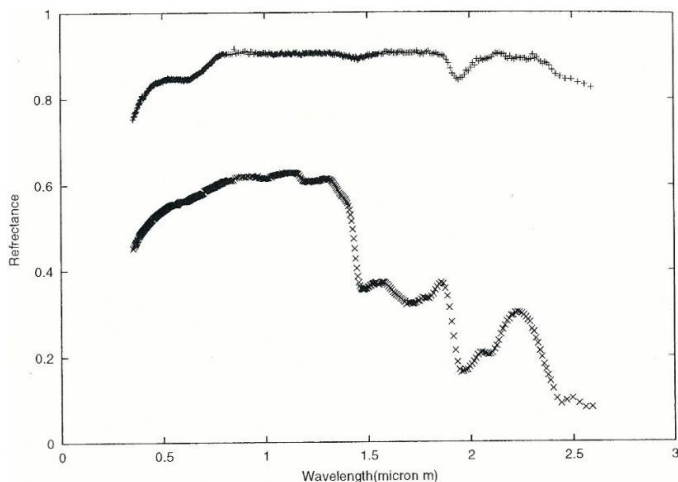


Fig. 4. Examples of the selected two ground cover materials of spectral characteristics which show a good a middle level and a poor correlation between both spectral characteristics

Using these spectral characteristics, un-mixing by means of the proposed matched filter based un-mixing method is attempted with changing mixing ratio as well as additive noises.

Root Mean Square Error: RMSE between designated and estimated mixing ratios is evaluated. The RMSE is evaluated for both the conventional SVD based method and the proposed method.

B. Simulation Results

Evaluated RMSE for both the conventional and the proposed methods are shown in Figure 5 as function of cross correlation between spectral characteristics extracted from the USGS spectral library. In this case, Mixels are created with two ground cover materials.

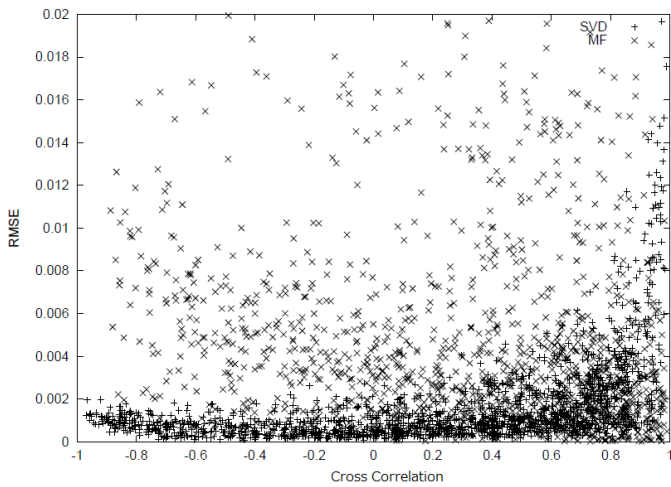


Fig. 5. Evaluated RMSE for both the conventional and the proposed methods as function of cross correlation between spectral characteristics extracted from the USGS spectral library

As shown in Figure 5, it is clear that RMSE for the proposed method is always smaller than that of the conventional method.

RMSE is also depending on the number of material of the Mixels used for simulation studies. Figure 6 shows RMSE as function of the number of ground cover materials of which the Mixels used are composed.

RMSE for the conventional un-mixing method varied greatly in comparison to that of the proposed method and is greater than that of the proposed method. It is concluded that there is a poor relation between RMSE and the number of ground cover materials of which the Mixels used for simulation. RMSE depends on the complexity of spectral characteristics of the ground cover materials and also depends on the correlation among the materials. RMSE is not function of the number of materials. Therefore, RMSE of the conventional method varied a lot comparing to the proposed method. The proposed method extracts the spectral characteristics from the mixed spectral characteristics so that RMSE is not varied too much.

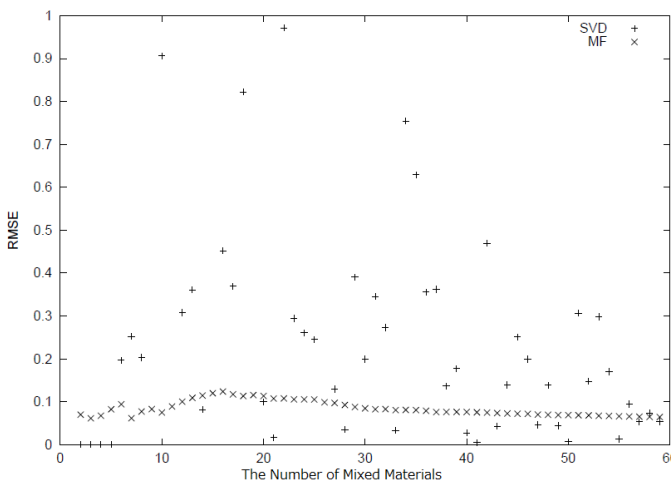


Fig. 6. Relation between the evaluated RMSE and the number of ground cover materials of mixels used for the simulation

Required computational time for un-mixing based on the proposed method, on the other hand, increases in accordance with the number of ground cover materials with which the Mixels used for simulation are composed as shown in Figure 7.

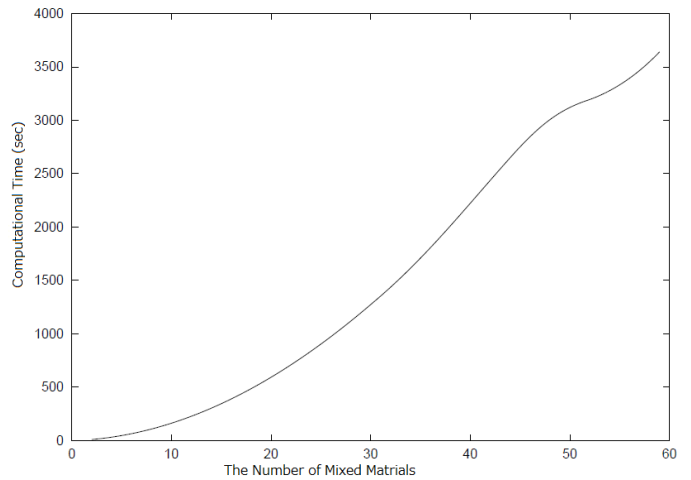


Fig. 7. Required computational time for un-mixing, on the other hand, increases in accordance with the number of ground cover materials with which the Mixels used for simulation are composed

Figure 8 shows the evaluated RMSE with the parameters of mixing ratio, signal to noise ratio and cross correlation for both the conventional and the proposed un-mixing methods. Two materials are mixed together when the Mixels used for simulation is created. There are three levels of correlation coefficients between two materials. Those are 0.0009, 0.5, and 0.99.

C. Experimental Results with Actual Airborne Based Hyper Spectrometer of AVIRIS

Actual hyper-spectral sensor data (AVIRIS) onboard aircraft is used for validation of the proposed method. Figure 9 shows the AVIRIS imagery data of Ivanpah playa in California, USA. The site is covered with silica Cray mostly.

From the image, silica Cray of pixel is extracted at the $x=54, y=479$, while asphalt pixel is also extracted from the pixel location at $x=81, y=405$, respectively. Meanwhile, four test pixels are extracted from the pixels in the Ivanpah playa. These pixels are situated on the Root # 15 of road so that the pixels are essentially covered with asphalt. Then the mixing ratio of silica Cray and Asphalt are estimated with the proposed Matched Filter: MF based method and the conventional Singular Value Decomposition: SVD based method. Estimated mixing ratios are shown in Table 1.

Although these test pixels seem to be covered with asphalt, mixing ratio of asphalt estimated with the conventional method is not so large in comparison to that with the proposed method. On the other hand, mixing ratio of silica Cray estimated with the conventional method is relatively large in comparison to that with the proposed method. From these facts, it is concluded that the proposed MF based un-mixing method is superior to the conventional SVD based method.

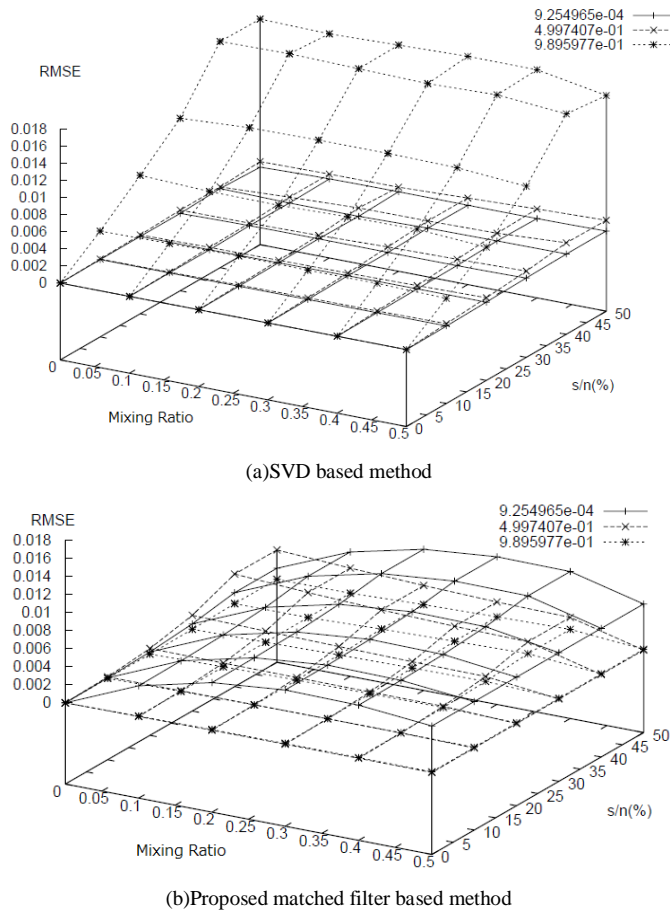


Fig. 8. Evaluated RMSE with the parameters of mixing ratio, signal to noise ratio and cross correlation for both the conventional and the proposed un-mixing methods

TABLE I. ESTIMATED MIXING RATIO OF SILICA CRAY AND ASPHALT ARE ESTIMATED WITH THE PROPOSED MATCHED FILTER: MF BASED METHOD AND THE CONVENTIONAL SINGULAR VALUE DECOMPOSITION: SVD BASED METHOD

| Pixel Location | Silica Cray | | Asphalt | |
|-------------------|-------------|------|---------|------|
| | SVD | MF | SVD | MF |
| Data #1 (96,402) | 0.32 | 0.21 | 0.54 | 0.76 |
| Data #2 (108,402) | 0.36 | 0.22 | 0.40 | 0.73 |
| Data #3 (128,402) | 0.33 | 0.21 | 0.51 | 0.75 |
| Data #4 (295,405) | 0.36 | 0.21 | 0.47 | 0.73 |

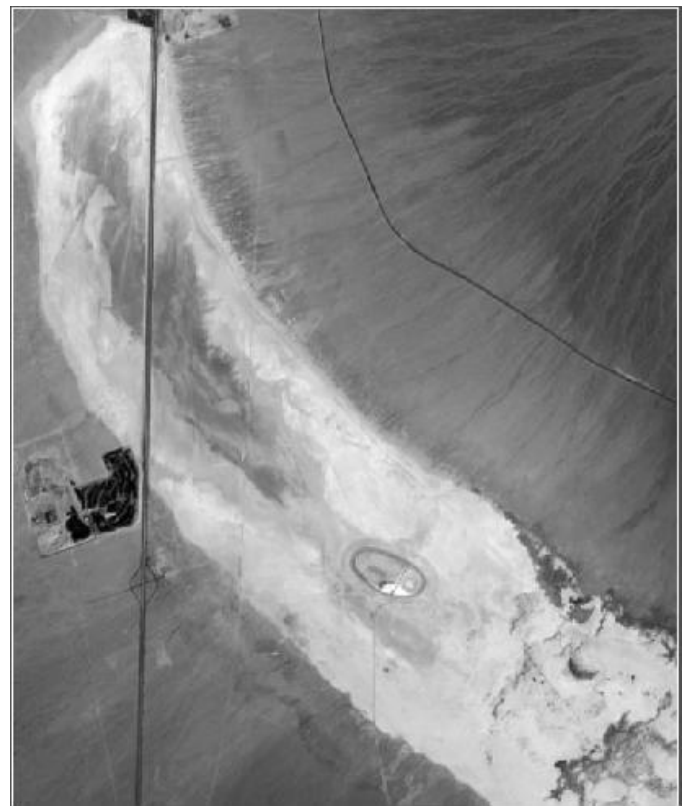


Fig. 9. AVIRIS imagery data of Ivanpah playa in California, USA.

IV. CONCLUSION

Category decomposition method based on matched filter for un-mixing of mixed pixels: Mixels which are acquired with spaceborne based hyper-spectral radiometers is proposed. Through simulation studies with simulated mixed pixels which are created with spectral reflectance data derived from USGS spectral library as well as actual airborne based hyper-spectral radiometer imagery data, it is found that the proposed method works well with acceptable decomposition accuracy

Through the experiment and simulation, it is found that the proposed Matched Filter based un-mixing method is superior to the conventional Singular Value Decomposition based un-mixing method for almost all cases. In particular, the estimated mixing ratio of asphalt which has a specific spectral feature derived from the proposed method shows better performance in comparison to that from the conventional method.

ACKNOWLEDGMENT

The author would like to thank Mr. Tadashi Yokota for his effort to conduct experiments.

REFERENCES

- [1] Lushalan Liao, Peter Jarecke, "Radiometric Performance Characterization of the Hyperion Imaging Spectrometer Instrument", Proc. Optical Science and Technology Symposium, Earth Observing Systems V, SPIE 1435, (2000)
- [2] Peter Jarecke, Karen Yokoyama, "Radiometric Calibration Transfer Chain from Primary Standards to the End-to-End Hyperion Sensor", Proc. Optical Science and Technology Symposium, Earth Observing Systems V, SPIE 1435, (2000).
- [3] Schurmer, J.H., Air Force Research Laboratories Technology Horizons, (2003)
- [4] Ellis, J., Searching for oil seeps and oil-impacted soil with hyperspectral imagery, Earth Observation Magazine (2001).
- [5] Smith, R.B. Introduction to hyperspectral imaging with TMIPS, MicroImages Tutorial Web site, (Accessed on July 14, 2012),
- [6] Lacar, F.M., et al., Use of hyperspectral imagery for mapping grape varieties in the Barossa Valley, South Australia, Geoscience and remote sensing symposium (IGARSS'01) - IEEE 2001 International, vol.6 2875-2877p. doi:10.1109/IGARSS.2001.978191, (2001)
- [7] Tilling, A.K., et al., Remote sensing to detect nitrogen and water stress in wheat, The Australian Society of Agronomy, (2006)
- [8] Fernández Pierna, J.A., et al., 'Combination of Support Vector Machines (SVM) and Near Infrared (NIR) imaging spectroscopy for the detection of meat and bone meat (MBM) in compound feeds' Journal of Chemometrics 18 341-349 (2004)
- [9] Holma, H., Thermische Hyperspektralbilddgebung im langwelligen Infrarot, Photonik, (2011),
- [10] Werff H. Knowledge based remote sensing of complex objects: recognition of spectral and spatial patterns resulting from natural hydrocarbon seepages, Utrecht University, ITC Dissertation 131, 138p. ISBN 90-6164-238-8 (2006),
- [11] Noomen, M.F. Hyperspectral reflectance of vegetation affected by underground hydrocarbon gas seepage, Enschede, ITC 151p. ISBN 978-90-8504-671-4 (2007),.
- [12] M. Chamberland, V. Farley, A. Vallières, L. Belhumeur, A. Villemaire, J. Giroux et J. Legault, "High-Performance Field-Portable Imaging Radiometric Spectrometer Technology For Hyperspectral imaging Applications," Proc. SPIE 5994, 59940N, September 2005.
- [13] Farley, V., Chamberland, M., Lagueux, P., et al., "Chemical agent detection and identification with a hyperspectral imaging infrared sensor," Proceedings of SPIE Vol. 6661, 66610L (2007).
- [14] Kevin C. Gross, Kenneth C Bradley and Glen P. Perram, "Remote identification and quantification of industrial smokestack effluents via imaging Fourier-transform spectroscopy," Environmental Sci Tech, 44, 9390-9397, 2010.
- [15] Tremblay, P., Savary, S., Rolland, M., et al., "Standoff gas identification and quantification from turbulent stack plumes with an imaging Fourier-transform spectrometer," Proceedings of SPIE Vol. 7673, 76730H (2010).
- [16] K.Arai, K. Yamaguchi, Atmospheric correction through estimation of atmospheric optical properties with hyperspectrometer data, Proceedings of the 46th General Assembly of Japan Society of Remote Sensing, 22, 2009.
- [17] Lillesand T. and R.Kiefer, Remote Sensing and Image Interpretation, 3rd ed., John Willey & Sons, Inc., 1994.
- [18] Vane G., R.Green, T.Chrien, H.Enmark, E.Hansen, and W.Porter, The airborne visible/infrared imaging spectrometer (AVIRIS), Remote Sensing of the Environment, 44, 127-143, 1993.
- [19] Adams J.B., and M.O.Smith, A new analysis of rock and soil types at the viking lander 1 site, J. of Geophysical Research, 91, B8, 8098-8112, 1986.
- [20] Arai K., Information extraction of inner pixel contents derived from satellite remote sensing imagery data, J. of Japanese Society for Photogrammetry and Remote Sensing, 30, 4, 30-34, 1991.
- [21] Keshava N. and J.Mustard, Spectral unmixing, IEEE Signal Processing Mag., 19, 1, 44-57, 2002.
- [22] Liangrocapt S. and M.Petrou, Mixed pixels classification, Proc. of the SPIE Conference on Image and Signal Processing for Remote Sensing IV, 3500, 72-83, 1998.
- [23] Arai K. and Y.Terayama, Label Relaxation Using a Linear Mixture Model, International Journal of Remote Sensing, 13, 16, 3217-3227, 1992.
- [24] Borel C.C. and S.A.Gerstl, Nonlinear spectral mixing models for vegetation and soil surface, Remote Sensing of the Environment, 47, 2, 403-416, 1994.
- [25] Arai K. and Reiko Inagaki, Nonlinear mixel model taking into account multiple reflections between ground cover targets and the atmosphere, Proceedings of the 33rd General Conference of Remote Sensing Society of Japan, 2002.
- [26] Settle J.J., On the relationship between spectral unmixing and subspace projection, IEEE Trans., Geosci. Remote Sensing, 34, 1045-1046, 1996.
- [27] Matsumoto M., H. Fujiku, K.Tsuchiya and K.Arai, Unmixing by means of maximum likelihood classification, J. of Japanese Society for Photogrammetry and Remote Sensing, 30, 2, 25-34, 1991.
- [28] Chang C.L, Hyperspectral Imaging: Techniques for spectral detection and classification, New York: Kluwer Academic, 2003.
- [29] Arai K., Y.Terayama, Y.Ueda, and M.Moriyama, Adaptive least square method for estimation of partial cloud coverage within a pixel, International J. of Remote Sensing, 16, 12, 2197-2206, 1995.
- [30] Mazer A.S., M.Martin, et al., Image processing software for imaging spectrometry data analysis, Remote Sensing of the Environment, 24, 1, 201-210, 1988.
- [31] Chang C., X.Zhao, M.L.G.Althouse, and J.J.Pan, Least squares subspace projection approach to mixed pixel classification for hyperspectral images, IEEE Trans. Geosci. Remote Sensing, 36, 3, 898-912, 1998.
- [32] Arai K., H.Chen, Unmixing based on subspace method with learning process, Proceedings of the 33rd General Conference of Remote Sensing Society of Japan, 2002.
- [33] Harsanyi J.C. and C.I.Chang, Hyperspectral image classification and dimensionality reduction: An orthogonal subspace projection approach, IEEE Trans. Geosci. Remote Sensing, 32, 4, 779-785, 1994.
- [34] Arai K. and K.Seto, Data hiding method based on a linear transformation to the subspace, Journal of the Visualization Society of Japan, 25, 5, Suppl.No.1, 55-58, 2005.
- [35] Parra L., K.R.Muller, C.Specce, A.Ziehe, and S.Sajda, Unmixing hyperspectral data, Advances in Neural Information Processing Systems, 12, 942-948, 2000.
- [36] Erkki O., Subspace methods of pattern recognition, Research Studies Press Ltd., 1983.

AUTHORS PROFILE

Kohei Arai, He received BS, MS and PhD degrees in 1972, 1974 and 1982, respectively. He was with The Institute for Industrial Science and Technology of the University of Tokyo from April 1974 to December 1978 also was with National Space Development Agency of Japan from January, 1979 to March, 1990. During from 1985 to 1987, he was with Canada Centre for Remote Sensing as a Post Doctoral Fellow of National Science and Engineering Research Council of Canada. He moved to Saga University as a Professor in Department of Information Science on April 1990. He was a councilor for the Aeronautics and Space related to the Technology Committee of the Ministry of Science and Technology during from 1998 to 2000. He was a councilor of Saga University for 2002 and 2003. He also was an executive councilor for the Remote Sensing Society of Japan for 2003 to 2005. He is an Adjunct Professor of University of Arizona, USA since 1998. He also is Vice Chairman of the Commission "A" of ICSU/COSPAR since 2008. He wrote 30 books and published 322 journal papers.

Parallelization of 2-D IADE-DY Scheme on Geranium Cadcam Cluster for Heat Equation

Simon Uzezi Ewedafe
Computing & IT. Baze University, Abuja
Baze University, Abuja
Abuja, Nigeria

Rio Hirowati Shariffudin
Institute of Mathematical Sciences
Universiti Malaya
Kuala Lumpur, Nigeria

Abstract—A parallel implementation of the Iterative Alternating Direction Explicit method by D'Yakonov (IADE-DY) for solving 2-D heat equation on a distributed system of Geranium Cadcam cluster (GCC) using the Message Passing Interface (MPI) is presented. The implementation of the scheduling of n tri-diagonal system of equations with the above method was used to show improvement on speedup, effectiveness, and efficiency. The Master/Worker paradigm and Single Program Multiple Data (SPMD) model is employed to manage the whole computation based on the use of domain decomposition. The completion of the execution can need task recovery and favorable configuration. The above mentioned details consist of a main report about the numerical validation of the parallelization through simulation to demonstrate the proposed method effectiveness on the cluster system. It was found that the rate of convergence decreases as the number of processors increases. The result of this paper suggests that the 2-D IADE-DY scheme is a good approach to solving problems, particularly when it is simulation with more processors.

Keywords—Parallel Implementation; Heat Equation; SPMD; IADE-DY; Domain Decomposition

I. INTRODUCTION

Software programmers developing parallel application do focus on some challenges in the area of parallel computing. According to [18] there are theoretical challenges such as task decomposition, dependence analysis, and task scheduling. Then there are practical challenges such as portability, synchronization, and debugging. An alternative and cost effective means of achieving a comparable performance is by way of distributed computing, using a system of processors loosely connected through a local area network [3]. For a global computational task with other processors, relevant data need to be passed from processors to processors through a message passing mechanism [7, 11, 28, 22]. There is greater demand for computational speed and computations must be completed within reasonable time period by using multiple processors on a single problem, hence, the demand for faster processors has been growing rapidly, which can only be met by the use of parallel computers for grand challenge problems [19, 30] and [4].

There are a number of important unresolved questions concerning multiprocessor computers, among these issues are: should they consist of a few, rather powerful processors or many very much less powerful processors, or something in between? According to [16] there is a natural expectation that the multiprocessors with a few, powerful processors will have

an MIMD architecture, and that the others will have SIMD architecture. Parallelization of heat equation has been proposed by [3], and recent developments have included a number of different applications [5, 2]. Another issue is the communication among the processors. How is the memory connected to the processors, and how are these processors connected to each other? The model proposed in this paper enhances overlap communication and computation to avoid unnecessary synchronization; hence, the method yields significant speedup by the use of the non-blocking communication.

While the theoretical properties of the 2-D IADE-DY algorithm employing the master/worker paradigm and SPMD model are promising, achieving good performance in practice can be challenging. In reference to [2] this is due to fundamental tradeoff between the reduction of the time required for an inherently sequential part of the algorithm, and an increase in the number of the iterations required to converge. Previous analysis of the IADE scheme in the literature did not consider the efficient parallelization and scheduling of tasks to improve scalability. Sequential numerical methods for solving time dependable problems have been explored extensively [25, 30].

A number of software tools have been developed for parallel implementation, MPI [19] is chosen since it has a large user group. The objective of our parallel focus is to improve performance. Due to our objective, parallelizing code has traditionally been paired with general code optimizations for performance, especially in the scientific and engineering area [18].

The main contribution of this paper is to present a detailed study of the parallelization using the 2-D IADE-DY algorithm employing master/worker paradigm and SPMD model to enhance overlapping communication with computation on the GCC cluster system running MPI that result in significant improved speedup, effectiveness, and efficiency across varying mesh sizes. The Master/Worker paradigm and SPMD model is employed to manage the whole computation based on the use of domain decomposition. The completion of the execution can need task recovery and favorable configuration. Our results demonstrate two properties that make this approach attractive for the platform of GCC: overlap communication and computation, and ability to arbitrary use various varying mesh sizes. The distribution done in the GCC reduces the memory pressure on the master while preserving parallel efficiency.

To obtain results with sufficient accuracy for the numerical prediction of the scalable parallel implementation of the AGE, IADE and ADI algorithm, fine discretization of the domain would be necessary. Due to the limitation in both processing element power and memory on sequential architectures and the dimension of full scale utility, only coarse grids are possible. A confine enhancement may be achieved if a domain decomposition method is used to allow locally refined meshes. The paper is organized as follows: section 2 emphasizes on previous related work, section 3 introduces the model for the 2-D heat equation and method and the 2D-IADE-DY scheme. Section 4 and 4 introduces the performance analysis and numerical experiment. Finally, a conclusion is included in section 6.

II. PREVIOUS WORK

Parallelization of Partial Differential Equations (PDE) by time decomposition was first proposed by [24]. The motivation for the paper was to achieve parallel real-time solutions. Recent improvements have included a number of different applications [5], and [2] emphasizes the scheduling of tasks in the Para real algorithm. The importance of loop parallelization and loop scheduling has been extensively studied [1]. This work is distinct while promoting flexibility, and applies standard parallel concepts. Several approaches to solving heat equation have been carried out in [6, 25, 26, 27] and [13, 29, 32]. We have applied the 2-D IADE-DY scheme by simulation to schedule the n tri-diagonal system of equations with the above method used to show improvement on speedup, effectiveness, and efficiency. Reference [10] and [12] show speedup and efficiency, while comparing to our results generated using GCC, the GCC results show better conformity to linearity for speedup and closeness to unity for efficiency than [10] as applied to the simple method using MPI. In [20], the unconditional stability of the alternating difference schemes has similarity to our scheme. Our implementation compared to [26] and [27, 6] is a way of proving stability and convergence in the GCC cluster system. We also note the various constant improvements on speedup, effectiveness, and efficiency analysis carried out in [33h] using the overlapping domain decomposition method. However, [32] proposed a generalized speedup formula as the ratio of the parallel to sequential speed. As in relation to the performance strategies implementation, a thorough study of speedup models together with their advantages is implemented in [30, 9, 28] show the same conformity to our implementation, but here we were able to achieve unity conformity in the message passing mechanism.

III. THE MODEL PROBLEM

The problem that is of interest to us is the heat equation in 2-dimension. We assume that the heat will spread within the field based on a dynamics described in [27, 31] and the Alternating Group Explicit [13] method by the following:

$$\frac{\partial U}{\partial t} = \frac{\partial^2 U}{\partial x^2} + \frac{\partial^2 U}{\partial y^2} + h(x, y, t), (x, y, t) \in R \times (0, T], \quad (3.1)$$

with the initial condition,

$$U(x, y, 0) = F(x, y), (x, y, t) \in R \times \{0\}, \quad (3.1a)$$

and $U(x, y, t)$ is specified on the boundary of $R, \partial R$ by

$$U(x, y, t) = G(x, y, t), (x, y, t) \in \partial R \times (0, T], \quad (3.1b)$$

where for simplicity we assume that the region R of the xy -plane is a rectangle. Consider the two-dimensional heat (3.1) with the auxiliary conditions (3.1a) and (3.1b). The region R is a rectangle defined by

$$R = \{(x, y) : 0 \leq x \leq L, 0 \leq y \leq M\}.$$

At the point $P(x_i, y_j, t_k)$ in the solution domain, the value of $U(x, y, t)$ is denoted by $U_{i,j,k}$ where $x_i = i\Delta x$, $y_j = j\Delta y$ for $0 \leq i \leq (m+1), 0 \leq j \leq (n+1)$ and $\Delta x = L/(m+1)$, $\Delta y = M/(n+1)$. The increment in the time t , Δt is chosen such that $t_k = k\Delta t$ for $k = 0, 1, 2, \dots$ for simplicity of presentation, we assume that m and n are chosen so that $\Delta x = \Delta y$ and consequently the mesh ratio is defined by $\lambda = \Delta t / (\Delta x)^2$.

A. The IADE-DY and DS-MF

By fractional splitting, each time step in the double sweep methods is split into two steps of size $\Delta t / 2$. The horizontal sweep advances from t_k to $t_{k+1/2}$ by using a difference approximation that is implicit in only the x -direction. Specifically, past values in the y -direction along the grid line $x = x_i$ are used, to yield the intermediate value $u_{i,j,k+1/2}$. Then, in the vertical sweep from $t_{k+1/2}$ to t_{k+1} , the solution is obtained by using an approximation implicit in only the y -direction and uses past values in the x -direction along the grid line $y = y_j$, to yield the final value $u_{i,j,k}$.

At the $(k+1/2)$ time level method, the solution of (3.1) uses a backward-difference approximation.

$$u_{i,j,k+1/2} - u_{i,j,k} = \frac{\lambda}{2} \delta_x^2 u_{i,j,k+1/2} + \frac{\lambda}{2} \delta_y^2 u_{i,j,k} \quad (3.2)$$

Where δ_x and δ_y are the usual central difference operators in the x and y coordinates respectively.

$$u_{i,j,k+1} - u_{i,j,k} = \frac{\lambda}{2} (u_{i-1,j,k+1/2} - 2u_{i,j,k+1/2} + u_{i+1,j,k+1/2}) + \frac{\lambda}{2} (u_{i,j-1,k} - 2u_{i,j,k} + u_{i,j+1,k}) \quad (3.3)$$

$$-\frac{\lambda}{2}u_{i-1,j,k+1/2} + (1+\lambda)u_{i,j,k+1/2} - \frac{\lambda}{2}u_{i+1,j,k+1/2} = \frac{\lambda}{2}u_{i,j+1,k} + (1-\lambda)u_{i,j,k} + \frac{\lambda}{2}u_{i,j-1,k} \quad (3.4)$$

From (3.4), for $j = 1, 2, \dots, n$

$$i = 1: (1+\lambda)u_{1,j,k+1/2} - \frac{\lambda}{2}u_{2,j,k+1/2} = \frac{\lambda}{2}u_{0,j,k+1/2} + \frac{\lambda}{2}u_{1,j+1,k} + (1-\lambda)u_{1,j,k} + \frac{\lambda}{2}u_{1,j-1,k} \quad (3.5)$$

$$i = 2, 3, \dots, m-1: -\frac{\lambda}{2}u_{i-1,j,k+1/2} + (1+\lambda)u_{i,j,k+1/2} - \frac{\lambda}{2}u_{i+1,j,k+1/2} = \frac{\lambda}{2}u_{i,j+1,k} + (1-\lambda)u_{i,j,k} + \frac{\lambda}{2}u_{i,j-1,k} \quad (3.6)$$

$$i = m: -\frac{\lambda}{2}u_{m-1,j,k+1/2} + (1+\lambda)u_{m,j,k+1/2} = \frac{\lambda}{2}u_{m+1,j,k+1/2} + \frac{\lambda}{2}u_{m,j+1,k} + (1-\lambda)u_{m,j,k} + \frac{\lambda}{2}u_{m,j-1,k} \quad (3.7)$$

let $a = 1 + \lambda$, $b = c = -\frac{\lambda}{2}$. Equation (3.5) – (3.7) can be written in a more compact matrix form as:

$$Au_j^{(k+1/2)} = f_k, \quad j = 1, 2, \dots, n. \quad (3.8)$$

where

$$u = (u_{1,j}, u_{2,j}, \dots, u_{m,j})^T, \quad f = (f_{1,j}, f_{2,j}, \dots, f_{m,j})^T$$

$$f_{1,j} = \frac{\lambda}{2}u_{1,j+1,k} + (1-\lambda)u_{1,j,k} + \frac{\lambda}{2}(u_{1,j-1,k} + u_{0,j,k+1/2})$$

$$f_{i,j} = \frac{\lambda}{2}u_{i,j+1,k} + (1-\lambda)u_{i,j,k} + \frac{\lambda}{2}u_{i,j-1,k} \quad i = 2, 3, \dots, m-1$$

$$f_{m,j} = \frac{\lambda}{2}u_{m,j+1,k} + (1-\lambda)u_{m,j,k} + \frac{\lambda}{2}(u_{m,j-1,k} + u_{m+1,j,k+1/2}) \quad (3.9)$$

at the $(k+1)$ time level, (3.1) is approximated by,

$$u_{i,j,k+1} - u_{i,j,k+1/2} = \frac{\lambda}{2}\delta_x^2 u_{i,j,k+1/2} + \frac{\lambda}{2}\delta_y^2 u_{i,j,k+1} \quad (3.10)$$

$$u_{i,j,k+1} - u_{i,j,k+1/2} = \frac{\lambda}{2}(u_{i-1,j,k+1/2} - 2u_{i,j,k+1/2} + u_{i+1,j,k+1/2}) + \frac{\lambda}{2}(u_{i,j-1,k+1} - 2u_{i,j,k+1} + u_{i,j+1,k+1}) \quad (3.11)$$

$$-\frac{\lambda}{2}u_{i,j-1,k+1} + (1+\lambda)u_{i,j,k+1} - \frac{\lambda}{2}u_{i,j+1,k+1} = \frac{\lambda}{2}u_{i-1,j,k+1/2} + (1-\lambda)u_{i,j,k+1/2} + \frac{\lambda}{2}u_{i+1,j,k+1/2} \quad (3.12)$$

from (3.4), for $i = 1, 2, \dots, m$.

$$j = 1: (1+\lambda)u_{i,1,k+1} - \frac{\lambda}{2}u_{i,2,k+1} = \frac{\lambda}{2}u_{i-1,1,k+1/2} + (1-\lambda)u_{i,1,k+1/2} + \frac{\lambda}{2}u_{i+1,1,k+1/2} + \frac{\lambda}{2}u_{i,0,k+1} \quad (3.13)$$

$$j = 2, 3, \dots, n-1: -\frac{\lambda}{2}u_{i,j-1,k+1} + (1+\lambda)u_{i,j,k+1} - \frac{\lambda}{2}u_{i,j+1,k+1} = \frac{\lambda}{2}u_{i-1,j,k+1/2} + (1-\lambda)u_{i,j,k+1/2} + \frac{\lambda}{2}u_{i+1,j,k+1/2} \quad (3.14)$$

$$j = n: -\frac{\lambda}{2}u_{i,n-1,k+1} + (1+\lambda)u_{i,n,k+1} = \frac{\lambda}{2}u_{i-1,n,k+1/2} + (1-\lambda)u_{i,n,k+1/2} + \frac{\lambda}{2}u_{i+1,n,k+1/2} \quad (3.15)$$

let $a = 1 + \lambda$, $b = c = -\frac{\lambda}{2}$. Equations (3.13) – (3.15) can be displayed in a more compact matrix form as:

$$Bu_i^{(k+1)} = g_{k+1/2}, \quad i = 1, 2, \dots, m \quad (3.16)$$

where

$$u_i^{(k+1)} = (u_{i,1}, u_{i,2}, \dots, u_{i,n})^T, \quad g = (g_{i,1}, g_{i,2}, \dots, g_{i,n})^T$$

$$g_{i,1} = \frac{\lambda}{2}u_{i+1,1,k+1/2} + (1-\lambda)u_{i,1,k+1/2} + \frac{\lambda}{2}(u_{i-1,1,k+1/2} + u_{i,0,k+1})$$

$$g_{i,j} = \frac{\lambda}{2}u_{i+1,j,k+1/2} + (1-\lambda)u_{i,j,k+1/2} + \frac{\lambda}{2}u_{i-1,j,k+1/2} \quad j = 2, 3, \dots, n-1$$

$$g_{i,n} = \frac{\lambda}{2}u_{i+1,n,k+1/2} + (1-\lambda)u_{i,n,k+1/2} + \frac{\lambda}{2}(u_{i-1,n,k+1/2} + u_{i,n+1,k+1}) \quad (3.17)$$

B. IADE-DY

The matrices A and B are respectively tridiagonal of size (mxm) and (nxn) . Hence, at each of the $(k + \frac{1}{2})$ and $(k + 1)$ time levels, these matrices can be decomposed into $G_1 + G_2 - \frac{1}{6}G_1G_2$, where G_1 and G_2 are lower and upper bidiagonal matrices given respectively by

$$G_1 = [l_i, 1], \quad \text{and} \quad G_2 = [e_i, u_i], \quad (3.18)$$

where

$$e_1 = \frac{6}{5}(a-1), u_i = \frac{6}{5}b,$$

$$e_{i+1} = \frac{6}{5}(a + \frac{1}{6}l_i u_i - 1),$$

$$l_i = \frac{6c}{6 - e_i} (e_i \neq 6) \quad i = 1, 2, \dots, m-1$$

hence, by taking p as an iteration index, and for a fixed acceleration parameter $r > 0$, the two-stage IADE-DY scheme of the form,

$$(rI + G_1)u^{(p+1/2)} = (rI - gG_1)(rI - gG_2)u^{(p)} + hf \quad \text{and}$$

$$(rI + G_2)u^{(p+1)} = u^{(p+1/2)} \quad (3.19)$$

can be applied on each of the sweeps (3.2) and (3.10). By carrying out the relevant multiplications in (3.19), the following equations for computation at each of the intermediate levels are obtained:

(i) at the $(p+1/2)^{th}$ iterate,

$$u_1^{(p+1/2)} = \frac{1}{d} (\hat{s}_1 s u_1^{(p)} + w_1 s u_2^{(p)} + hf_1)$$

$$u_i^{(p+1/2)} = \frac{1}{d} (-l_{i-1} u_{i-1}^{(p+1/2)} v_{i-1} s_{i-1} u_{i-1}^{(p)} +$$

$$(v_{i-1} w_{i-1} + s_i \hat{s}) u_i^{(p)} + w_i \hat{s} u_{i+1}^{(p)} + hf_i), \quad (3.20)$$

$$i = 2, 3, \dots, m-1$$

$$u_m^{(p+1/2)} = \frac{1}{d} (-l_{m-1} u_{m-1}^{(p+1/2)} v_{m-1} s_{m-1} u_{m-1}^{(p)} +$$

$$(v_{m-1} w_{m-1} + s_m \hat{s}) u_m^{(p)} + hf_m)$$

Where,

$$g = \frac{6+r}{6}, \quad h = \frac{r(12+r)}{6}, \quad d = 1+r,$$

$$s = r - g, \quad s_i = r - g e_i, \quad i = 1, 2, \dots, m$$

$$\text{and } v_i = -g l_i, \quad w_i = -g u_i \quad i = 1, 2, \dots, m-1.$$

(ii) at the $(p+1)^{th}$ iterate,

$$u_m^{(p+1)} = \frac{u_m^{(p+1/2)}}{d_m},$$

$$u_i^{(p+1)} = \frac{1}{d_i} (u_i^{(p+1/2)} - u_i u_{i+1}^{(p+1)}), \quad (3.21)$$

$$\text{where } d_i = r + e_i, \quad i = m-1, \dots, 2, 1$$

IV. PERFORMANCE ANALYSIS AND PARALLEL ALGORITHM

All experiment were performed on the GCC of 8 nodes with Gigabit Ethernet interconnect. Each node consists of dual core processors (3.0GHZ) with 16 GB of RAM. The MPI implementation was implemented in C/MPI. A parallel platform design to run numerical application has to be efficient [8]. The platform contains more computations on large set of varying mesh sizes, and its evaluation has to be large to benchmarking. Performance concerns not only the cost of functions of the schemes, but resource accesses and code placement on computing resources [8]. Making declaration for placement of data at the beginning of computation, it does not accept any perturbation. The 2D IADE-DY scheme is extremely tested using the GCC cluster system for its implementation. The objective is to evaluate the overhead it introduces and its ability to exploit the inherent parallelism of an iterative computation as stated in [18]. The scalability across varying number of processors and mesh sizes is observed. To obtain any speedup we need convergence in fewer than N iterations. The closer the coarse propagator is to the fine propagation, the faster will be the convergence. If they are too similar, then the sequential part of the algorithm will significantly degrade the speedup. A simple speedup analysis according to [2] produces the following:

$$\varphi = \frac{N}{Nr(K+1) + K}, \quad (4.1)$$

Where r is the ration of the time taken by coarse propagation to fine propagation over the same time interval, K is the number of iterations required for convergence, and communication overhead is ignored.

In the limit $r \rightarrow 0$, $\varphi \rightarrow \frac{N}{K}$, therefore, the efficiency

will be $\frac{1}{K}$. Full efficiency can be achieved if the algorithm converges in one iteration. To make r smaller, the coarse propagator must be less than accurate due to larger time step or coarse spatial grid, which in turn requires more iteration to converge [17]. As treated in [14, 15], the algorithm for the scheme is performed on a distributed memory system of p processors, assumes that each processors initially stores $n = N/p$ objects distributed over the entire physical domain. In the

first iteration of the algorithm, the domain is decomposed into two sub-domains so that the difference between the sums of the weight of the sub-domain is as small as possible. Then the same process is applied to two sub-domains in parallel, and process is repeated recursively, for log p iteration. In other words, during iteration i , $1 \leq i \leq \log p$, the p processors are group into 2^{i-1} groups of $p / 2^{i-1}$ processors each. At the beginning of the iteration, the problem domain is already partitioned into 2^{i-1} sub-domains and the objects in each sub-domain are stored in single group of processors. At the end of the iteration, each processor group is divided into two groups, and the corresponding sub-domain is divided into two sub-groups with the object in one sub-domain residing in one half the processors and the other objects in the other sub-domain residing in the other half of processor. Data parallelism originated the SPMD [23]. Thus, the finite difference approximation can be treated as a SPMD problem; essentially the same computation must be performed for multiple data sets. The multiple data are different parts of the overall grid, each sent to a different computer node (processor). The main issues that arise in parallelizing a finite difference grid are: the determination of how best to partitioned the grid among processors, and how to pass instructions about grid boundaries from node to node.

The domain decomposition is used to distribute data between different processors, in order to minimize the idle time static load balancing is used to distribute the data such that each processor gets almost the same number of computational points. The partitioning and load balancing is done in the pre-processing stage, wherein, separate grid files are generated for each processor along with other necessary information about partitioning. Thus there is no need to allocate any extra storage or scatter the grid data when the parallel program is executed. At the end of the parallel computation each process writes the output into separate files suitable for verification.

V. NUMERICAL EXPERIMENTS AND DISCUSSION

The algorithm was tested on the 2-D heat equation and the application of the above mentioned algorithm is now demonstrated on meshes of 100x100, 200x200 and 300x300 respectively. Tables 1 – 3, show the various performance timing. Consider the 2-D parabolic equation of the form:

$$\frac{\partial^2 U}{\partial x^2} + \frac{\partial^2 U}{\partial y^2} = \frac{\partial U}{\partial t} \tag{5.1}$$

The boundary conditions and initial condition posed are:

$$\left. \begin{aligned} U(0, y, t) &= 0 \\ U(1, y, t) &= 100 \\ U(x, 0, t) &= 0 \\ U(x, 1, t) &= 100 \end{aligned} \right\} t \geq 0 \tag{5.1a}$$

$$\begin{aligned} U(x, y, 0) &= \text{Sin}(\pi x)\text{Sin}(\pi y) \\ (0 \leq x \leq 1, 0 \leq y \leq 1) \end{aligned} \tag{5.1b}$$

The exact solution is given by

$$U(x, y, t) = e^{-\pi^2 t} \text{Sin}(\pi x)\text{Sin}(\pi y).$$

TABLE I. 100x100 meshes with MPI

| Scheme | N | T_w | T_m | T_{sd} | S_{par} | E_{par} |
|--------|---|-------|-------|----------|-----------|-----------|
| IADE | 1 | 334.3 | 8.6 | 3.3 | 1.000 | 1.000 |
| | 2 | 285.6 | 8.5 | 3.2 | 1.516 | 0.758 |
| | 3 | 198.7 | 8.5 | 3.1 | 2.172 | 0.724 |
| | 4 | 141.6 | 8.5 | 3.1 | 2.764 | 0.691 |
| | 5 | 128.1 | 8.5 | 3.1 | 3.165 | 0.633 |
| | 6 | 108.5 | 8.5 | 3.1 | 3.588 | 0.598 |
| | 7 | 98.1 | 8.5 | 3.1 | 3.787 | 0.541 |
| | 8 | 83.8 | 8.5 | 3.1 | 4.144 | 0.518 |

TABLE II. 200x200 meshes with MPI

| Scheme | N | T_w | T_m | T_{sd} | S_{par} | E_{par} |
|--------|---|-------|-------|----------|-----------|-----------|
| IADE | 1 | 486.4 | 14.9 | 5.8 | 1.000 | 1.000 |
| | 2 | 392.8 | 14.7 | 5.6 | 1.782 | 0.891 |
| | 3 | 308.5 | 14.7 | 5.6 | 2.562 | 0.854 |
| | 4 | 286.7 | 14.7 | 5.6 | 3.244 | 0.811 |
| | 5 | 203.1 | 14.7 | 5.6 | 3.91 | 0.782 |
| | 6 | 189.6 | 14.7 | 5.6 | 4.302 | 0.717 |
| | 7 | 163.5 | 14.7 | 5.6 | 4.795 | 0.685 |
| | 8 | 142.9 | 14.7 | 5.6 | 4.952 | 0.619 |

TABLE III. 300x300 meshes with MPI

| Scheme | N | T_w | T_m | T_{sd} | S_{par} | E_{par} |
|--------|---|-------|-------|----------|-----------|-----------|
| IADE | 1 | 685.4 | 18.6 | 9.5 | 1.000 | 1.000 |
| | 2 | 536.8 | 18.5 | 9.3 | 1.798 | 0.899 |
| | 3 | 482.1 | 18.5 | 9.3 | 2.658 | 0.886 |
| | 4 | 413.8 | 18.5 | 9.3 | 3.476 | 0.869 |
| | 5 | 386.9 | 18.5 | 9.3 | 4.24 | 0.848 |
| | 6 | 251.8 | 18.5 | 9.3 | 4.926 | 0.821 |
| | 7 | 210.1 | 18.5 | 9.3 | 5.572 | 0.796 |
| | 8 | 189.6 | 18.5 | 9.3 | 5.976 | 0.747 |

Here, we observed in our experiments designed to test the effectiveness of our approach that as the mesh size increases, the execution time increases as well with a proportionate decrease in time as processors increases for three mesh sizes in Tables 1 – 3. T_w is the time for the worker, T_m is the master time, T_{sd} is the worker domain decomposition time for worker allocation, S_{par} is the speedup, and E_{par} is the efficiency. This phenomenon shows that as the number of processors increases, though it might lead to a decrease in execution time but will get to a point that increasing the processors will not have much impact on total execution time. The time spend in data exchange will be significant compared to the time spend in computation and the parallel efficiency goes down. Hence, when the number of processors increases, balancing the number of computational cells per processors will become a difficult task due to significant load imbalance. When the number of processors increases, execution time suddenly increases for certain number of processors mesh sizes. This gain is due to the uneven distribution of the computational cells when a large number of processors are used, execution time had a very small change due to domain decomposition influence on performance in parallel computation. The larger the mesh sizes show that up to certain number, the speedup improvement is near linearity. The performance begins to degrade with an effect caused by increase in communication overheads.

The problem size is scaled up following the memory-bounded constraint. This phenomenon is well under expected since the implicit replacement has a very low computation overhead as implemented on the three problems. However, these jumps in communication time which are relatively larger than the others are mainly caused by the architecture of the communication between the processors, that is, due to the underlying machine architecture not the algorithm. This rate of performance decrease is fairly shown for parallel computing, especially for experiments conducted under non-dedicated environments which show that the proposed algorithm scales well. Our experiment shows reliability by conforming to convergence, and how memory is been distributed to access main data. This step is made possible by the Master/Worker computation process.

VI. CONCLUSION

We have explained in this paper how the role of GCC in the parallelization of the 2-D IADE-DY scheme is a good approach to solving problems, particularly when it is simulation with more processors. The objective is to present a design of paradigm adapted architecture for distributed computation, because they depend on empirical concern (data and code). The algorithm presented shows significant improvement when implemented on the above number of processors. In addition to the ease of use compared to other common approaches, the results show negligible overhead with effective load scheduling which produce the expected inherent speedups. It was also confirmed that the domain decomposition, and the use of SPMD are important and this is easy with our parallel platform of GCC. The performance of the 2D IADE-DY with the parallel paradigm is in many cases superior. As the number of processors increases, the bottleneck of parallel computation appears and the global

reduction consumes a large part of time, then the improvement becomes significant.

REFERENCES

- [1] J. Aguilar, E. Leiss, 'Parallel loop scheduling approaches for distributed and shared memory system,' *Parallel Process Letter* 15 (1 – 2), 131 – 152, 2005.
- [2] E. Aubanel, 'Scheduling of tasks in the parareal algorithm,' *Parallel Computing* 37 (3), 172 – 182, 2011.
- [3] W. Barry, A. Michael, 'Parallel programming techniques and application using networked workstation and parallel computers,' Prentice Hall, New Jersey, 2003.
- [4] D. Callahan, K. Kennedy, 'Compiling programs for distributed memory multiprocessors,' *Journal of supercomputer* 2, pp 151 – 169, 1988.
- [5] E. Celledoni, T. Kvamsdal, 'Parallelization in time for thermo-viscoplastic problems in extrusion aluminium,' *Int'l Journal for numerical methods in engineering* 75 (5), 576 – 598, 2009.
- [6] H. Chi-Chung, G. Ka-Kaung, 'Solving partial differential equations on a network of workstations,' *IEEE*, pp 194 – 200, 1994.
- [7] P.J Coelho, M.G Carvalho, 'Application of a domain decomposition technique to the mathematical modeling of utility boiler' *Journal of numerical methods in eng.*, 36 pp 3401 – 3419, 1993.
- [8] D. Cyril, M. Fabrice, 'Jacobi computation using mobile agent,' *Int'l Journal of Computer Science & Information Technologies*, 1 (5), 392 – 401, 2010.
- [9] D'Ambra P., M. Danelutto, S. Daniela, L. Marco, 'Advance environments for parallel and distributed applications: a view of current status,' *Parallel Computing* 28, pp 1637 – 1662, 2002.
- [10] H.S Dou, Phan-Thien, 'A Domain decomposition implementation of the simple method with PVM,' *Computational Mechanics* 20 pp 347 – 358, 1997.
- [11] F. Durst, M. Perie, D. Chafer, E. Schreck, 'Parallelization of efficient numerical methods for flows in complex geometries,' *Flow simulation with high performance computing I*, pp 79 – 92, Vieweg, Braunschweig, 1993.
- [12] J.H. Eduardo, M.A. Yero, H. Amaral, 'Speedup and scalability analysis of master-slave application,' 2007.
- [13] D.J. Evans, M.S. Sahimi, 'The alternating group explicit iterative method for parabolic equations I: 2-dimensional problems,' *Intern. j. compt. math.*, Vol. 24, (1988) pp. 311-341
- [14] S. U. Ewedafe, R. H. Shariffudin, 'Armadillo generation distributed system with geranium cadcam cluster for solving 2-d telegraph problem,' *Intern. j. compt. math.*, vol. 88, 589 – 609, 2011.
- [15] S. U. Ewedafe, R. H. Shariffudin, 'Parallel implementation of 2-d telegraphic equation on MPI/PVM cluster,' *Int. j. parallel prog.*, 39, 202 – 231, 2011.
- [16] A. Fatoohi, E.G. Chester, 'Implementation of an ADI method on parallel computers,' *Journal of scientific computing* 2 (2), 1987.
- [17] M. J. Gander, S. Vandewall, 'Analysis of the parareal time-parallel time-integration method,' *SIAM jour. on scientific computing* 29 (2), 556 – 578, 2007.
- [18] N. Giacaman, O. Sinnen, 'Parallel iterator for parallelizing object-oriented applications,' *Intl journal of parallel programming*, 39 (2) 223 – 269, 2011.
- [19] W. Groop, E. Lusk, A. Skjellum, 'Using MPI, portable and parallel programming with the message passing interface,' 2nd Ed., Cambridge MA, MIT Press, 1999.
- [20] Y. Guangwei, H. Xudeng, 'Parallel iterative difference schemes based on prediction techniques for Sn transport method,' *Applied numerical mathematics* 57, 746 – 752, 2007.
- [21] M. Gupta, P. Banerjee, 'Demonstration of automatic data partitioning for parallelizing compilers on multi-computers,' *IEEE trans. parallel distributed system*, 3, vol. 2, pp 179 – 193, 1992a.
- [22] K. Jaris, D.G. Alan, 'A High-performance communication service for parallel computing on distributed systems,' *Parallel computing* 29, pp 851 – 878, 2003.

- [23] H. Laurant, 'A method for automatic placement of communications in SPMD parallelization,' *Parallel computing* 27, 1655 – 1664, 2001.
- [24] J. L. Lions., Y. Maday, G. Turinki, 'Parareal in time discretization of PDE,' *Comptes, rendus de l'academie des sciences – series 1 – mathematics* 332 (7), 661 – 668, 2011.
- [25] A. R. Mitchell, G. Fairweather, 'Improved forms of the Alternating direction methods of Douglas, Peaceman and Rachford for solving parabolic and elliptic equations,' *Numer. maths*, 6, 285 – 292, 1964.
- [26] J. Noye, 'Finite difference methods for partial differential equations,' *Numerical solutions of partial differential equations*. North-Holland publishing company, 1964.
- [27] D.W Peaceman, H.H Rachford, 'The numerical solution of parabolic and elliptic differential equations,' *Journal of soc. indust. applied math.* 8 (1) pp 28 – 41, 1955.
- [28] L. Peizong, Z. Kedem, 'Automatic data and computation decomposition on distributed memory parallel computers,' *ACM transactions on programming languages and systems*, vol. 24, number 1, pp 1 – 50, 2002.
- [29] M. S. Sahimi, E. Sundararajan, M. Subramaniam, and N. A. A Hamid, 'The D'Yakonov fully explicit variant of the iterative decomposition method,' *International journal of computers and mathematics with applications*, 42, 1485 – 1496, 2001.
- [30] V. T Sahni, 'Performance metrics: keeping the focus in routine. IEEE parallel and distributed technology, Spring pp 43 – 56, 1996.
- [31] G.D Smith, 'Numerical solution of partial differential equations: finite difference methods 3rd Ed.,' Oxford university press New York, 1985.
- [32] X.H Sun, J. Gustafson, 'Toward a Better Parallel Performance Metric,' *Parallel Computing* 17, 1991.
- [33] M. Tian, D. Yang, 'Parallel finite-difference schemes for heat equation based upon overlapping domain decomposition,' *Applied maths and computation*, 186, pp 1276 – 1292, 2007.

An Efficient Routing Protocol under Noisy Environment for Mobile Ad Hoc Networks using Fuzzy Logic

Supriya Srivastava, A. K. Daniel

^{1,2}Computer Science & Engineering Department M M M Engineering College,
Gorakhpur U.P. (India)

Abstract—A MANET is a collection of mobile nodes communicating and cooperating with each other to route a packet from the source to their destinations. A MANET is used to support dynamic routing strategies in absence of wired infrastructure and centralized administration. In this paper, we propose a routing algorithm for the mobile ad hoc networks based on fuzzy logic to discover an optimal route for transmitting data packets to the destination. This protocol helps every node in MANET to choose next efficient successor node on the basis of channel parameters like environment noise and signal strength. The protocol improves the performance of a route by increasing network life time, reducing link failure and selecting best node for forwarding the data packet to next node.

Keywords—Fuzzy Logic; Noise; Signal Strength; MANET

I. INTRODUCTION

Mobile ad hoc network is a collection of mobile devices which can communicate through wireless links. The task of routing protocol is to direct packets from source to destination. This is particularly hard in mobile ad hoc networks due to the mobility of the network elements and lack of centralized control. Source routing is a routing technique in which the sender of a packet determines the complete sequence of nodes through which it forwards the packet. The sender explicitly lists this route in the packet's header, identifying each forwarding "hop" by the address of the next node to which to transmit the packet on its way to the destination host. When a host needs a route to another host, it dynamically determines one based on cached information and on the results of a route discovery protocol, unlike conventional routing protocols.

Routing in MANET using the shortest hop count is not a sufficient condition to construct high-quality routes, because minimum hop count routing often chooses routes that have significantly less capacity than the best routes that exist in the network [1]. The routes selected based on hop count alone may be of bad quality since the routing protocols do not ignore weak quality links which are typically used to connect to remote nodes. The weak quality of a link can be the result of under considered metrics like Energy, SNR, Packet Loss, Maximum available bandwidth, load etc. The links usually have poor signal-to-noise ratio (SNR), hence higher frame error rates and lower throughput [2] [3].

All real measurements in any network are disturbed by noise. This includes electronic noise, but can also include

external events that affect the measured phenomenon—wind, vibrations, gravitational attraction of the moon, variations of temperature, variations of humidity, etc., depending on its measurement and of the sensitivity of the device. It is not possible to reduce the noise by controlling the environment. Otherwise, when the characteristics of the noise are known and are different from the signals, it is possible to filter it or to process the signal. In MANET, it is always needed to choose a channel with lower noise that result in reduction of number of dropped packets to increase the quality of service. The possibility that a packet will drop due to poor signal of the assigned transmission channel is called as "Dropped Call". The dropped packet rate is dependent on the following factors:

- The Channel Capacity
- Level of Traffic in the system
- Probability that noise is above unavoidable frequency.
- Probability that Residual Energy of nodes is below threshold
- Probability that Signal Strength is below Receiver threshold.
- Probability that Signal is below the specified Co-Channel interference level.

The proposed approach is called An Efficient Routing Protocol under Noisy Environment for Mobile Ad Hoc Networks using Fuzzy Logic (ERP). In this paper, the proposed protocol enhances Dynamic Source Routing protocol by considering Signal strength and Noise constraints to improve its performance. The fuzzy logic based technique uses two important parameters as noise factor and signal strength for route selection that results in best possible combinations to choose a route. The proposed protocol defines how a fuzzy logic based technique is effective to select routes, avoid link failure and increase network lifetime. A control mechanism like fuzzy logic is used to make mobile nodes intelligent. Fuzzy logic is basically the extension of crisp logic that includes the intermediate values between absolutely true and absolutely false. It has the efficiency to solve the system uncertainties.

The rest of the paper is organized as follows: related work and design issue in Section 2, the proposed protocol in Section

3, validation and analysis in Section 4 and finally Conclusion in Section 5.

II. DESIGN ISSUES AND RELATED WORK

The movement of the nodes, packet collision and bad channel condition are the various reasons for the data packets to loss. Packet losses are subjected to occur due to continuous period of intermittent failure during the communication between nodes. The fading conditions cause certain nodes to completely lose their connectivity. Signal-to-Noise ratio is an important issue over a link; the links that usually have bad signal-to-noise ratio (SNR) have higher frame error rates and lower throughput, resulting in link failure. Signal-to-noise ratio (SNR or S/N) compares the level of a desired signal to the level of background noise [4].

- SNR is defined as the ratio of signal power to the noise power. A ratio higher than 1:1 indicates more signal than noise.

$$SNR = \frac{P_{Signal}}{P_{noise}}$$

Where P is average power

- Both signal and noise power must be measured at the same and equivalent points in a system, and within the same system bandwidth. If the signal and the noise are measured across the same impedance, then the SNR can be obtained by calculating the square of the amplitude ratio:

$$SNR = \frac{P_{Signal}}{P_{noise}} = \left(\frac{A_{Signal}}{A_{noise}} \right)^2$$

Where A is root mean square (RMS) of amplitude

- In decibels, the SNR is defined as

$$SNR_{dB} = 10 \log_{10} \left(\frac{P_{Signal}}{P_{noise}} \right) \\ = P_{signal, dB} - P_{noise, dB}$$

- Noise Limited System, $\mu \rightarrow 0$

Here, we are considering only noise limited system, so the effect of receiver threshold signal can be considered and also assumed that there will not be any Co-Channel interference. In such a case, $\mu \rightarrow 0$ and the expression for dropped packet rate is

$$D = \sum_{n=0}^N a_n D_n = \sum_{n=0}^N a_n [1 - (1 - \delta)^n]$$

- Interference Limited System, $\delta \rightarrow 0$

Here, we are consider only interference-limited system, so the effect of Co-Channel interference can be considered and also assumed that there will not be any kind of noise which is

introducing in the system. In such a case, $\delta \rightarrow 0$ and the expression for dropped packet rate is

$$D = \sum_{n=0}^N a_n D_n = \sum_{n=0}^N a_n [1 - (1 - \mu)^n]$$

Many algorithms have been proposed for route selection in Mobile Ad-Hoc network in recent years. Some of them are:

Devi M. [5] propose a fuzzy based route recovery technique. It consists of two phases, Proactive failure discovery, and Route failure recovery. Nodes in the network estimate the metrics Link Expiration Time (LET), Received Signal Strength (RSS), Available Band Width (ABW) and Residual Energy (RE) and using fuzzy logic, the type of node is estimated as weak, normal or strong.

Fuad Alnajjar et al. [4] has proposed a mechanism to provide an efficient QoS routing protocol to enhance the performance of existing routing protocols in Mobile ad hoc network environment.

Supriya Srivastava et al [6] proposes an Energy-Efficient Routing protocol that will improve the utilization of link by balancing the energy consumption between utilized and underutilized nodes. It also proposed a method for maintenance of the route during a link failure.

Junghwi Jeon et al. [7] have proposed a fast route recovery scheme to solve the link failure problem caused by node movement, packet collision or bad channel condition.

Merlinda Drini [8] explained that the mobility of the nodes, packet collision and bad channel condition are the various reasons for the data packets to fail. Packet losses are subjected to occur due to continuous period of intermittent failure during the communication between nodes. The fading conditions cause certain nodes to completely lose their connectivity.

Nityananda Sarma et al. [9] have proposed a simple model for computing link stability and route stability based on received signal strengths.

Tomonori Kagi et al. [10] have proposed a reliability improvement method in mobile ad hoc networks by applying network coding encoded by a relay node. Therefore, reliability is improved without requiring the source node to send redundant encoding packets.

Srinivas Sethi et al [11] have proposed an Optimized Reliable Ad hoc On-demand Distance Vector (ORAODV) scheme that offers quick adoption to dynamic link conditions, low processing and low network utilization in ad hoc network.

V. Ramesh et al [12] have proposed a dynamic source routing protocol in which the mobile node uses signal power strength from the received packets to predict the link breakage time, and sends a warning to the source node of the packet if the link is soon-to-be-broken.

Khalid Zahedi et al [13] have proposed and implemented a new approach for solving the problem of link breakages in MANET in Dynamic Source Routing (DSR) routing protocol.

Senthilkumar Maruthamuthu et al [14] have discussed the new protocol QPHMP-SHORT with multiple QoS constraints based on the QoS parameters namely delay, jitter, bandwidth, and cost metrics between source and destination.

III. PROPOSED MODEL FOR NODE SELECTION USING FUZZY LOGIC BASED TECHNIQUE

The proposed protocol uses Fuzzy based decision making technique to verify the status of a node. As an outcome of fuzzy decision rules, the node status can be considered as Little Strong, Strong, Very Strong, Lower Medium, Medium, Higher Medium, Little Weak, Weak, and Very Weak. Before a node transmits the data to the next node, it checks the status of that node. This estimated decision is stored in a routing table and is exchanged among all neighbors using a status flag with RREQ message. Data packets are transmitted through intermediate nodes that are in the routing table, whenever the source node sends data to the destination. If the status of a node is Little Weak, Weak or Very Weak then the sending does not transmit the packet to that node, if the status of a node is Lower Medium, Medium or Higher then that node is considerable for receiving the packet from sender node but if the status of a node is Little Strong, Strong, Very Strong then the sending node will choose this node for efficient data packet transmission. The process of node selection consists of two input functions that transform the system inputs into fuzzy sets such as Noise Factor and Signal Strength of paths between any two nodes. Fuzzy set for Noise Factor and Signal Strength in the protocol can be defined as,

$$A = \{(d, \mu_A(n))\}, n \in N_s$$

And

$$B = \{(e, \mu_B(s))\}, s \in S_i$$

Where,

N_s are universe of discourse for Noise and S_i is a universe of discourse for Signal Strength,

n and s are particular elements of N_s and S_i respectively,

$\mu_A(n)$, $\mu_B(s)$ are membership functions, find the degree of membership of the element in a given set.

Membership functions for Noise and Signal Strength are defined from Figure 1, as follows:

$$\mu_A(n) = \left\{ \begin{array}{ll} 0, & \text{if } n > TH_2 \\ (n - TH_1) / TH_1 - TH_2, & \text{if } TH_1 \geq n \geq TH_2 \\ 1, & \text{if } n \leq TH_1 \end{array} \right\}$$

$$\mu_B(s) = \left\{ \begin{array}{ll} 0, & \text{if } s \leq TH_1 \\ (TH_1 - s) / TH_1 - TH_2, & \text{if } TH_1 < s < TH_2 \\ 1, & \text{if } s \geq TH_2 \end{array} \right\}$$

Where,

TH_1 = Threshold to activate system

TH_2 = Threshold which identifies the level of activeness

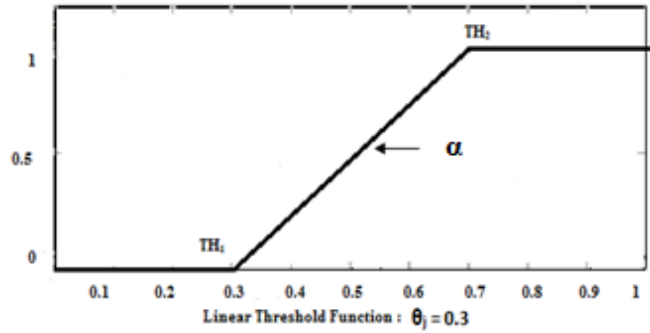


Fig. 1. GRAPH SHOWING MINIMUM AND MAXIMUM THRESHOLD FOR ANY INPUT VARIABLE

A fuzzy relation is a relation between elements of N_s and elements of S_i , described by a membership function,

$$\mu_{N_s \times S_i}(n, s), n \in N_s \text{ and } s \in S_i$$

Now applying AND fuzzy operator i.e. $\min(\wedge)$ on fuzzy relation,

$$\mu_A(n) \wedge \mu_B(s) = \min(\mu_A(n), \mu_B(s)) = \left\{ \begin{array}{ll} \mu_A(n), & \text{if and only if } \mu_A(n) \leq \mu_B(s) \\ \mu_B(s), & \text{if and only if } \mu_A(n) \geq \mu_B(s) \end{array} \right\}$$

A. Rule Evaluation

The proposed protocol is a fuzzy logic based protocol for the selection of successor node for data packet transmission. The process of route selection consists of two input functions that transform the system inputs into fuzzy sets such as Noise Factor and Signal Strength of paths between any two nodes. The Table 1 of Input Function uses three membership functions to show the varying degrees of input variables.

TABLE I. INPUT FUNCTION

| Input | Membership | | |
|-----------------|------------|----------|--------|
| Noise Factor | Light | Medium | Heavy |
| Signal Strength | Weak | Adequate | Strong |

In Table 2, 9 membership functions are defined that represent the varying probabilities of the fuzzy output defined for each of the rules in the rule set and the graph for the same is shown in Figure 2. Then an aggregation of these fuzzy probabilistic values into a single fuzzy output is represented in a detailed rule-set (Table 3).

TABLE II. OUTPUT FUNCTION

| Output | Membership |
|--------|------------|
|--------|------------|

| | |
|-----------------------------------|--|
| Probability (P _{ni}) | Little Strong, Strong, Very Strong, Lower Medium, Medium, Higher, Medium, Little Weak, Weak, Very Weak |
|-----------------------------------|--|

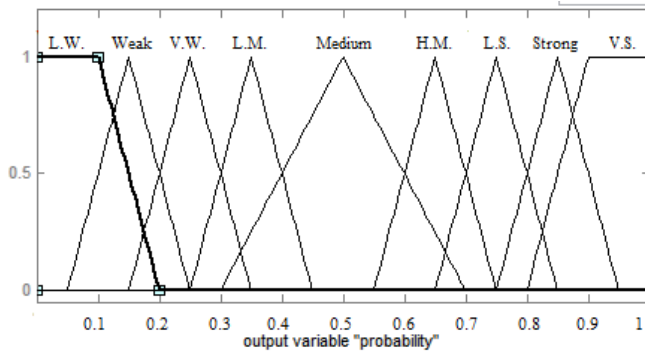


Fig. 2. GRAPH SHOWING ALL POSSIBLE PROBABILITIES OF OUTPUT VARIABLE

B. The Proposed Rule set

The given protocol defines all the possible combinations of the different membership functions for the two input variables that results in 9 rules for the fuzzy inference shown in Table 3.

TABLE III. RULE SET TABLE

| Noise Factor | Signal Strength | Probability |
|--------------|-----------------|---------------|
| Light | Weak | Higher Medium |
| Light | Adequate | Strong |
| Light | Strong | Very Strong |
| Medium | Weak | Little Weak |
| Medium | Adequate | Medium |
| Medium | Strong | Little Strong |
| Heavy | Weak | Very Weak |
| Heavy | Adequate | Weak |
| Heavy | Strong | Lower Medium |

IV. VALIDATION AND ANALYSIS

Let us consider a network of 5 nodes and 6 edges.

Now suppose the noise factor at each edge as:

$$N_s = \{0.1, 0.3, 0.4, 0.7, 0.8, 0.9\}$$

And the signal strength at each edge as:

$$S_i = \{0.2, 0.3, 0.5, 0.6, 0.9, 0.1\}$$

A membership function based on the noise at each edge and its graphical representation is shown in Figure-2

$$\mu_{\text{Noise}}(n) = \begin{cases} 0, & \text{if } \text{Noise}(n) \geq 0.8 \text{ (TH}_2\text{)} \\ (0.8 - \text{Noise}(n))/0.2, & \text{if } 0.6 < \text{Noise}(n) < 0.8 \\ 1, & \text{if } \text{Noise}(n) \leq 0.6 \end{cases}$$

- Rule 1**
IF Noise Factor is Light AND Signal Strength is Weak
THEN Probability is Higher Medium
- Rule 2**
IF Noise Factor is Light AND Signal Strength is Adequate
THEN Probability is Strong
- Rule 3**
IF Noise Factor is Light AND Signal Strength is Strong
THEN Probability is Very Strong
- Rule 4**
IF Noise Factor is Medium AND Signal Strength is Weak
THEN Probability is Little Weak
- Rule 5**
IF Noise Factor is Medium AND Signal Strength is Adequate
THEN Probability is Medium
- Rule 6**
IF Noise Factor is Medium AND Signal Strength is Strong
THEN Probability is Little Strong
- Rule 7**
IF Noise Factor is Heavy AND Signal Strength is Weak
THEN Probability is Very Weak
- Rule 8**
IF Noise Factor is Heavy AND Signal Strength is Adequate
THEN Probability is Weak
- Rule 9**
IF Noise Factor is Heavy AND Signal Strength is Strong
THEN Probability is Lower Medium

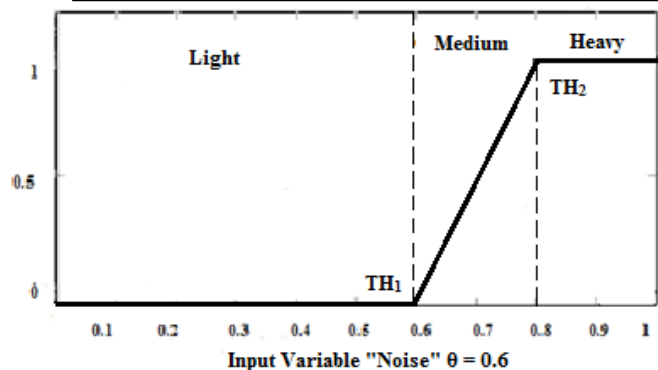


Fig. 2. Graph showing membership functions for input variable "Noise"

A membership function based on the Signal Strength at each edge and its graphical representation is shown in Figure-3

$$\mu_{\text{Signal}}(s) = \begin{cases} 0, & \text{if } \text{Signal}(s) \leq 0.3(\text{TH}_1) \\ (\text{Signal}(s) - 0.3)/0.4, & \text{if } 0.3 < \text{Signal}(s) < 0.7 \\ 1, & \text{if } \text{Signal}(s) \geq 0.7 \end{cases}$$

{0.2| weak, 0.3| weak, 0.4| Adequate, 0.7| Adequate, 0.8| Strong, 0.9| Strong}

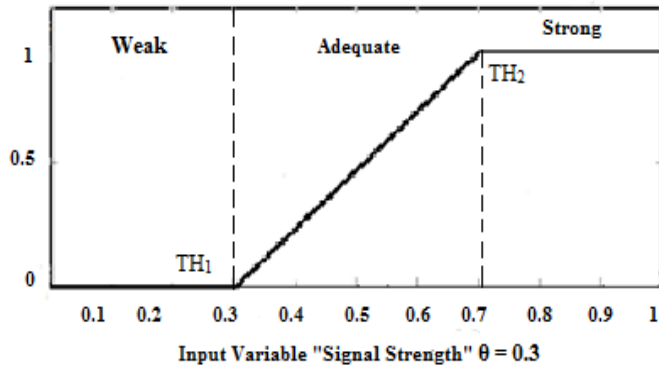


Fig. 3. GRAPH SHOWING MEMBERSHIP FUNCTIONS FOR INPUT VARIABLE "SIGNAL STRENGTH"

Now calculate the degree of membership of Noise and Signal Strength using the above defined membership functions for both of these input variables which is shown in Table 4 and Table 5.

Degree of membership of Noise

| Noise (Ns) | Degree of Lightness |
|------------|---------------------|
| 0.1 | 1 |
| 0.3 | 1 |
| 0.4 | 1 |
| 0.7 | 0.5 |
| 0.8 | 0 |
| 0.9 | 0 |

In Table 4 for the Noise factors {0.1, 0.3, 0.4, 0.7, 0.8, 0.9} the degree of memberships are {1, 1, 1, 0.5, 0, 0} respectively. According to fuzzy output the membership of the above noise factors are,

{0.1| weak, 0.3| weak, 0.4| weak, 0.7| Considerable, 0.8| Considerable, 0.9| heavy}

TABLE IV. DEGREE OF MEMBERSHIP OF SIGNAL STRENGTH

| Signal (Si) | Degree of Strongness |
|-------------|----------------------|
| 0.2 | 0 |
| 0.3 | 0 |
| 0.5 | 0.5 |
| 0.6 | 0.75 |
| 0.9 | 1 |
| 01 | 1 |

In Table 5 for the Signal Strengths {0.2, 0.3, 0.5, 0.6, 0.9, 1} the degree of memberships are {0, 0, 0.5, 0.75, 1, 1} respectively. According to fuzzy output the memberships of the above Signal Strengths are,

Now create Table 6 that shows the fuzzy relation between membership functions of noise factor and signal strength.

TABLE V. FUZZY RELATION ON MEMBERSHIP VALUE OF SIGNAL STRENGTH AND NOISE

| $\frac{Si}{Ns}$ | 0.2 | 0.3 | 0.5 | 0.6 | 0.9 | 1 |
|-----------------|----------------|----------------|------------------|-------------------|----------------|----------------|
| 0.1 | 1 \wedge 0 | 1 \wedge 0 | 1 \wedge 0.5 | 1 \wedge 0.75 | 1 \wedge 1 | 1 \wedge 1 |
| 0.3 | 1 \wedge 0 | 1 \wedge 0 | 1 \wedge 0.5 | 1 \wedge 0.75 | 1 \wedge 1 | 1 \wedge 1 |
| 0.4 | 1 \wedge 0 | 1 \wedge 0 | 1 \wedge 0.5 | 1 \wedge 0.75 | 1 \wedge 1 | 1 \wedge 1 |
| 0.7 | 0.5 \wedge 0 | 0.5 \wedge 0 | 0.5 \wedge 0.5 | 0.5 \wedge 0.75 | 0.5 \wedge 1 | 0.5 \wedge 1 |
| 0.8 | 0 \wedge 0 | 0 \wedge 0 | 0 \wedge 0.5 | 0 \wedge 0.75 | 0 \wedge 1 | 0 \wedge 1 |
| 0.9 | 0 \wedge 0 | 0 \wedge 0 | 0 \wedge 0.5 | 0 \wedge 0.75 | 0 \wedge 1 | 0 \wedge 1 |

The result of the AND (\wedge) operation process on membership values of Signal Strength and Noise shown in Table 7.

TABLE VI. RESULT AFTER AND FUZZY OPERATION

| $\frac{Si}{Ns}$ | 0.2 | 0.3 | 0.5 | 0.6 | 0.9 | 1 |
|-----------------|-----|-----|-----|------|-----|-----|
| 0.1 | 0 | 0 | 0.5 | 0.75 | 1 | 1 |
| 0.3 | 0 | 0 | 0.5 | 0.75 | 1 | 1 |
| 0.4 | 0 | 0 | 0.5 | 0.75 | 1 | 1 |
| 0.7 | 0 | 0 | 0.5 | 0.5 | 0.5 | 0.5 |
| 0.8 | 0 | 0 | 0 | 0 | 0 | 0 |
| 0.9 | 0 | 0 | 0 | 0 | 0 | 0 |

The possible combinations of distance and energy with higher membership value shown in Table 8:

TABLE VII. OUTPUT TABLE

| $\frac{Si}{Ns}$ | 0.9 | 1 |
|-----------------|-----|---|
| 0.1 | 1 | 1 |
| 0.3 | 1 | 1 |
| 0.4 | 1 | 1 |

The degree of membership of noise and signal is shown in Table 9.

TABLE VIII. OUTPUT TABLE WITH THE DEGREE OF MEMBERSHIP

| Noise (Ns) | Degree of membership (Noise) | Signal (Si) | Degree of Strongness (Signal) |
|------------|------------------------------|-------------|-------------------------------|
| 0.1 | Light | 0.9 | Strong |
| 0.3 | Light | 1 | Strong |
| 0.4 | Light | | |

The output probability for these values is "Very Strong" as "Noise is Light and Signal strength is strong". Now all the

resultant possible combinations of noise and signal strength are:

- Noise factor = 0.1 and Signal strength = 0.9
- Noise factor = 0.1 and Signal strength = 1
- Noise factor = 0.3 and Signal strength = 0.9
- Noise factor = 0.3 and Signal strength = 1
- Noise factor = 0.4 and Signal strength = 0.9
- Noise factor = 0.4 and Signal strength = 1.

The effective edge to be selected can have any of the above combinations. But the perfect combination among all combinations is when noise factor is 0.1 and signal strength is 1, which will be perfect for transmission of data packet to next successor node.

A. Performance Evaluation

The proposed protocol is a fuzzy logic based protocol for the efficient successive edge selection for data packet transmission. The best possible outcomes obtained from the above proposed fuzzy logic based protocol helps a mobile Ad-Hoc network to choose an efficient edge on the basis of parameters like environment noise and signal strength.

The protocol improves the performance of a route by increasing network life time, reducing link failure and selecting best node for forwarding the data packet to next node.

V. CONCLUSIONS

The proposed protocol an Efficient Routing Protocol under Noisy Environment for Mobile Ad Hoc Networks using Fuzzy Logic (ERP) is efficient for transmission of data. The status of the node is verified before a node transmits the data to the next node. The designed fuzzy logic controller determines, best outcome from all the possible combinations of offered signal strength and noise. If the status is normal or strong, then it transmits the packet to the next node. The validation shows that the fuzzy based effective edge selection technique increases packet delivery ratio, decreases link failure, lowers error rate and increases throughput.

REFERENCES

- [1] Wing Ho Yuen, Heung-no Lee and Timothy D. Andersen "A simple and effective cross layer networking system for Mobile Ad Hoc Networks", in: PIMRC 2002, vol. 4, September 2002, pp. 1952-1956.
- [2] H.M. Tsai, N. Wisitpongphan, and O.K. Tonguz, "Link-quality aware AODV protocol," in Proc. IEEE International Symposium on Wireless Pervasive Computing (ISWPC) 2006, Phuket, Thailand, January 2006
- [3] E. Royer and C.-K. Toh, "A review of current routing protocols for Ad Hoc mobile wireless networks," IEEE Personal Communications Magazine, vol. 6, No. 2, April 1999.
- [4] Fuad Alnajjar and Yahao Chen "SNR/RP aware routing algorithm cross-layer design for MANET" in International Journal of Wireless & Mobile Networks (IJWMN), Vol 1, No 2, November 2009.
- [5] H Devi M. and V. Rhymend Uthariaraj "Fuzzy based route recovery technique for Mobile Ad Hoc Networks" in European Journal of Scientific Research ISSN 1450-216X Vol.83 No.1 (2012), pp.129-143.
- [6] Supriya Srivastava, A.K. Daniel "Energy-efficient position based routing protocol for MANET in proceedings of International Conference in computing, engineering and information technology (ICCEIT), 2012.
- [7] Junghwi Jeon., Kiseok Lee., and Cheeha Kim., "Fast route recovery scheme for Mobile Ad Hoc Networks", IEEE International Conference on Information Networking, 2011.
- [8] Merlinda Drini & Tarek Saadawi . "Modeling wireless channel for Ad-Hoc network routing protocol", ISCC Marakech Morocco, July 2008, Page(s): 549-555
- [9] Nityananda Sarma., and Sukumar Nandi., "Route stability based QoS routing in mobile Ad Hoc networks", IEEE international Conference on Emerging Trends in Engineering and Technology, 2008.
- [10] Tomonori Kagi., and Osamu Takahashi., "Efficient reliable data transmission using network coding in MANET multipath routing environment", Springer, KES, 2008.
- [11] Srinivas Sethi., and Siba K. Udgata., "Optimized and reliable AODV for MANET", International Journal of Computer Applications, 2010.
- [12] V.Ramesh., Dr.P.Subbaiah., and K.Sangeetha Supriya., "Modified DSR (Preemptive) to reduce link breakage and routing overhead for MANET using Proactive Route Maintenance (PRM)", Global Journal of Computer Science and Technology, 2010.
- [13] Khalid Zahedi., and Abdul Samad Ismail., "Route maintenance approach for link breakage prediction in mobile Ad Hoc networks", International Journal of Advanced Computer Science and Applications ((IJACSA), 2011.
- [14] Senthilkumar Maruthamuthu., and Somasundaram Sankaralingam., "QoS aware power and hop count constraints routing protocol with mobility prediction for MANET using SHORT", International Journal of Communications, Network and System Sciences, 2011.

Lecturer's e-Table (Server Terminal) Which Allows Monitoring the Location at Where Each Student is Looking During Lessons with e-Learning Contents Through Client Terminals

Kohei Arai

Graduate School of Science and Engineering
Saga University
Saga City, Japan

Abstract—Lecturer's e-Table (Server Terminal) which allows monitoring the location at where each student is looking during lessons with e-learning contents through Client Terminals is proposed. Through the lessons with e-learning contents through client terminal, it is obvious that student can take the lessons much efficiently when the student are looking at the appropriate location at where the lecturers would like the students look at. It, however, is not always that the student is looking at the appropriate location even if the system indicates the appropriate location. The proposed system of lecturer's e-table of server terminal allows monitoring the location at where each student is looking. Therefore, lecturer can make a caution to the student for the appropriate location at where the student has to be looking at. Through experiments with students, it is found that the achievement test score with the indication of appropriate location is much better than that without the indication. Also, learning efficiency with the caution is much greater than that without the caution.

Keywords—e-learning; line of sight estimation; e-table for lecturers; eye based Human-Computer Interaction;

I. INTRODUCTION

e-learning is widely used for supplemental lessons with face-to-face lectures in a worldwide basis. The current problems of e-learning system is improvement of learning efficiency, effective e-learning contents (comprehensive), band width limitation, limitation of display size, question answering system, and authentication of students, etc. Other than these, students' manner for taking lessons is another problem. It is not always that the students' attitude for the lessons is properly right. Some of the students are looking at a different location at where e-learning content creators would like the students are looking at. Therefore, the achievement test score of the students is not good enough.

Lecturer's e-Table (Server Terminal) which allows monitoring the location at where each student is looking during lessons with e-learning contents through Client Terminals is proposed.

Through the lessons with e-learning contents through client terminal, it is obvious that student can take the lessons much efficiently when the student are looking at the

appropriate location at where the lecturers would like the students look at. It, however, is not always that the student is looking at the appropriate location even if the system indicates the appropriate location.

The proposed system of lecturer's e-table of server terminal allows monitoring the location at where each student is looking. Therefore, lecturer can make a caution to the student for the appropriate location at where the student has to be looking at. Through experiments with students, it is found that the achievement test score with the indication of appropriate location is much better than that without the indication. Also, learning efficiency with the caution is much greater than that without the caution.

Computer key-in system by human eyes only (just by sight) is proposed [1], [2]. The system allows key-in when student looks at the desired key (for a while or with blink) in the screen keyboard displayed onto computer screen. Also blink detection accuracy had to be improved [3], [4].

Meanwhile, influence due to students' head pose, different cornea curvature for each student, illumination conditions, background conditions, reflected image (environmental image) on students' eyes, eyelashes affecting to pupil center detection, un-intentional blink, etc. are eliminated for gaze detection accuracy improvement [5]-[11]. Also e-learning system with student confidence level evaluation is proposed [12]. Furthermore, gaze estimation method and accuracy evaluation are well reported [13]-[23].

The following section describes the proposed system followed by implementation of the system. Then some experiments with students is describes together with achievement test score. Finally, conclusion is described with some discussions.

II. PROPOSED SYSTEM

A. System Configuration of the Proposed e-learning System with e-table for Lecturer

Figure 1 shows the system configuration of the proposed e-learning system with e-table for lecturer.

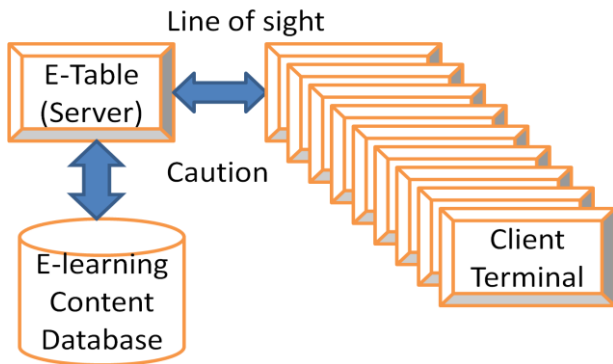


Fig. 1. system configuration of the proposed e-learning system with e-table for lecture

There is e-learning content database under the e-learning server. The server provides e-learning contents to the client terminals through e-Table of the e-learning server. In the client terminal, line of sight estimation system is equipped. Therefore, the lecturers can identify the location at where the students are looking. The location can be identified on the e-learning contents. The lecturers may choose the client display image by student by student. Therefore, the lecturers may awake the difference between the location at where lecturers would like the student in concern is looking and the location at where the student in concern is looking. If the location difference is too large, then the lecturers may give a caution to the student. It also can be done automatically. The system program measures the difference then the system provides a caution when it is beyond a threshold.

B. Server and Client Display Layout

Fundamentally, the proposed e-learning system assumes synchronized mode of e-learning because the synchronized mode is much effective than on-demand mode. Therefore, lecturers may change e-learning operations freely. The proposed e-learning system may be used in on-demand mode as well.

There is e-Table for the lecturer as server machine with e-learning content database under the e-table. On the other hand, there are some clients terminals for students with line of sight estimation system which allows monitoring the display monitor location at where the student is looking. Lecture can monitor the students are looking on the display monitor during lessons by using the system.

Figure 2 shows the proposed e-Table server display image layout. The e-Table server display layout is divided into three portions, (a) portion of client display image with switch radio button for selection of student number of client display image, (b) server display image, and (c) control panel for manipulation of e-learning operations including stage selection. Using this e-Table server, lecturers can take a look at the client display image in concern by selecting the student with radio button. Lecturers also can control e-learning operation.

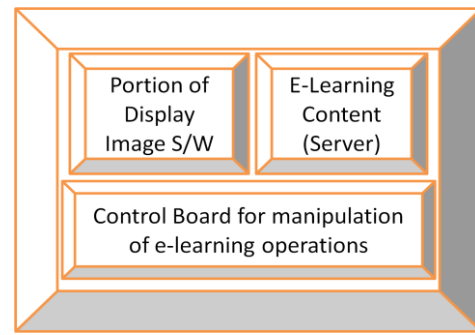


Fig. 2. Proposed e-Table server display image layout (Functions)

C. Line of Sight Estimation

One of the key issues here is line of sight estimation. Students wear a two Near Infrared: NIR cameras (NetCowBoy, DC-NCR130¹) mounted glass. One camera acquires student eye while the other camera acquires computer screen which displays e-learning content. Outlook of the glass is shown in Figure 3 while the specification of NIR camera is shown in Table 1, respectively.



Fig. 3. Proposed glass with two NIR cameras

TABLE I. SPECIFICATION OF NIR CAMERA

| | |
|----------------------|-------------------------|
| Resolution | 1,300,000pixels |
| Minimum distance | 20cm |
| Frame rate | 30fps |
| Minimum illumination | 30lx |
| Size | 52mm(W)x70mm(H)x65mm(D) |
| Weight | 105g |

An example of the acquired eye image with the NIR camera is shown in Figure 4 together with the binarized detected cornea and the extracted pupil image. In the NIR eye image shows a clearly different cornea from the sclera. In this case, although influence due to eyelash and eyelid is situated at the end of eye, not so significant influence is situated in the eye center. Also pupil is clearly extracted from the cornea center. NIR camera which shown in Table 1 has the six NIR Light Emission Diode: LEDs² which are situated along with the circle shape. The lights from the six LEDs are also detected in the extracted cornea.

¹ <http://www.digitalcowboy.jp/support/drivers/dc-ncr130/index.html>

² <http://www.digitalcowboy.jp/>

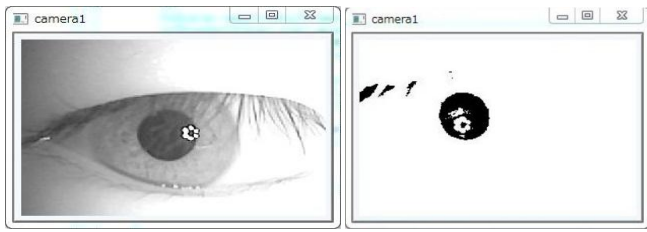


Fig. 4. An example of the acquired eye image with the NIR camera together with the binarized detected cornea and the extracted pupil image

Firstly, student has to conduct calibration for adjust the distance between the student and the computer display. In the calibration, student has to look at the four corners of the checkerboard which is displayed on the computer screen as shown in Figure 5.

Red rectangles in Figure 6 indicate the programming commands, the detected binarized cornea, and three corners of the checkerboard images.

Two images which are acquired with the camera 1 for student's eye and the camera 2 for the image of which student is now looking at.

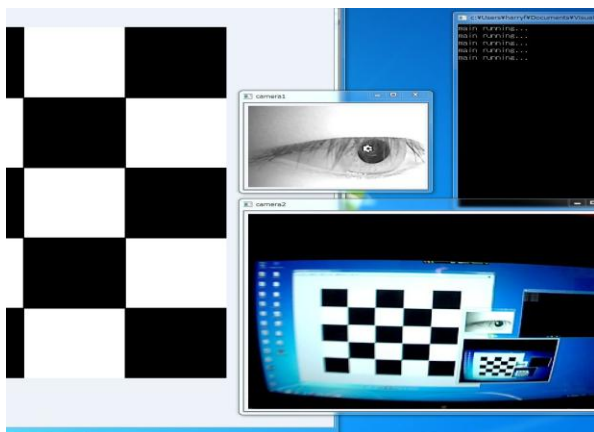


Fig. 5. An example of computer screen image which is showing commands for the computer program, student's eyes image together with checkerboard for calibration which allows estimation of distance between student and the computer screen.

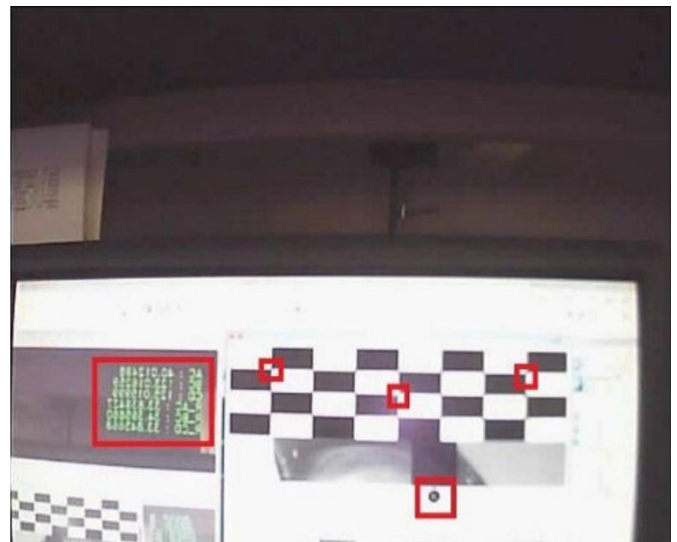


Fig. 6. The programming commands, the detected binarized cornea, and three corners of the checkerboard images.

At the bottom right in Figure 7 shows the image which is acquired with the camera 2. With the camera 1 acquired image, the system can estimate the gaze location. At the same time, the system can acquire the image of which the student is looking at.

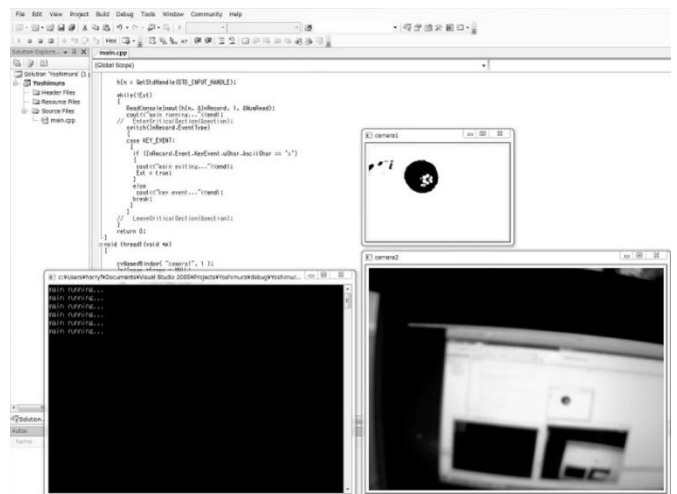


Fig. 7. Example of the image which is acquired with the camera 2 at the bottom right.

III. IMPLEMENTATION AND EXPERIEMENTS

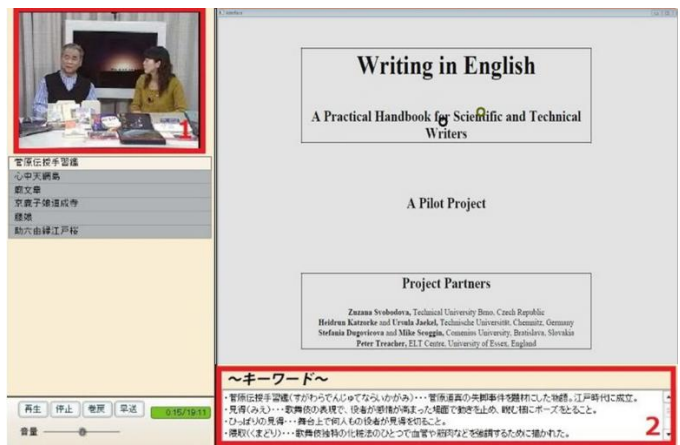
A. Implementation

Figure 8 (a) shows an example of screen shot image of the proposed e-Table server display monitor of the e-table while Figure 8 (b) shows example of the display terminal of the client machine. On the top right portion of Figure 7 (a), there is e-learning content provided by the server while the client image can be seen on the top left portion with the black circle which indicates the location at where the lecturer would like the student is looking and with the green circle which indicates the location at where the student is looking. Also the student number is included in the client display image with radio button. Therefore, the lecture can change the client display image by student by student.

On the bottom right portion of Figure 8 (a), there is control panel for e-learning content reproducing while there is the other functionalities of the e-learning system is situated on the bottom left portion. There are functions, Question and Answer: Q/A system, Bulletin Board System: BBS, Chatting, Making a Caution: MaC and so on.

Figure 8 (b) shows client display image. The location at where the lecturer would like the student is looking is indicated with red circle by frame by frame.

The experiment is conducted with the Document entitled "Writing in English –A Practical Handbook for Scientific and Technical Writers–" created by the European Commission of Leonard da Vinci Programme³.



(b)Client display layout

Fig. 8. Example of server and client display layout

B. Gaze Estimation Accuracy Evaluation

The gaze instability is essential parameter in our system. It could influence typing accuracy. The ideal eye-based HCI should have gaze instability close to zero. Unfortunately, the zero gaze instability is difficult to be reached due to several causes such as flicker of the camera, noise, etc. Our proposed method will benefit on system with high gaze instability (unstable gaze output). We conducted gaze instability measurement by user follows the target point while we recorded the trajectory point of the gaze. The result is shown in **Error! Reference source not found.9**.



(a)E-Table server display layout

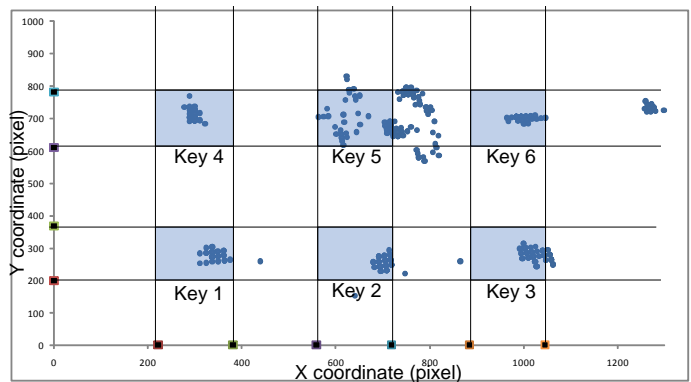


Fig. 9. Gaze instability. A single person looks at fixed five points on the screen while we recorded the trajectory points.

³ <http://afendirojan.files.wordpress.com/2010/04/writing-in-english-a-practical-handbook-for-scientific-and-technical-writers-2000.pdf>

TABLE II. STANDARD DEVIATION OF GAZE INSTABILITY

| Key | Standard Deviation (pixels) | |
|-----|-----------------------------|----------|
| | x | y |
| 1 | 13.19866 | 11.73971 |
| 2 | 11.38451 | 13.10489 |
| 3 | 20.65958 | 15.30955 |
| 4 | 7.167983 | 13.73321 |
| 5 | 108.7133 | 60.40783 |
| 6 | 100.1875 | 13.07776 |

In Error! Reference source not found.9, the trajectory points were taken while user was looking at 6 keys serially. This figure shows that at key 5, the gaze result has more scattered than others. It was caused by the position of eye at this key little bit occluded and it made the gaze result become unstable (the instability become increase). In other key, there is significant disturbance. The only noise from camera made the instability.

The standard deviation of gaze instability of each key is shown in Figure 9. It shows that our gaze estimation method has worst instability on key number five about 124 pixels. Therefore, gaze estimation accuracy is not good enough to identify one specific key.

Figure 10 shows a relation between blinking and the distance between the locations at where the student is looking and at where the lecturer would like the student is looking. As shown in Figure 10, it is fund that the timings are coincident between blinking and the distance is large as shown with red lines in Figure 10.

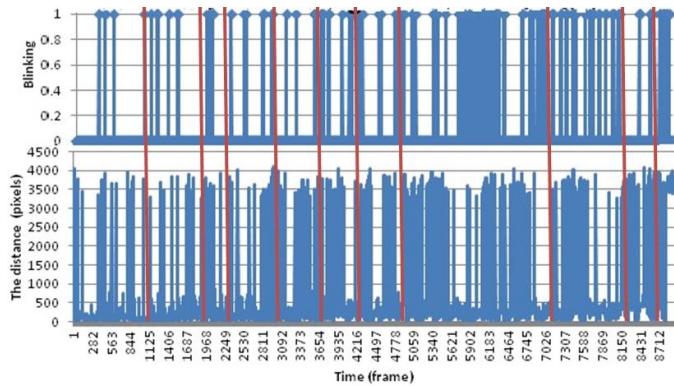


Fig. 10. Relation between blink timing and the timing at when the distance between the locations at where the student is looking and at where the lecturer would like the student is looking is large

IV. CONCLUSION

Lecturer's e-Table (Server Terminal) which allows monitoring the location at where each student is looking during lessons with e-learning contents through Client Terminals is proposed. Through the lessons with e-learning contents through client terminal, it is obvious that student can take the lessons much efficiently when the student are looking at the appropriate location at where the lecturers would like the students look at. It, however, is not always that the student

is looking at the appropriate location even if the system indicates the appropriate location.

The proposed system of lecturer's e-table of server terminal allows monitoring the location at where each student is looking. Therefore, lecturer can make a caution to the student for the appropriate location at where the student has to be looking at. As the results from the experiment through e-learning lessons with Writing in English document, it is found that students made blinking when the distance between the location at where the lecturer would like the student to look and the location at where the student is looking is large. This implies that the student loses his/her concentration to the content. Therefore, achievement test result is good when the distance is small and vice versa.

Through experiments with students, it is found that the achievement test score with the indication of appropriate location is much better than that without the indication. Also, learning efficiency with the caution is much greater than that without the caution.

ACKNOWLEDGMENT

The author would like to thank Mr. Kagoyama his efforts through experiments and simulations.

REFERENCES

- [1] Arai K. and H. Uwataki, Computer key-in based on gaze estimation with cornea center determination which allows students' movement, Journal of Electrical Engineering Society of Japan (C), 127, 7, 1107-1114, 2007
- [2] Arai K. and H. Uwataki, Computer input system based on viewing vector estimation with iris center detection from face image acquired with web camera allowing students' movement, Electronics and Communication in Japan, 92, 5, 31-40, John Wiley and Sons Inc.,2009.
- [3] Arai K., and M. Yamaura, Blink detection accuracy improvements for computer key-in by human eyes only based on molforgic filter, Journal of Image Electronics Engineering Society of Japan, 37, 5, 601-609, 2008.
- [4] Arai K. and R. Mardiyanto, Real time blinking detection based on Gabor filter, International Journal of Human Computer Interaction, 1, 3, 33-45, 2010.
- [5] Arai K. and R. Mardiyanto, Camera mouse and keyboard for handicap person with trouble shooting capability, recovery and complete mouse events, International Journal of Human Computer Interaction, 1, 3, 46-56, 2010.
- [6] Arai K. and M. Yamaura, Computer input with human eyes only use two Purkinje images which work in a real time basis without calibration, International Journal of Human Computer Interaction, 1, 3, 71-82, 2010.
- [7] Arai K., and K. Yajima, Communication aid based on computer key-in with human eyes only, Journal of Electric Engineering Society of Japan, (C), 128 -C, 11, 1679-1686, 2008.
- [8] Djoko P., R. Mardiyanto and K. Arai, Electric wheel chair control with gaze detection and eye blinking, Artificial Life and Robotics, AROB Journal, 14, 694,397-400, 2009.
- [9] Arai K. and K. Yajima, Communication Aid and Computer Input System with Human Eyes Only, Electronics and Communications in Japan, 93, 12, 1-9, John Wiley and Sons, Inc., 2010.
- [10] Arai K., R. Mardiyanto, A prototype of electric wheel chair control by eye only for paralyzed student, Journal of Robotics and Mechatronics, 23, 1, 66-75, 2010.
- [11] Arai K. and K. Yajima, Robot arm utilized having meal support system based on computer input by human eyes only, International Journal of Human Computer Interaction, 2, 1, 120-128, 2011.
- [12] K.Arai, E-learning system which allows students' confidence level evaluation with their voice when they answer to the questions during

- achievement tests, International Journal of Advanced Computer Science and Applications, 3, 9, 80-84, 2012.
- [13] Ibanga. s.l. : <http://abcnews.go.com/GMA/OnCall/story?id=7385174&page=1>, April 21, 2009.
- [14] Foundation, Christopher and Dana Reeve. s.l. : <http://www.christopherreeve.org/>.
- [15] Hawking, Official website of Professor Stephen W. s.l. : <http://www.hawking.org.uk>.
- [16] EyeWriter: low-cost, open-source eye-based drawing system. s.l. : <http://www.crunchgear.com/2009/08/25/%20eyewriter-low-cost-%20open-source-eye-%20based-drawing-system/>, 2011.
- [17] Improvement of blinking detection in determination of key selection of computer input system with line of sight vector estimation by means of morphologic filter. Kohei, Arai and Yamaura. 5, 2008, Journal of Digital Image, Vol. 37, pp. 601-608.
- [18] *Eye-controlled human/computer interface using the line-of-sight and the intentional blink*. Park K.S., Lee K.T. s.l. : Computers and Industrial Engineering, 1993. Vols. 30-3, pp. 463-473.
- [19] *EyeKeys: A Real-Time Vision Interface Based on Gaze Detection from a Low-Grade Video Camera*. John J. Magee, Matthew R. Scott, Benjamin N. Waber, Margrit Betke. 2004. Conference on Computer Vision and Pattern Recognition Workshop (CVPRW'04). Vol. 10, p. 159.
- [20] *The Indirect Keyboard Control System by Using the Gaze Tracing Based on Haar Classifier in OpenCV*. ChangZheng Li, Chung-Kyue Kim, Jong-Seung Park. 2009. Proceedings of the International Forum on Information Technology and Applications. pp. 362-366.
- [21] *Scrollable keyboards for casual eye typing*. Spakov, O., & Majaranta, P. 2009. PsychNology Journal. Vol. 7, pp. 159-173.
- [22] Text Input Methods for Eye Trackers Using Off-Screen Targets. Isokoski, P. 2000. Proceedings of the ETRA'00. pp. 15-21.
- [23] *Improving hands-free menu selection using eye gaze glances and fixations*. Tien, G. and Atkins, M. S. 2008. Proceedings of the 2008 Symposium on Eye Tracking Research & Applications. pp. 47-50.

AUTHORS PROFILE

Kohei Arai, He received BS, MS and PhD degrees in 1972, 1974 and 1982, respectively. He was with The Institute for Industrial Science and Technology of the University of Tokyo from April 1974 to December 1978 also was with National Space Development Agency of Japan from January, 1979 to March, 1990. During from 1985 to 1987, he was with Canada Centre for Remote Sensing as a Post Doctoral Fellow of National Science and Engineering Research Council of Canada. He moved to Saga University as a Professor in Department of Information Science on April 1990. He was a councilor for the Aeronautics and Space related to the Technology Committee of the Ministry of Science and Technology during from 1998 to 2000. He was a councilor of Saga University for 2002 and 2003. He also was an executive councilor for the Remote Sensing Society of Japan for 2003 to 2005. He is an Adjunct Professor of University of Arizona, USA since 1998. He also is Vice Chairman of the Commission "A" of ICSU/COSPAR since 2008. He wrote 30 books and published 322 journal papers

Method for 3D Rendering Based on Intersection Image Display Which Allows Representation of Internal Structure of 3D objects

Kohei Arai¹

¹Graduate School of Science and Engineering
Saga University
Saga City, Japan

Abstract—Method for 3D rendering based on intersection image display which allows representation of internal structure is proposed. The proposed method is essentially different from the conventional volume rendering based on solid model which allows representation of just surface of the 3D objects. By using afterimage, internal structure can be displayed through exchanging the intersection images with internal structure for the proposed method. Through experiments with CT scan images, the proposed method is validated. Also one of other applicable areas of the proposed for design of 3D pattern of Large Scale Integrated Circuit: LSI is introduced. Layered patterns of LSI can be displayed and switched by using human eyes only. It is confirmed that the time required for displaying layer pattern and switching the pattern to the other layer by using human eyes only is much faster than that using hands and fingers.

Keywords—3D object display; volume rendering; solid model; afterimage; line of sight vector

I. INTRODUCTION

Computer input by human eyes only is proposed and implemented [1]-[3] together with its application to many fields, communication aids, electric wheel chair controls, having meal aids, information collection aids (phoning, search engine, watching TV, listening to radio, e-book/e-comic/e-learning/etc., domestic helper robotics and so on [4]-[15]. In particular, the proposed computer input system by human eyes only does work like keyboard as well as mouse. Therefore, not only key-in operations but also mouse operations (right and left button click, drag and drop, single and double click) are available for the proposed system.

It is well known that hands, fingers operation is much slower than line of sight vector movements. It is also known that accidental blink is done within 0.3 second. Therefore, the proposed computer input system by human eyes only decides the specified key or location when the line of vector is fixed at the certain position of computer display for more than 0.3 second. In other words, the system can update the key or the location every 0.3 second. It is fast enough for most of all application fields.

Meanwhile, 3D image display and manipulation can be done with 3D display. Attempts are also done with 2D display for 3D image display and manipulation, on the other hands. Most of previous attempts are based on touch panel based

manipulation by hands and fingers. As aforementioned, eyes operations are much faster than hands & fingers operations. Therefore, 3D image display and manipulation method by human eyes only is proposed in this paper.

The proposed method is essentially different from the conventional volume rendering based on solid model which allows representation of just surface of the 3D objects. By using afterimage, internal structure can be displayed through exchanging the intersection images with internal structure for the proposed method. Through experiments with CT scan images, the proposed method is validated. Also one of other applicable areas of the proposed for design of 3D pattern of Large Scale Integrated Circuit: LSI is introduced. Layered patterns of LSI can be displayed and switched by using human eyes only. It is confirmed that the time required for displaying layer pattern and switching the pattern to the other layer by using human eyes only is much faster than that using hands and fingers.

The following section describes the proposed method for 3D volume rendering together with theoretical background followed by some experiments with CT scan of imagery data. Then its applicability for LSI pattern design of 3D display of the layered pattern is discussed. After that, conclusion is described together with some discussions.

II. PROPOSED METHOD AND SYSTEM

A. Basic Idea for the Proposed Method

3D model that displays a picture or item in a form that appears to be physically present with a designated structure. Essentially, it allows items that appeared flat to the human eye to be display in a form that allows for various dimensions to be represented. These dimensions include width, depth, and height.

3D model can be displayed as a two-dimensional image through a process called *3D rendering* or used in a computer simulation of physical phenomena. The model can also be physically created using 3D printing devices.

Models may be created automatically or manually. The manual modeling process of preparing geometric data for 3D computer graphics is similar to plastic arts such as sculpting.

There are some previously proposed methods for 3D display such as tracing object contour and reconstruct 3D object with line drawings, and wireframe representation and display 3D object with volume rendering. There is another method, so called OCT: Optical Coherence Tomography. It, however, quit expensive than the others.

Fundamental idea of the proposed method is afterimage. Response time of human eyes is that the time resolution of human eyes: 50ms~100ms. An afterimage or ghost image or image burn-in is an optical illusion that refers to an image continuing to appear in one's vision after the exposure to the original image has ceased. One of the most common afterimages is the bright glow that seems to float before one's eyes after looking into a light source for a few seconds.

Afterimages come in two forms, negative (inverted) and positive (retaining original color). The process behind positive afterimages is unknown, though thought to be related to neural adaptation. On the other hand, negative afterimages are a retinal phenomenon and are well understood.

Example of 3D image on to 2D display is shown in Figure 1. This is the proposed system concept. In the example, "A" marked 3D image of multi-fidus which is acquired with CT scanner is displayed onto computer screen. "B", "C", ... are behind it.

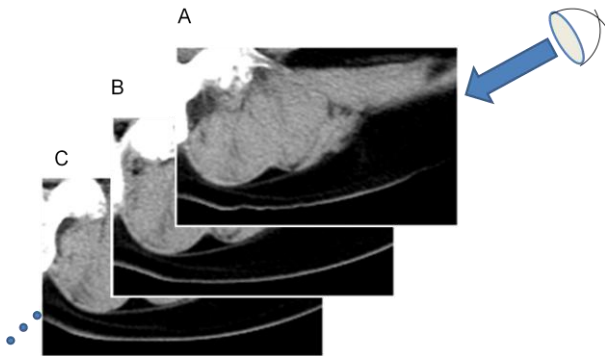


Fig. 1. System Concept

Such this layered 3D images are aligned with depth direction. Attached character "A" to "Z" are transparent and displayed at just beside the layered image at the different locations.

Therefore, user can recognize the character and can select one of those characters by their eye. Arrow shows the line of sight vector. Curser can be controlled by human eyes only. By sweeping the character, 3D images are displayed by layer by layer. Therefore, it looks like time division delay of 3D images.

B. Automatic Mode and Eye Cotroll Mode

There are two modes of 3D display, automatic and eye control modes. In the automatic mode, the layered intersection of images is switched in accordance with the layer order for displays while the displayed intersection of image is switched by human eye in the eye control mode.

III. IMPLEMENTATION AND EXPERIMENTAL RESULTS

C. Displayed Image in Automatic Mode

Implementation of the proposed system is conducted. By using mouse operation by human eyes only, 3D image with different aspects can be recreated and display. It is confirmed that conventional image processing and analysis can be done with mouse operation by human eyes only.

Figure 2 shows the example of displayed layered images. In this example, 1024 of layer images are prepared for 3D object. By displaying the prepared layered images alternatively in automatic mode, 3D object appears on the screen. Furthermore, as shown in Figure 2, internal structure is visible other than the surface of the 3D object. It looks like a semi transparent 3D surface and internal structure in side of the 3D objects.

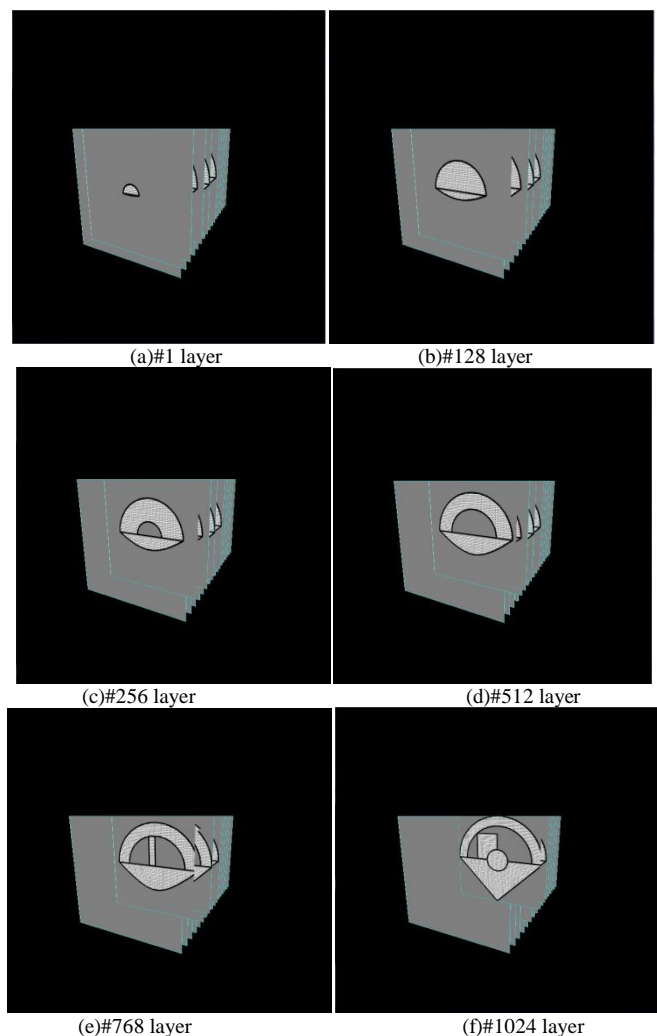


Fig. 2. Example of displayed layered images.

D. Displayed Image in Eye Cotroll Mode

The configuration of the proposed system is shown in Figure 3. As shown in the figure, a user looking at the screen while camera put on top of screen display.

Only camera which mounted on top of screen display is required. Optiplex 755 dell computer with Core 2 Quad 2.66 GHz CPU and 2G RAM is used. We develop our software under C++ Visual Studio 2005 and OpenCv Image processing Library which can be downloaded as free on their website. The specification of IR camera is shown in Table 1. The pointing value is determined based on head poses and eye gaze.

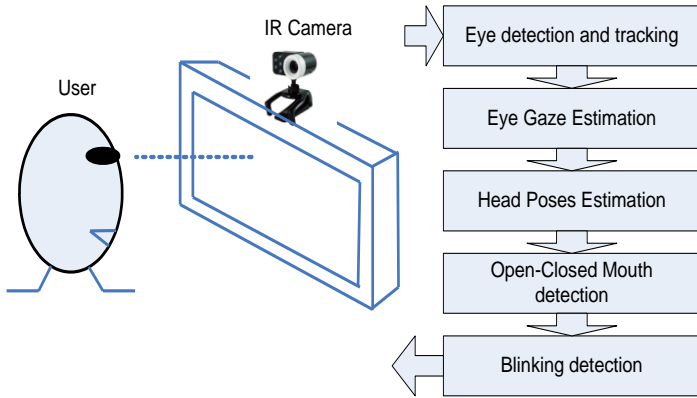


Fig. 3. Camera mouse configurations.

TABLE I. SPECIFICATION OF IR CAMERA

| | |
|---------------------|---------------------------------------|
| Pixel Resolution | 1.3 M 1280×1024 |
| Frame rate | 1280 x 1024: 7.5fps, 640 x 480: 30fps |
| Dimension | 52mm (W) × 65mm (D) × 70mm (H) |
| Weight | 85g |
| Operating condition | 0 - 40deg.C |
| Interface | USB 2.0 |
| IR Illumination | 7 IR LED |

Figure 4 shows definition of success criteria of key input by human eye only.

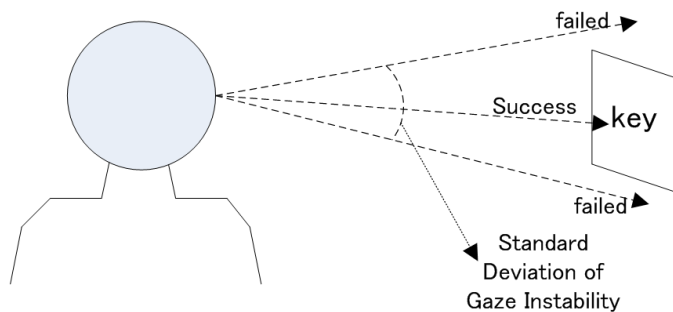


Fig. 4. Accuracy affected by gaze instability and key size

We classify the parameters affected by eye-based Human Computer Interaction: HCI in regard to accuracy as:

- instability of gaze,
- Size of keys and number of keys,
- Position of keys (“zero position” has maximum accuracy because it seems ideal for the eye).

Figure 4 shows how accuracy is affected by gaze instability and key size. The targeted key could be wrong hit if

gaze instability is larger than key size. Gaze instability could be caused by:

- Poor camera image resolutions
- Noise,
- Environmental disturbances such as external light source.

As a result, the method for detecting eye performance has become somewhat unreliable. In addition to the aforementioned factors, distance between eye and target display have also played a part. Accuracy decreases with distance of subject from key and increases when subject gets closer. This phenomenon is a result of the flicker of the camera influencing the calculation of eye gaze, and accuracy is proportional to distance from the key.

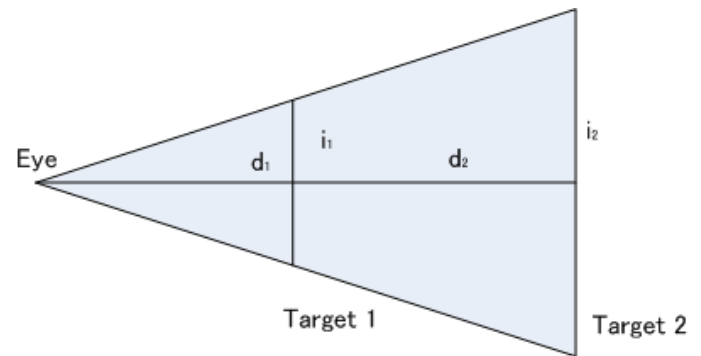


Fig. 5. Instability affected by distance of user-target

The relationship between instability and distance is depicted in **Error! Reference source not found.5**. It shows that the instability is proportional with distance formatted as follow,

$$\frac{i_1}{i_2} = \frac{d_1}{d_2} \tag{1}$$

where i and d are instability and distance respectively. Although gaze instability could be minimized, making it become perfect is difficult due to external disturbances. Now, we would like to show how we achieved perfect accuracy allowing for disturbances. If we assume that key size is S and the instability of gaze result is SD , the accuracy can be formulated as,

$$A \approx \frac{S}{SD} \times 100\% , \text{ if } SD \geq S \tag{2}$$

$$A \approx 100\% , \text{ if } SD < S \tag{3}$$

Gaze estimation accuracy is measured at the middle center to horizontally aligned five different locations with the different angles as shown in Figure 6. The experimental result shows the gaze estimation error at the center middle (No.1) shows zero while those for the angle ranges from -5 to 15 degrees is within 0.2 degree of angle estimation error as shown in Table 2. Because the user looks at the center middle with 5 degree allowance results in 0.2 degree of gaze estimation accuracy.

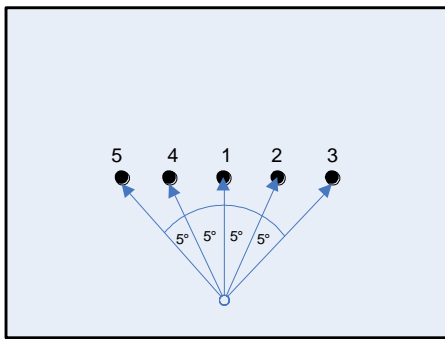


Fig. 6. Measuring accuracy

TABLE II. GAZE ESTIMATION ACCURACY AT THE DESIGNATED VIEWING ANGLES

| Point | 1 | 2 | 3 | 4 | 5 |
|---------------|---|-----|-----|-----|------|
| Error(degree) | 0 | 0.2 | 0.2 | 0.2 | 3.12 |

In the eye control mode of 3D display, layer images are switched with human eyes only. Accidental blink is done within 0.3 seconds. Therefore, layer image is changed when user look at the corner of the image (the number of frame is written here) for more than 0.3 seconds (in this case, it is set at 0.7 seconds: 0.3 by 2 +0.1 second of margin). At the corner of the layer image, there is enlarged frame number as shown in Figure 7.

The frame number is displayed about one quarter of the screen size. Therefore, it does not require too much accuracy of the line of sight estimation. It is peripheral visual field; or peripheral vision for intersection of 3D object while the frame number is focused image.

Viewing at around the center of field of view allows acquisition of color and shape information of the objective 3D image while viewing of the peripheral visual fields allows movement and the location of 3D object pattern, in general. Therefore, throughout looking at frame number, user is looking at the 3D object in the peripheral visual fields and is looking at the frame number precisely in the eye control mode.

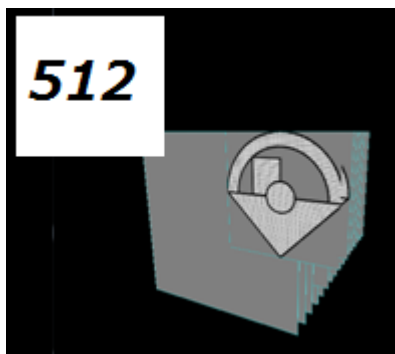


Fig. 7. User can select layer image by frame by frame by looking at the corner of the layer image

Thus layer selection for display can be done with human eye only. One of the applications of the proposed 3D object display is that LSI patter design as shown in Figure 8. It is getting easier to check through holes connectivity between layers by switching the displayed layer image by human eye only. Now a day, new model of LSI for mobile phone has to be delivered every three months. Therefore, there is a strong demand of LSI pattern design as much as they could. In this connection, the proposed eye control mode of layered image pattern representation is desired for this.

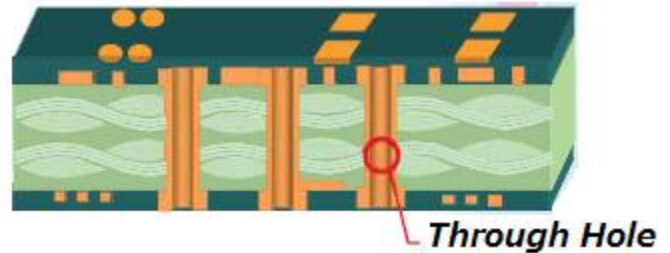


Fig. 8. Check the through holes of the layered LSI pattern with the proposed 3D object display method

E. Comparison of Processing Time Required for Switching Layer Images by between Using Hands and Fingers and Human Eye

Processing time by eye is as follows,
 Eye fixation = 230 [it is ranged from 70 to 700] milliseconds
 Eye movement = 30 milliseconds
 Perceptual Processor = 100 [it is ranged from 50 to 200] milliseconds
 Cognitive Processor = 70 [it is ranged from 25 to 170] milliseconds

On the other hand, the time required for press a key or button is as follows,
 Best typist = 0.08 seconds
 Good typist = 0.12 seconds
 Average skilled typist = 0.20 seconds
 Average non-secretary = 0.28 seconds
 Typing random letters = 0.50 seconds
 Typing complex codes = 0.75 seconds
 Worst typist = 1.2 seconds
 These are measured by Card, Moran and Newell [16].

Meanwhile, the time required for point with a mouse (excluding click) = 1.1 seconds. Furthermore, the time required for move hands to keyboard from mouse (or vice-versa) = 0.4 seconds in addition to mentally prepare = 1.35 seconds.

Another experiments show that, in the eye control mode, it requires around 700 milliseconds for selection of function by human eye. On the other hand, it requires 1.5 to 2 seconds for selection of function by human hand and fingers.

As a conclusion, the time required for mouse operations and or key-in operations by human eye is faster than that by hand and or fingers. Therefore, eye control mode of operations is faster than hand / finger operations. In particular for LSI pattern design of which it requires quick operation, eye control

mode is useful because through hole between LSI layers can be checked easily and fast.

IV. CONCLUSION

Method for 3D rendering based on intersection image display which allows representation of internal structure is proposed. The proposed method is essentially different from the conventional volume rendering based on solid model which allows representation of just surface of the 3D objects. By using afterimage, internal structure can be displayed through exchanging the intersection images with internal structure for the proposed method.

Through experiments with CT scan images, the proposed method is validated. Also one of other applicable areas of the proposed for design of 3D pattern of Large Scale Integrated Circuit: LSI is introduced. Layered patterns of LSI can be displayed and switched by using human eyes only. It is confirmed that the time required for displaying layer pattern and switching the pattern to the other layer by using human eyes only is much faster than that using hands and fingers. It is also found the followings,

Afterimage based 3D object representation onto 2D display works well

Automatic and manual (eye control) modes are available

Automatic mode works for continuous display while manual mode works for detail display in accordance with users' intension.

ACKNOWLEDGMENT

The author would like to thank Mr. Guo XiaoYu of Saga University and Arai's laboratory members for their valuable discussions and suggestions through this research works.

REFERENCES

- [1] K.Arai, H.Uwataki, Computer input by human eyes only based on cornea center extraction which allows users' movements, Journal of Institute of Electric Engineering of Japan, C-127, 7, 1107-1114, 2007.
- [2] K.Arai, M.Yamaura, Improvement of blink detection performance based on Morphologic filter for computer input by human eyes only, Journal of Image Electronics Engineering Society of Japan, 37, 5, 601-609, 2008.
- [3] K.Arai, K.Yajima, Communication aid based on computer input by human eyes only, Journal of Institute of Electric Engineering of Japan, C-128, 11, 1679-1686, 2008.
- [4] D. Purwanto, R. Mardiyanto and K. Arai, Electric wheel chair control with gaze detection and eye blinking, Artificial Life and Robotics, AROB Journal, 14, 694,397-400, 2009.

- [5] K.Arai, R. Mardiyanto, Computer input by human eyes only with blink detection based on Gabor filter, Journal of Visualization Society of Japan, 29,Suppl.2, 87-90,2009.
- [6] K. Arai and R. Mardiyanto, Real time blinking detection based on Gabor filter, International Journal of Human Computer Interaction, 1, 3, 33-45, 2010.
- [7] K. Arai and M. Yamaura, Computer input with human eyes only using two Purkinje images which works in a real time basis without calibration, International Journal of Human Computer Interaction, 1, 3, 71-82, 2010.
- [8] [8] K. Arai and R. Mardiyanto, Camera mouse and keyboard for handicap person with trouble shooting capability, recovery and complete mouse events, International Journal of Human Computer Interaction, 1, 3, 46-56, 2010.
- [9] K. Arai, R. Mardiyanto, A prototype of electric wheel chair control by eye only for paralyzed user, Journal of Robotics and Mechatronics, 23, 1, 66-75, 2010.
- [10] K. Arai, K. Yajima, Robot arm utilized having meal support system based on computer input by human eyes only, International Journal of Human-Computer Interaction, 2, 1, 120-128, 2011.
- [11] Kohei Arai, Ronny Mardiyanto, Autonomous control of eye based electric wheel chair with obstacle avoidance and shortest path finding based on Dijkstra algorithm, International Journal of Advanced Computer Science and Applications, 2, 12, 19-25, 2011.
- [12] K. Arai, R. Mardiyanto, Eye-based human-computer interaction allowing phoning, reading e-book/e-comic/e-learning, Internet browsing and TV information extraction, International Journal of Advanced Computer Science and Applications, 2, 12, 26-32, 2011.
- [13] K. Arai, R. Mardiyanto, Eye based electric wheel chair control system-I(eye) can control EWC-, International Journal of Advanced Computer Science and Applications, 2, 12, 98-105, 2011.
- [14] K. Arai, R. Mardiyanto, Evaluation of users' impact for using the proposed eye based HCI with moving and fixed keyboard by using eeg signals, International Journal of Research and Reviews on Computer Science, 2, 6, 1228-1234, 2011.
- [15] K. Arai, R. Mardiyanto, Electric wheel chair controlled by human eyes only with obstacle avoidance, International Journal of Research and Reviews on Computer Science, 2, 6, 1235-1242, 2011.
- [16] Card, Stuart; Thomas P. Moran and Allen Newell (1983). The Psychology of Human Computer Interaction. Lawrence Erlbaum Associates. ISBN 0-89859-859-1.

AUTHORS PROFILE

Kohei Arai He received BS, MS and PhD degrees in 1972, 1974 and 1982, respectively. He was with The Institute for Industrial Science and Technology of the University of Tokyo from April 1974 to December 1978 and also was with National Space Development Agency of Japan from January, 1979 to March, 1990. During from 1985 to 1987, he was with Canada Centre for Remote Sensing as a Post Doctoral Fellow of National Science and Engineering Research Council of Canada. He moved to Saga University as a Professor in Department of Information Science on April 1990. He was a councilor for the Aeronautics and Space related to the Technology Committee of the Ministry of Science and Technology during from 1998 to 2000. He was a councilor of Saga University for 2002 and 2003. He also was an executive councilor for the Remote Sensing Society of Japan for 2003 to 2005. He is an Adjunct Professor of University of Arizona, USA since 1998. He also is Vice Chairman of the Commission-A of ICSU/COSPAR since 2008. He wrote 30 books and published 332 journal papers.

3D Map Creation Based on Knowledgebase System for Texture Mapping Together with Height Estimation Using Objects' Shadows with High Spatial Resolution Remote Sensing Satellite Imagery Data

Kohei Arai¹

Graduate School of Science and Engineering
Saga University
Saga City, Japan

Abstract—Method for 3D map creation based on knowledgebase system for texture mapping together with height estimation using objects' shadows with high spatial resolution of remote sensing satellite imagery data is proposed. Through the experiments with IKONOS imagery data, the proposed method is validated.

Keywords—texture mapping; remote sensing satellite; 3D map; object height estimation;

I. INTRODUCTION

3D geographic maps are available for public use such as Google map. 3D scenery of major intersections, in particular, is needed to be created for public use. In order to create 3D scenery of image, cameras mounted on automobiles are used for acquisition of 3D images. It requires huge resources, human resources, time consumable computational resources, and so on. This is referred to the conventional method.

On the other hand, there is the method for 3D map creation with high spatial resolution of remote sensing satellite images, such as Early Bird, Quick Bird¹ [1], OrbView², IKONOS³, etc. Using these satellite imagery data, 3D image can be created. Essentially, satellite acquires images from space with off nadir angle (observation angle). Therefore, top view of 3D object can be acquired while side views are difficult to acquire. Some portion of side view images, however, can be acquired depending on off nadir angle. From the acquired side view images, knowledge about side view image, in particular, texture information can be acquired. Using such knowledge, it is possible to make a texture mapping to the 3D map. This is referred to the proposed method based on knowledgebase system.

Meanwhile, it is also possible to estimate the objects' height in concern. Using the acquisition time and location of the pixel in concern, then solar zenith angle is calculated. Then objects' height can be estimated with the estimated solar zenith angle and the length of the objects' shadow. The height information estimated by the aforementioned method can be

used for a confirmation of 3D view of the object in concern. The proposed method uses this procedure of the confirmation of objects' height.

The following section describes the proposed 3D map creation based on knowledgebase system together with the height estimation and confirmation followed by some experiments with IKONOS imagery data. Then conclusion is described together with some discussions.

II. PROPOSED METHOD

A. Conventional Method

3D maps are widely used in public domain. Google map is the most popular 3D map. In order to create 3D maps, cameras mounted vehicles are mostly used. There are major instruments which allow acquisition of 3D images, range cameras, stereoscopic cameras, etc. In Japan, stereoscopic cameras mounted vehicles are used for acquisition of 3D images at around 5400 of major intersections in the relatively large cities every year. It takes one year to update the created 3D image maps in Japan.

In order to save the time required for creation of 3D maps, aerial laser profilers as well as high resolution of remote sensing satellite imagery data are used. The former is to estimate the height of objects, essentially. The later can acquire not only height information but also off nadir view of images are acquired. Therefore, there is a possibility to create 3D maps with such high spatial resolution of remote sensing satellite images.

There is another method for creation of 3D maps. That is conversion method from existing 2D maps to 3D maps. Merits and demerits of these three methods are as follows,

(1) Stereoscopic cameras:

- Relatively high spatial resolution
- It is hard to create automatically

(2) Laser radars:

- It is easy to create automatically
- Relatively low spatial resolution

¹ <http://www.satimagingcorp.com/gallery-quickbird.html>

² <http://ja.wikipedia.org/wiki/GeoEye>

³ <http://ja.wikipedia.org/wiki/GeoEye#IKONOS>

(3) Map conversion:

- It is easy to resample 2D maps to 3D maps
- Re-sampled data is usually distorted and has ambiguity

B. Proposed Method

One of the purposes of the 3D map creation is pedestrian navigation. Therefore, 3D maps have to be comprehensive visually. This implies that comprehensive maps are better than accurate maps (high geometric fidelity). In other words, geometric fidelity is not needed. Therefore, imitated texture derived from the off nadir view of high resolution remote sensing satellite imagery data is used for assumed side view of 3D maps.

C. Objects' Height Estimation

Because pixel location of longitude and latitude as well as elevation is known, and also acquisition time is know, then object's height can be estimated with satellite altitude and with length of shadow. Illustrative view of the method for object's height estimation is shown in Figure 1.

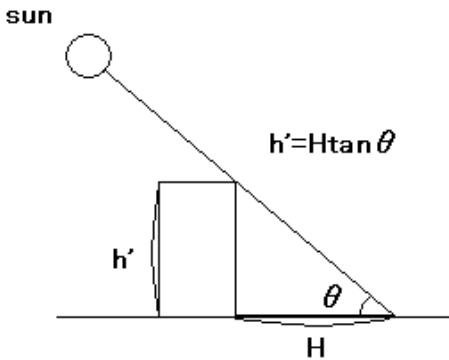


Fig. 1. Object's height estimation

Let z be solar zenith angle. Then cosine of solar zenith angle can be expressed in equation (1).

$$\cos(z) = \sin(a)\sin(b)+\cos(a)\cos(b)\cos(c) \quad (1)$$

Where a , b , and c denotes latitude of the location in concern, solar latitude, and solar time angle, respectively.

D. Texture Extraction from the Satellite Images

Because the acquired high spatial resolution of remote sensing satellite images are distorted and occluded due to the fact that satellite acquires images with off nadir viewing. Therefore, geometric correction with Affine transformation and anti-aliasing is required for extraction of side view of images from the off nadir view of images. Then these images can be used for texture mapping. Occluded portion of side view images can be assumed with knowledge base system.

3D Affine transformation can be expressed as follows,

$$\begin{bmatrix} x' \\ y' \\ z' \end{bmatrix} = \begin{bmatrix} v_{11} & v_{12} & v_{13} \\ v_{21} & v_{22} & v_{23} \\ v_{31} & v_{32} & v_{33} \end{bmatrix} \begin{bmatrix} x \\ y \\ z \end{bmatrix} + \begin{bmatrix} a \\ b \\ c \end{bmatrix} \quad (2)$$

Where $(x,y,z)_t$ and $(x',y',z')_t$ denotes the coordinate before and after the geometric correction. V matrix denotes magnification, aspect ratio conversion, skew and rotation matrix, and $(a,b,c)_t$ denotes offsets in directions of x , y , z .

Due to the fact that affine transformation induces aliasing noises. A single off nadir view of high spatial resolution of satellite image, essentially, would not be enough to create 3D map images. Spatial resolution for side view or opposite side view of images is not good enough for a single off nadir view of the high spatial resolution of remote sensing satellite images. Therefore, anti-aliasing is needed. Anti-aliasing can be done with smoothing filter which allows conversion from zigzag shaped edges to smooth edges.

E. Knowledge Base System

Occluded portion of side view images have to be assumed with knowledge base system. Also, unclear side view images have to be improved in terms of image quality and have to be assumed some portion of images by using knowledge base system. Knowledge about the artificial constructed objects is as follows,

Knowledge #1: Because object height can be estimated, the number of floor can be assumed with the knowledge about the floor height.

Knowledge #2: If windows are aligned on the one side view of the artificial constructed objects, then the opposite side of the artificial constructed objects has same window arrays.

Knowledge #3: If stairs are attached to one side of the artificial constructed objects, then there is no such stair on the other side of the artificial constructed objects.

III. EXPERIMENTS

A. Data Used

Table 1 shows major specification of IKONOS imagery data which is used for the experiments.

TABLE I. MAJOR SPECIFICATION

| Satellite_Name | IKONOS |
|----------------|-----------------------|
| Provider | Space_Imaging_Co_Ltd. |
| Launch_data | Septembe_25_1999 |
| Mission_life | 7_years |
| Revisit_period | 11_days |
| Inclination | 98.12_deg. |
| Altitude | 680_km |

Figure 2 shows an example of image of IKONOS. The example image includes shadow of the buildings, unclear side view images of the buildings, one side view image of the buildings, and so on.



Fig. 2. Example of IKONOS image used for the experiment.

B. 3D Maps from Four Different Aspects of Images Derived from the Single Off Nadir View of KINOS Image

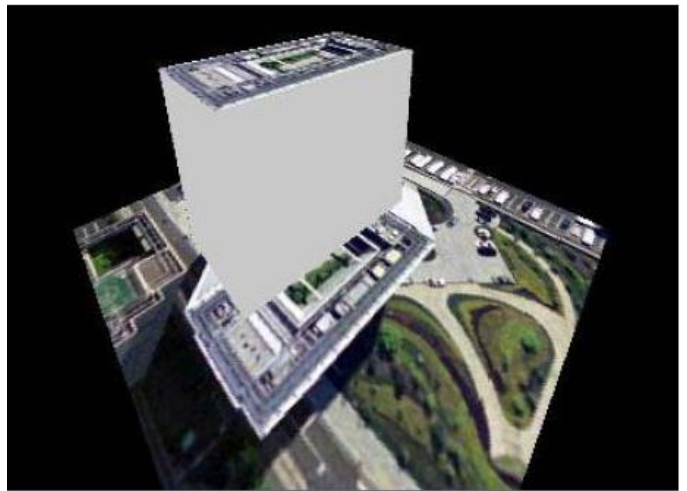
From the acquired IKONOS image of Figure 2, the following four different aspects of 3D map images are created. Figure 3 (a) shows front view of the created image while Figure 3 (b) shows side view of the created image.

On the other hand, Figure 3 (c) shows rear view of the created image while Figure 3 (d) shows opposite side view of the created image.

The locations of corners of the building are known. Therefore, geometric conversion can be done in accordance with the different viewing angles using Affine transformation. In the created images, there are so much aliasing noises induced by the Affine transformation. It would be better to remove these aliasing noises. Anti-aliasing can be done with smoothing filter which allows conversion from zigzag shaped edges to smooth edges.



(b)Side view



(c)Rear view



(a)Front view

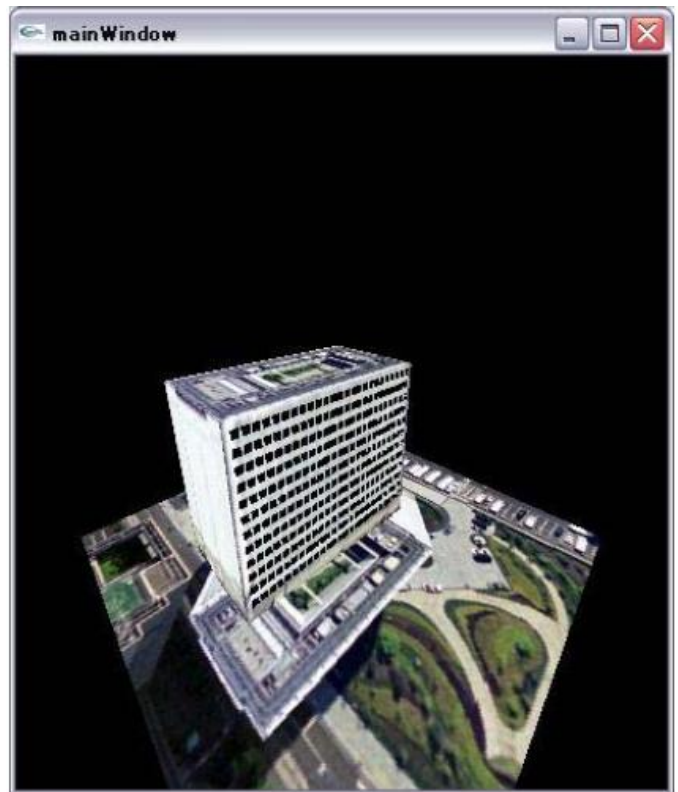


(d)Opposite side view

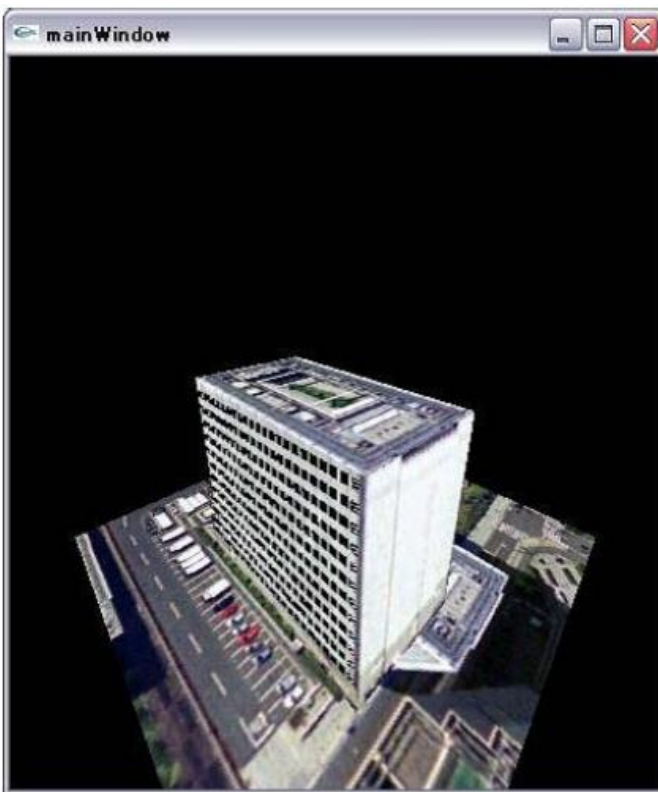
Fig. 3. Four different aspects of 3D map images derived from a single off nadir view of IKONOS image.

Moreover, opposite side plane and rear view images cannot be obtained obviously because these planes are occluded. Furthermore, details of the front view and not occluded side view images are unclear due to not enough spatial resolution of IKONOS image for these two planes. Therefore, some image quality improvements are needed for creation of 3D map images. In order to improve the image quality for these planes, the proposed method based on knowledge base system is applied. Firstly, building height is estimated. Then using typical height per one floor (290 cm) together with the estimated number of floors of the building, texture is derived from the actual acquired IKONOS image. In the same time, anti-aliasing noise reduction is applied to the acquired image to improve image quality.

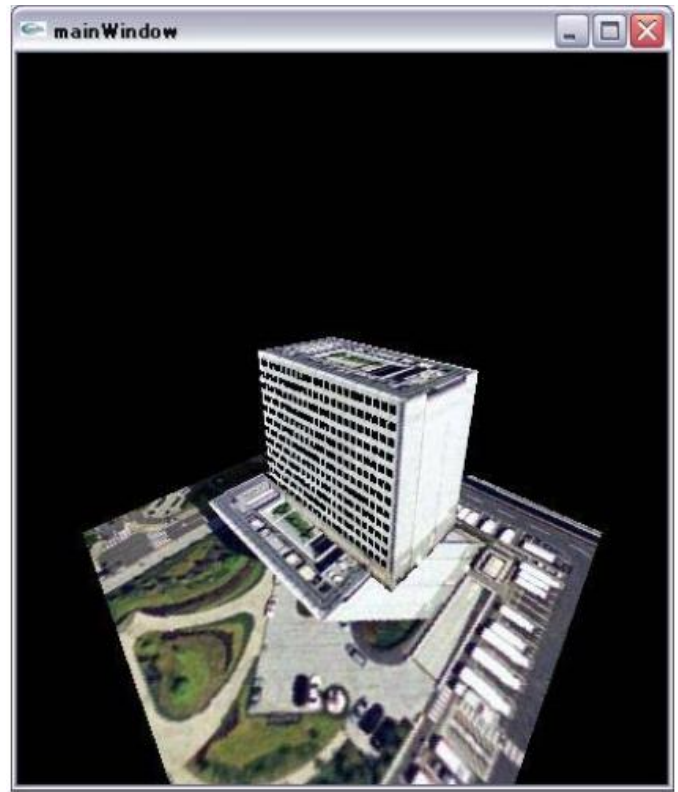
Front view of 3D map image is used for the rear view of 3D map image. Namely the same images are mapped onto the front and the rear planes of the building. This is one of knowledge (or assumption). This is the same thing for two side view of images. The created texture of the side view of 3D map image derived from the acquired from the IKONOS satellite is mapped onto the opposite side of the building plane which is occluded. Thus 3D map image of four different aspects of images are created. Figure 4 shows the resultant images. In comparison between the created 3D map image of four different aspects of images with (proposed method) and without (the conventional method) consideration of knowledge base system, image quality for the proposed method is superior to that for the conventional method.



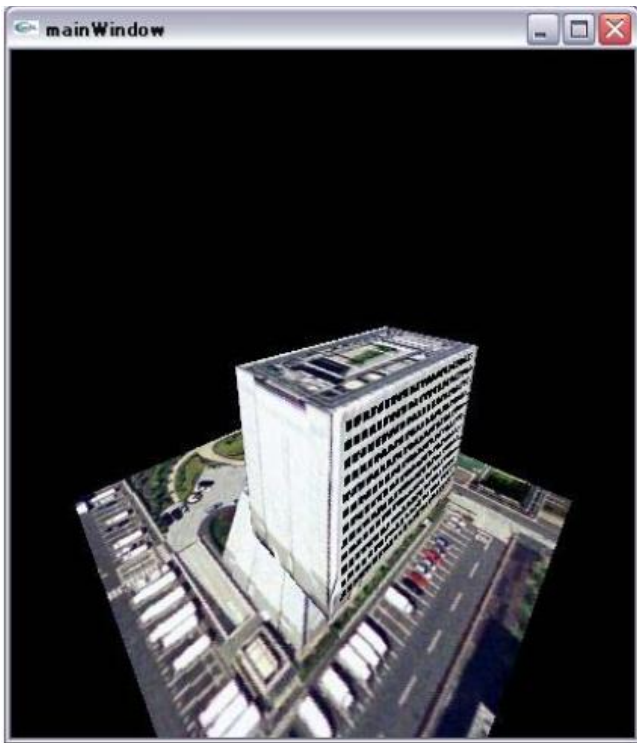
(b)Side view



(a)Front view



(c)Rear view



(d)Opposite side view

Fig. 4. Created 3D map image of four different aspects of images

IV. CONCLUSION

Method for 3D map creation based on knowledgebase system for texture mapping together with height estimation

using objects' shadows with high spatial resolution of remote sensing satellite imagery data is proposed. Through the experiments with IKONOS imagery data, the proposed method is validated.

In comparison between the created 3D map image of four different aspects of images with (proposed method) and without (the conventional method) consideration of knowledge base system, it is found that the image quality for the proposed method is superior to that for the conventional method.

ACKNOWLEDGMENT

The author would like to thank Mr. Kazunori Kinoshita for his effort to conduct experiments.

REFERENCES

- [1] Mehuron, Tamar A., Assoc. Editor (August 2008). "2008 USAF Space Almanac - Major Civilian Satellites in Military Use". *Air Force Magazine* (Pub: Air Force Association) 91 (8): pp.49-50. ISSN: 0730-6784..

AUTHORS PROFILE

Kohei Arai, He received BS, MS and PhD degrees in 1972, 1974 and 1982, respectively. He was with The Institute for Industrial Science and Technology of the University of Tokyo from April 1974 to December 1978 and also was with National Space Development Agency of Japan from January, 1979 to March, 1990. During from 1985 to 1987, he was with Canada Centre for Remote Sensing as a Post Doctoral Fellow of National Science and Engineering Research Council of Canada. He moved to Saga University as a Professor in Department of Information Science on April 1990. He was a councilor for the Aeronautics and Space related to the Technology Committee of the Ministry of Science and Technology during from 1998 to 2000. He was a councilor of Saga University for 2002 and 2003. He also was an executive councilor for the Remote Sensing Society of Japan for 2003 to 2005. He is an Adjunct Professor of University of Arizona, USA since 1998. He also is Vice Chairman of the Commission A of ICSU/COSPAR since 2008. He wrote 30 books and published 332 journal papers.

Monte Carlo Ray Tracing Based Adjacency Effect and Nonlinear Mixture Pixel Model for Remote Sensing Satellite Imagery Data Analysis

Kohei Arai¹

Graduate School of Science and Engineering
Saga University
Saga City, Japan

Abstract—Monte Carlo Ray Tracing: MCRT based adjacency effect and nonlinear mixture pixel model is proposed for remote sensing satellite imagery data analysis. Through simulation and actual visible to near infrared radiometer onboard spaceborne data utilizing experiment, the proposed model is confirmed and validated. Therefore, influences due to adjacency effect and nonlinearity of mixed pixel can be taken into account in the remote sensing satellite imagery data analysis.

Keywords—adjacency effect; nonlinear mixed pixel model; Monte Carlo method; Ray tracing method

I. INTRODUCTION

All land pixels in remote sensing imagery are essentially mixed pixels that consist of multiple ground cover materials. Currently, there are two types of models aiming to untangle these contributions: linear and non-linear mixture models. The linear mixture models assume negligible interactions among distinct ground cover materials while the nonlinear mixture models assume that incident solar radiation is scattered within the scene itself and that these interaction events may involve several types of ground cover materials. R.Singer and T.B.McCord (1979) [1], B.Hapke (1981) [2] and R.N.Clark and T.I.Roush (1984) [3] proposed linear mixture models while R.Singer (1974) [4], B.Nash and J.Conel (1974) [5] proposed nonlinear mixture models for the mixed pixels containing different mineral resources. Meanwhile, C.C.Borel and S.A.Gerst (1994) [6] proposed another nonlinear mixture model for vegetated areas. These nonlinear mixture pixel models, however, did not take into consideration the influence of topographic features nor the influence of multiple scattering in the atmosphere.

A nonlinear mixture model for the interpretation of mixed pixels in remote sensing satellite images is proposed. The proposed model is a Monte Carlo ray-tracing model that takes into account interactions among the ground cover materials (multiple reflections among the materials on the surface). The proposed model also takes into account topographic features (slope) of the ground surface. As an example, Top of the Atmosphere: TOA radiance of mixed pixels of forested areas which are composed of grasses and trees are simulated with the proposed model and compared to actual remote sensing satellite data of ASTER/VNIR over these forested areas. It was found that the influence due to multiple scattering interactions between trees depends on the tree distance and

ranges from 8 to 10 %. It is also found that the proposed model is useful to interpret mixed pixels. Namely, it is suggested that actual reflectance of the trees is higher than apparent reflectance that is calculated with the satellite data. Also it is suggested that it is possible to estimate forest parameters such as tree distance, tree shape.

This paper proposes a nonlinear mixed pixel model that takes into account topographic features of the surface and multiple scattering in the atmosphere. Furthermore, the proposed nonlinear mixed pixel model takes into account interactions among ground cover materials (trees) separated by different distances and having different shapes (crowns). Since multiple scattering interactions in 3D media are not so easy to solve using the radiative transfer equation, the proposed mixture model is based on Monte Carlo Ray-Tracing: MCRT.

Section 2 describes the proposed nonlinear mixed pixel model together with details of the MCRT algorithm. Section 3 presents experimental results showing the influence of multiple scattering interactions between trees, the shape of the trees, the slope of the terrain, and the atmospheric optical depth. Finally, the model derived Top-of-the-Atmosphere: TOA radiance over forested area is compared to actual remote sensing satellite observations by the visible and near-infrared radiometer, ASTER/VNIR: Advanced Spaceborne spectral-radiometer for Thermal Emission and Reflection / Visible and Near Infrared Radiometer onboard Terra satellite data.

II. PROPOSED MODEL

A. The Monte Carlo Ray-Tracing:MCRT Simulation Model

Nonlinear mixture model and brief description of Monte Carlo Ray-Tracing model: MCRT. Nonlinear mixing model proposed here is composed with more than two ground cover materials and is based on the MCRT model. In order to take into account the geographical feature, slope of the ground surface can be changed. Also any ground cover materials can be set for the ground surface together with different shape of ground cover materials. The simulation with MCRT model is called MCRT Simulation, MCRTS (Arai, 2005) [7]. In MCRTS, 50 by 50 by 50km of simulation cell size is assumed. The ground surface is composed with two planes, surface A and B, with the different slopes, α and β and with surface reflectance, Γ_A and Γ_B as is shown in Figure 1. a and b show IFOV on the ground for the surface A and B.

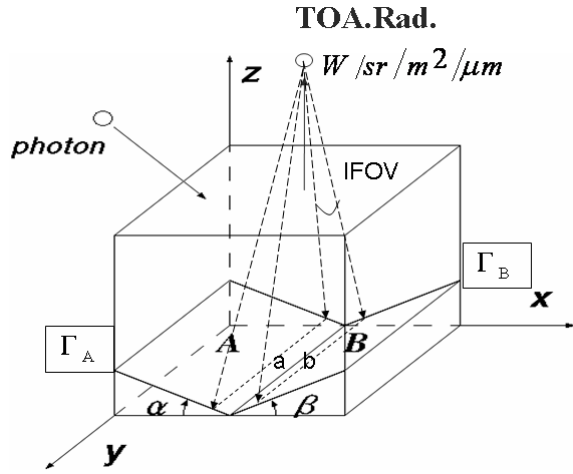


Fig. 1. Nonlinear mixed pixel model based on Monte Carlo Ray-Tracing Simulation model with 50x50x50km cell and two ground surfaces (The pixels situated along with border between two surface are mixed pixels).

A photon is put in the simulation cell from the top of the cell with the incidence angle that depends on the specified solar zenith angle. The position of which the photon is put in is changed by time by time in accordance with the uniformly distributed random numbers.

Depending on the optical depth of the atmosphere, free travel length L of photon is determined as follows,

$$L = -L_0 \log(Rnd) \quad (1)$$

$$L_0 = \frac{h}{\tau_{all}} \quad (2)$$

where L_0 is called free travel length, denoting the average distance of interaction of a photon from one position to another. Rnd is uniformly distributed random numbers ranges from 0 to 1. h denotes the physical height of the atmosphere (50km in this case) while τ_{all} denotes the optical depth of the atmosphere which is determined as follows,

$$\tau_{all} = \tau_{aero} + \tau_{mol} \quad (3)$$

where the subscript *aero* is associated with aerosols while *mol* with molecules. Here, it is assumed that atmosphere consists of aerosols and air molecules. Because the wavelength in concern ranges from 450 to 1050nm so that optical depth of ozone and water vapors are assumed to be negligible except 936nm of water vapor absorption band. A small absorption due to ozone is situated from 500 to 650nm around.

The photon meets aerosol particles or molecule when the photon travels in the atmosphere then scattering due to the aerosols or molecules occurs. The probability of the collision to the aerosols or molecules depends on their optical depths. If the endpoint of photon travel is in the atmosphere, the photon

meets aerosol or molecule. The probability of the photon meets aerosol is τ_{aero} / τ_{all} while that of the photon meets molecule is τ_{mol} / τ_{all} . In accordance with the phase function of aerosols or molecules, the photon is scattered. Strength of scattering as a function of scattering angle θ is determined by the phase function, $P(\theta)$, the Rayleigh for molecules, equation (4) and Heyney-Greestein function, equation (5) (it is just an approximation function of which the phase function is monotonically decreasing) for aerosols. Actual phase function can be determined with MODTRAN 4.0 of Mie code with the measured refractive index of aerosols through field experiments. By using uniformly distributed random numbers, scattering direction is determined. The phase function as $P(\theta)$, where θ is the angle between the incident direction and the scattering direction.

For molecules, the Rayleigh phase function is as follows,

$$P(\theta) = (3/4)(1 + \cos^2 \theta) \quad (4)$$

While that for aerosols, we use the Heyney-Greenstein approximation function of the following,

$$P(\theta) = \frac{1 - g_\lambda^2}{(1 + g_\lambda^2 - 2g_\lambda \cos \theta)^{3/2}} \quad (5)$$

Where g_λ is the asymmetry factor of the aerosol phase function which depends on the wavelength of the radiation and the compositions, sizes, and the shapes of the aerosol particles.

In the calculation of TOA radiance, the number of photons, N which comes out from the top of the atmosphere within the angle range which corresponds to the Instantaneous Field of View: IFOV of the sensor in concern is used thus the normalized TOA radiance, Rad is determined as follows,

$$Rad = \frac{\mu_0 \mu \Delta \mu}{2} \left(\frac{N}{N_{total}} \right) \quad (6)$$

where $\mu_0 = \cos \theta_0$, $\mu = \cos \theta$, θ_0 is the solar zenith angle and θ is a viewing solid angle. $\Delta \mu$ is a view solid angle, i.e., FOV (field of view). N_{total} is the number of photons which are put in the cell in total. If you multiply solar irradiance to Rad in unit of (W/m²/str/μm), then the TOA radiance in the same unit is calculated.

The input parameters are determined by field experimental data. They are (1) Material reflectance which is albedo of the entire ground cover material, (2) Background surface material reflectance, (3) Material-material distance, (4) Optical depth of aerosol and molecule, (5) Solar zenith and azimuth angles, (6) IFOV of the sensor, (7) Sensor direction (view zenith angle) and height. On the other hand, output parameters include TOA radiance and ten groups of photons. They are (1) Photons that are put in the atmosphere from the top of cell in total, (2) Photons that are come from the top of the cell within the range of IFOV, (3) Photons that are reflected by material,

(4) Photons that are absorbed by material, (5) Photons that are reflected on the background, (6) Photons that are absorbed on the background, (7) Photons that are scattered by aerosols, (8) Photons that are absorbed by aerosols, (9) Photons that are scattered by molecules and (10) Photon that are absorbed by molecule. A photon equation must be formed, that is, the number of put-in-photons must be equal to the sum of come-out-photons which are come-out from the top of cell and the photons which are absorbed by aerosols and molecules, material and background. Each simulation has proved this equation.

From the results from the preliminary MCRTS with a plenty of input parameters, it is concluded that 700,000 of put-in-photons would be enough for the MCRTS in many cases.

B. Parameters and more detailed description of Monte Carlo ray tracing

Wavelength for MCRTS can be set freely and is set the coverage from 450 to 1050nm in this case. Solar azimuth and zenith angles can also be set freely and are set at 17 and 58 degrees, respectively in this case (those at Terra/ ASTER satellite over path time on December 15 2004 when the field campaign was conducted). Optical depth of molecule and aerosol are designated within a range from 0 to 0.5 for typical conditions. The actual phase function used in the MCRTS is shown in Figure 2. Mie phase function used for MCRTS is determined by using Mie code of MODTRAN 4.0 with the measured refractive index using skyradiometer, POM-I which allows measurements of direct, diffuse and aureole of solar irradiance in Saga city on December 15 2004.

The measured size distributions of aerosol as well as optical depths of total atmosphere, water vapor, molecule, total column ozone, and aerosol are shown in Figure 3 and 4, respectively. Size distribution shows bi-modal characteristics, one peak is situated at the 0.2 μ m, while the other peak is situated at 1.2 μ m. Junge distribution is assumed for simplifying calculation. The measured Junge parameter (3 in this case) is used for MCRTS. The test site is situated in the Saga city, Japan near by the Ariake Sea so that aerosol are mixed aerosol of relatively small particles of water soluble and comparatively large size of oceanic sea salt aerosols.

In the Figure 4, the measured optical depth of total atmosphere that measured with MicroTops-II (Optical depth specification: 340, 500, 675, 870, 1020nm) is shown with green colored cross marks. Also column ozone and water vapor are measured at the test site with MicroTops-II (Ozone and water vapor measurement specification). With the measured optical depth, solid lines of smooth characteristics of optical depth of total atmosphere, ozone and water vapor are calculated with MODTRAN 4.0 through a curve fitting. Optical depth of molecule can be calculated with measured atmospheric pressure and wavelength. Then optical depth of aerosol is estimated by subtracting optical depth of ozone, water vapor and molecule from that of total atmosphere.

$$P(\theta)$$

C. Verification of Monte Carlo ray-tracing simulations

The proposed MCRTS is validated with the MODTRAN 4.0 of atmospheric code that allows estimation of TOA radiance with the atmospheric and ground surface parameters. A flat Lambertian surface with reflectance of 0.2 (vegetated area) is assumed together with the Mid.-Latitude-Winter of the other default parameters. Optical depth of aerosol ranges from 0.1 to 0.5. Meanwhile molecule optical depth is around 0.1 at 550nm, center wavelength of band 1 of ASTER/VNIR in accordance with atmospheric model of Mid.-Latitude-Winter of MODTRAN 4.0 while those of aerosol (refractive index=1.44-0.005i which are estimated with the field campaign data which was conducted in Saga test site on December 15 2004) for optical depth of 0.1, 0.2, 0.3, 0.4, and 0.5 those are corresponding to the visible range of 70, 30, 20, 15 and 13 km, respectively. Table 1 shows the TOA radiance at 550 nm derived from MODTRAN 4.0 and those derived from MCRTS.

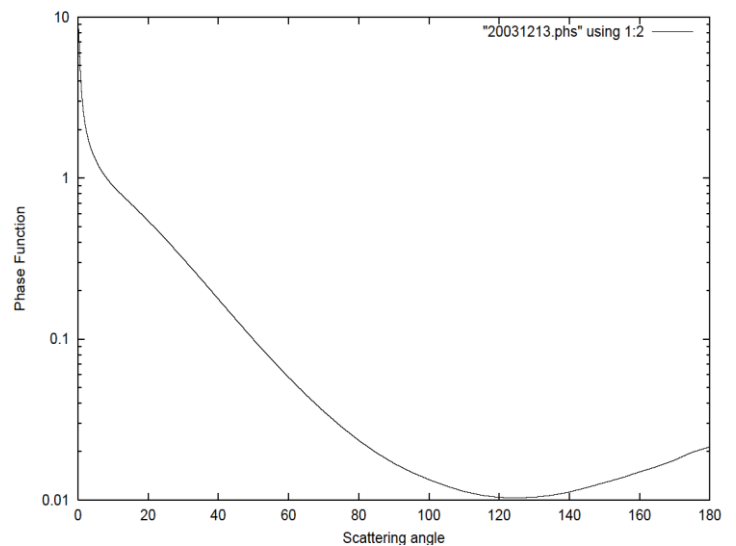


Fig. 2. Mie phase function used for MCRTS (By using Mie code of MODTRAN 4.0 with the measured refractive index using skyradiometer, POM-III in Saga city on December 15 2004.

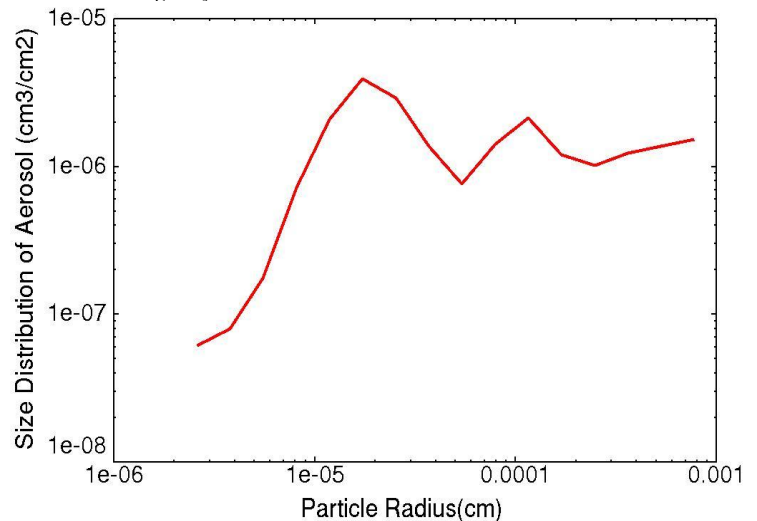


Fig. 3. Measured size distribution of aerosol at the Saga test site in Japan on December 15 2004.

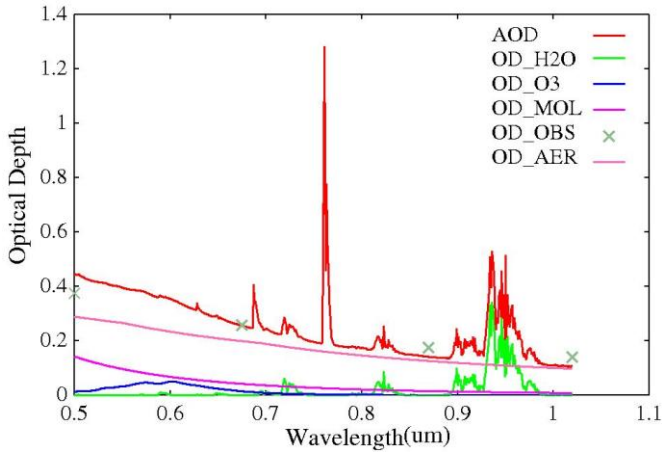


Fig. 4. Measured optical depths of total atmosphere (AOD), water vapor (OD_H2O), column ozone (OD_O3), molecule (OD_MOL), and aerosol (OD_AER) at Saga test site in Japan on Dec.15 2004. OD_OBS denotes observed optical depth.

On the other hand, molecule optical depth of the Mid-Latitude Winter of MODTRAN4.0 is 0.02 at 810 nm, center wavelength of band 3 of ASTER/VNIR while aerosol optical depth of 0.1, 0.2, 0.3, 0.4 are corresponding to the visible range of 55, 25, 18 and 12 km, respectively. Reflectance of the vegetation is assumed around 0.5 at 810 nm. TOA radiance at 810 nm is shown in Table 2. In accordance with increasing of aerosol optical depth, TOA radiance is increased due to the fact that the path radiance is increased with increasing of aerosol optical depth in the 550nm wavelength region while TOA radiance decreases in accordance with increasing of optical depth in the 810 nm because path radiance is rather small in comparison to that in the 550 nm region. In accordance with increasing of aerosol optical depth, TOA radiance is increased due to the fact that the path radiance is increased with increasing of aerosol optical depth in the 550 nm wavelength region while TOA radiance decreases in accordance with increasing of optical depth in the 810 nm because path radiance is rather small in comparison to that in the 550 nm region.

As the results from the comparisons with the typical atmospheric and surface conditions, the difference between both is within a range of 2 %. There are two systematic discrepancies between both. One is the TOA radiance derived from MODTRAN is greater than that from the proposed MCRTS. The other one is the difference depends on optical depth.

TABLE I. COMPARISON BETWEEN MCRTS AND MODTRAN DERIVED TOA RADIANCE AT ASTER/VNIR BAND 1(550NM)

| Optical Depth | | Visible Range (km) | TOA Radiance (W/m ² /str/μm) | | % difference between MCRTS and MODTRAN |
|---------------|---------|--------------------|---|---------|--|
| Molecule | Aerosol | | MCRTS | MODTRAN | |
| 0.1 | 0.1 | 70 | 106.7 | 107.1 | -0.4 |
| 0.1 | 0.2 | 30 | 106.2 | 106.7 | 0.5 |
| 0.1 | 0.3 | 20 | 106.3 | 107.0 | 0.7 |
| 0.1 | 0.4 | 15 | 106.4 | 107.7 | 1.2 |
| 0.1 | 0.5 | 13 | 106.8 | 108.8 | 1.8 |

TABLE II. COMPARISON BETWEEN MCRTS AND MODTRAN DERIVED TOA RADIANCE AT ASTER/VNIR BAND 3(810NM)

| Optical Depth | | Visible Range (km) | TOA Radiance (W/m ² /str/μm) | | % difference between MCRTS and MODTRAN |
|---------------|---------|--------------------|---|---------|--|
| Molecule | Aerosol | | MCRTS | MODTRAN | |
| 0.02 | 0.1 | 55 | 144.7 | 145.1 | 0.3 |
| 0.02 | 0.2 | 25 | 141.9 | 143.0 | 0.8 |
| 0.02 | 0.3 | 18 | 139.7 | 141.8 | 1.5 |
| 0.02 | 0.4 | 12 | 137.2 | 140.1 | 2.1 |

III. EXPERIEMNTS

A. Slope Effect

The effects of geographic feature, slope, and tree shape as well as tree-tree interaction on TOA radiance were investigated. Solar azimuth and zenith angles are set at 17, 58 degrees, respectively. As the atmospheric influence to TOA radiance in 550nm is greater than that in 810nm so that MCRTS is conducted in the 550nm.

Forested areas are assumed for the ground surface material together with bare soil and grass fields. Two types of trees, deciduous and coniferous trees are assumed. The different tree shapes, ellipsoidal and cone shaped Lambertian surface, respectively, are assumed for deciduous and coniferous trees. Also geographical feature, slopes are taken into account. Furthermore, two surfaces with area of 25km by 50km are assumed on the ground in the simulation cell in order to concentrate the mixed pixels that are situated along with the center of the ground. IFOV of sensor is set at 15m on the ground. Adjacency effect from the neighboring pixels is investigated with MCS. Through a comparison of the number of photons coming from the IFOV of the pixels that are situated at the center of the ground surface in the simulation cell to that from the IFOV of the neighboring pixels, the adjacency effect is calculated.

Slope effect with the different situation of two different slopes, Slope A and Slope B with the same surface reflectance of 0.3 at 550nm is shown in Table 3. Optical depth of aerosol and molecule are 0.35 and 0.14, respectively. Two different flat surfaces with the different slope that ranges from 0 to 30degrees with 15degrees step are assumed. The other parameters are the same mentioned above. In accordance with slope angle, TOA radiance is decreased due to the fact that the number of photons of which multiple reflections on the ground is occurred.

TABLE III. SLOPE EFFECT WITH THE DIFFERENT SITUATION OF TWO DIFFERENT SLOPES, SLOPE A AND SLOPE B WITH THE SAME SURFACE REFLECTANCE OF 0.3 (FLAT LAMBERTIAN SURFACE) AT 550NM (SOLAR AZIMUTH AND ZENITH ANGLES ARE 17 AND 58DEG.)

| Slope A and B | 0 and 0 | 15 and 0 | 30 and 0 |
|---------------|---------|----------|----------|
| TOA Radiance | 101.19 | 101.00 | 98.62 |

B. Tree-tree interaction and the effect of tree shape

Coniferous trees are simplified with cone shape of Lambertian surface while deciduous trees are ellipsoidal shape of Lambertian surface as are shown in Figure 5. These simplified models of trees are aligned with tree distance in the two dimensional ground surface of the simulation cell. By comparing the TOA radiance for the different types of trees, the effect of tree shape (types) is investigated. In the investigation, the number of photons of which multiple reflections among trees are occurred ((d) and (e) in the Figure 6) as a tree-tree interaction.

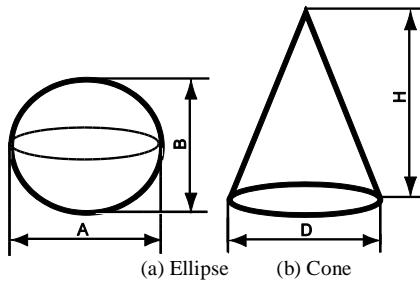


Fig. 5. Two types of trees, (a) ellipsoidal shape of deciduous trees and (b) cone shape of coniferous trees.

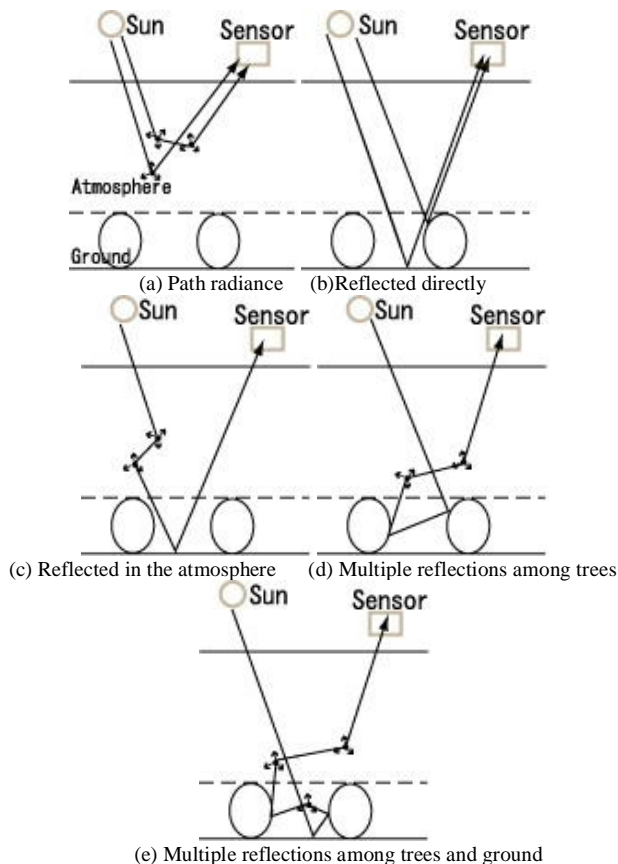


Fig. 6. Sun-atmosphere-ground paths (Each tree is treated as each individual ellipse: deciduous or cone: coniferous trees)

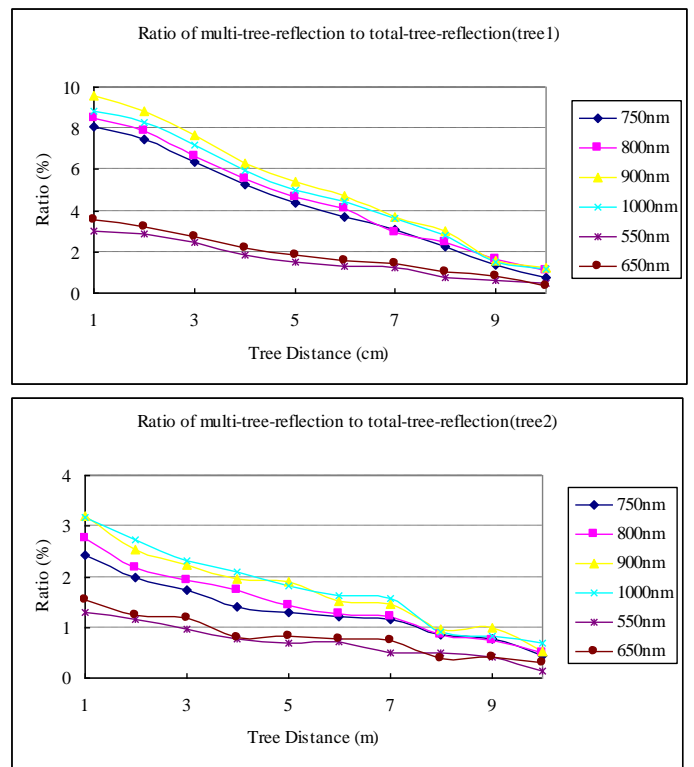


Fig. 7. Percentage ratio of multiple reflections among trees to the total TOA (the Top of the Atmosphere) radiance for deciduous trees (Left) and for coniferous trees (Right)

In the investigation of tree-tree interaction with MCRTS, (Tree 1): $A=1m, B=1m$ of spherical deciduous trees and (Tree 2): $D=1m, H=2m$ of cone shaped coniferous trees are assumed and aligned on the ground with tree distance ranges from 1 to 10m. The ratios of tree-tree interaction to the total TOA radiance are calculated. As are shown in Fig.7, tree-tree interaction of ellipsoidal deciduous trees is greater than that of cone shaped coniferous trees. The former ranges from 3 to 9.5% depending on the wavelength while the latter ranges from 1.2 to 3.3%. Also it is found that tree-tree interaction decreases in accordance with tree distance.

C. Interpretation of the mixed pixels in the Terra/ASTER/VNIR imagery data

In order to validate the proposed nonlinear mixed pixel model and to interpret the mixed pixels, multiple scattering in the atmosphere and geographical feature, shape of the ground cover materials, material-material interaction, experiments are conducted with actual Terra/ASTER/VNIR data of vegetated and forested areas of Saga, Japan, which was acquired at 11:09 on December 15 2004. Weather on that day in Saga is: fair and ground air temperature is 15.7 degree Celsius. Relative humidity is 60 % while atmospheric pressure is 1023.7 hPa. Meanwhile, wind direction is East-North-East and wind speed is 5.1 m/s. A portion of natural color image together with three intensive study areas is shown in Figure 8.

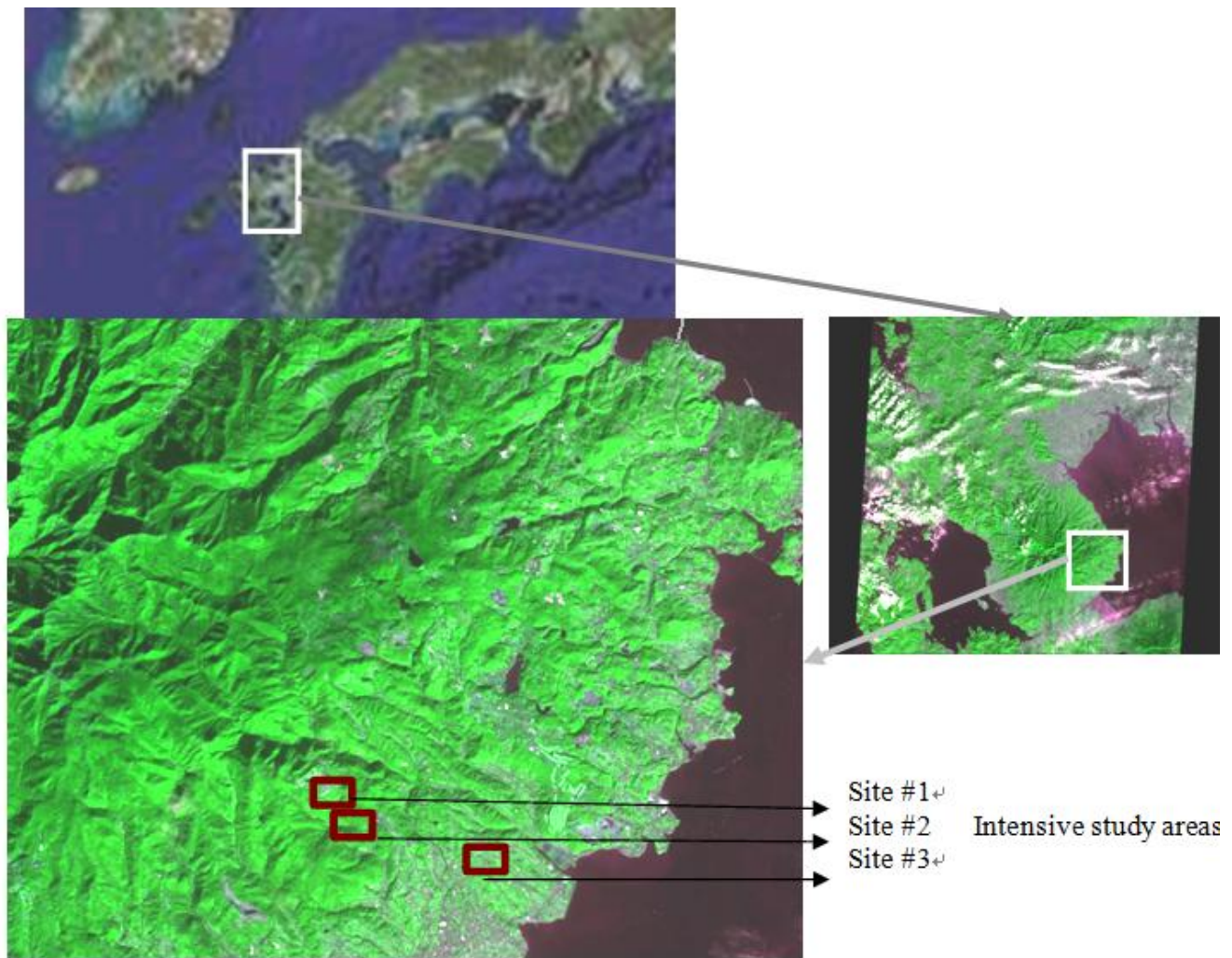


Fig. 8. Terra/ASTER/VNIR image data used and the intensive study areas

Three intensive study areas are situated at Ochiaigawa and the surrounding areas of Korai-cho in Nagasaki prefecture, Japan. The latitude and longitude of the centre location is as follows, Site1: (32°57.30N , 130°7.19E), Site2: (32°56.33N , 130°7.25E) and Site3: (32°56.13N , 130°10.21E).

Solar azimuth and zenith angles are 17 and 58 degrees, respectively. Figure 9 shows geographical feature and ground cover materials of the site #1, #2 and #3 while Figure 10 shows topographic maps and a portion of VNIR image including mixed pixels of the site #1, #2 and #3. The slopes and the ground cover materials of the test sites are known. Optical depth of aerosol, molecule, ozone and water vapor at the wavelength of 550nm were 0.35, 0.14, 0.009, 0.001, respectively so that optical depth of ozone and water vapor are negligible in the MCRTS while optical depth of aerosol and molecule at 810nm are 0.16 and 0.02, respectively and the other influencing factors are also negligible.

The detailed parameters for the site #1, #2 and #3 are shown in Table 4. Table 5 shows the experimental results of ASTER/VNIR derived at sensor radiance, MCRTS derived TOA radiance with the proposed nonlinear and linear mixed pixel models. TOA radiance of the mixed pixels of the site #1, #2, #3 is estimated with MCRTS assuming two homogeneous sloped ground surfaces with the different materials and with the same area of 25km by 50km. Two dimensionally aligned A=1m, B=1m, d=2m of deciduous trees with surface grass (the reflectance are same as paddy field) is assumed for surface A of the site #1 and #3 while two dimensionally aligned D=1m, H=2m, d=2m of coniferous trees with the same surface grass mentioned above is assumed for surface B of the site #1 #2. Flat surface is assumed for bare soil and paddy field for surface A of the site #2 and surface B of the site #3. It is not easy to simulate the real situation ground surface materials so that only the mixed pixel is concentrated for interpretation

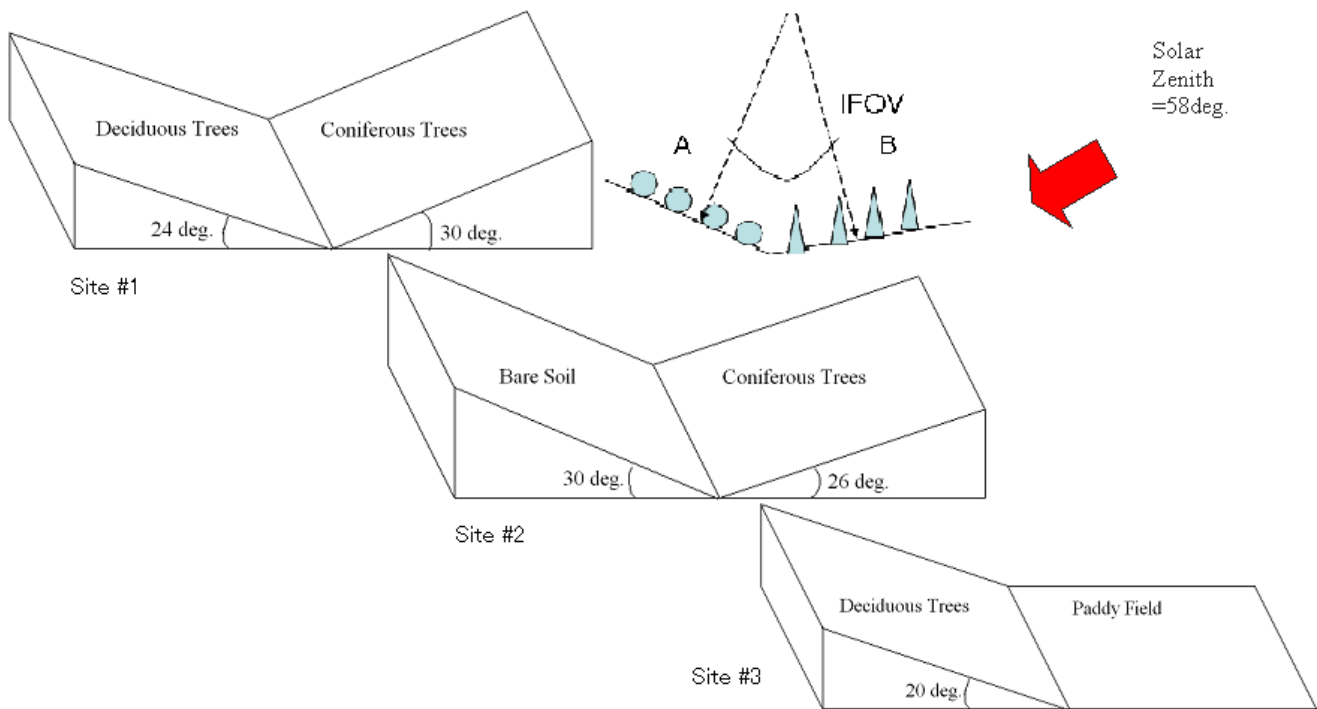


Fig. 9. Geographical features and ground cover types of the site 1, 2 and 3.

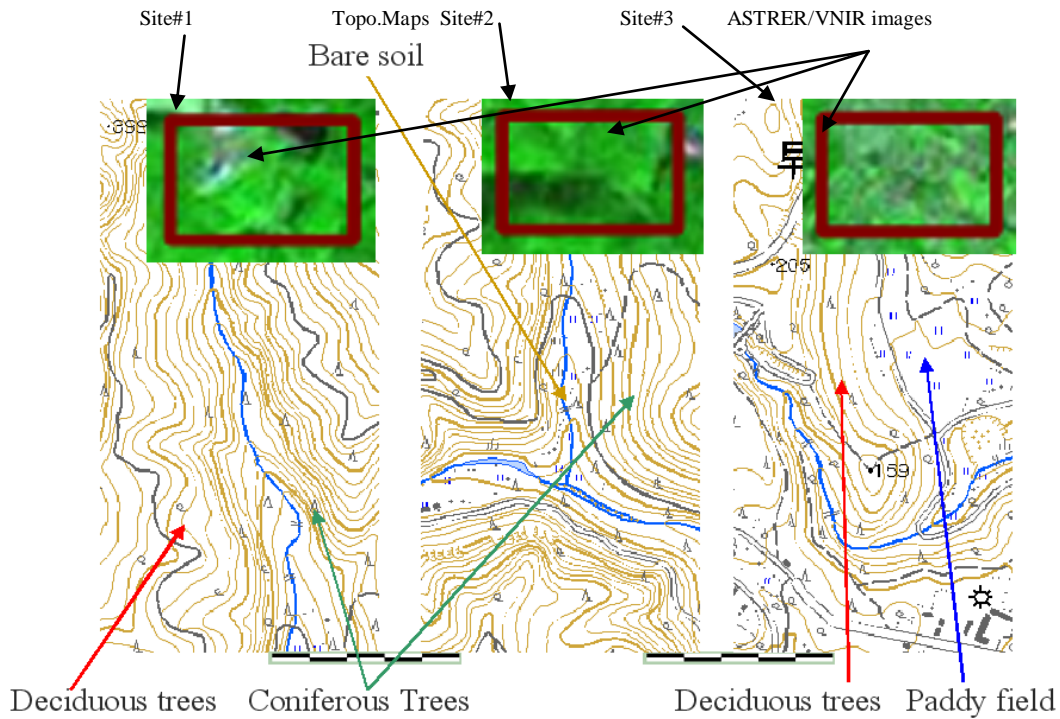


Fig. 10. Portion of ASTER/VNIR images of the intensive study areas of site #1, #2, and #3 including mixed pixels and the corresponding topographical maps.

TABLE IV. ANGLES OF THE SLOPES, GROUND COVER MATERIALS, REFLECTANCE AND OPTICAL DEPTH OF AEROSOL AND MOLECULE OF THE SITE #1, #2 AND #3 (Γ_{AX} DENOTES REFLECTANCE AT X NM OF WAVELENGTH).

| | Site #1 | Site #2 | Site #3 |
|---|----------------------|----------------------|---------------------|
| Slope α | 24 deg. (Deciduous) | 30 deg. (Bare soil) | 20 deg. (Deciduous) |
| Slope β | 28 deg. (Coniferous) | 26 deg. (Coniferous) | 0 deg. (Paddy) |
| Reflectance Γ_{A550} , Γ_{A810} | 0.14, 0.52 | 0.20, 0.13 | 0.14, 0.52 |
| Reflectance Γ_{B550} , Γ_{B810} | 0.08, 0.42 | 0.08, 0.48 | 0.12, 0.11 |

TABLE V. COMPARISON BETWEEN ASTER/VNIR DERIVED RADIANCE ($W/M^2/STR/MM$), ESTIMATED RADIANCE BASED ON LINEAR AND NONLINEAR MIXTURE MODELS

| | Site #1 | Site #2 | Site #3 |
|---------------------------|--------------|--------------|--------------|
| ASTER/VNIR (Band1, Band3) | 104.9, 144.7 | 105.9, 138.2 | 104.1, 137.6 |
| Linear (Band1, Band3) | 104.7, 138.2 | 106.7, 139.6 | 106.0, 136.9 |
| Nonlinear (Band1, Band3) | 109.5, 141.1 | 111.3, 142.2 | 110.4, 141.9 |

Table 6 shows a comparison of estimated reflectance of the mixed pixels based on linear and nonlinear mixed pixel models and the percent difference between both. It seems that the estimated radiance based on linear mixed pixel model is much closer than those for nonlinear mixed pixel model.

The ASTER/VNIR derived radiance is calculated based on onboard calibration data. There is approximately 10% of discrepancy between onboard calibration data and vicarious calibration data for band 1 while that for the band 3 is around 3%. Thus if the vicarious calibration is more reliable than onboard calibration, then the VNIR derived at sensor radiance of band 1 would be 115.4, 116.5, 114.5 for the site 1, 2 and 3, respectively while those for band 3 are 108.0, 109.1 107.2 so that the estimated TOA radiance based on nonlinear mixture model is much closer than those for linear mixed pixel model except for the Site3.

It seems that the site3 consists of flat paddy and 20deg. sloped deciduous trees so that not so significant tree-tree interaction and slope effect are occurred. TOA or at sensor radiance are estimated so that the surface reflectance can be derived because up/down-ward radiance on the ground can be estimated. The estimated reflectance of the mixed pixels together with the percent difference between the estimated reflectance based on linear and nonlinear mixture models are shown in Table 5.

The percent difference ranges from about 2 to 10%. In the linear mixture model, TOA radiance of the mixed pixel is expressed with linear combination of plural material (reflectance and mixing ratio). It may conclude that apparent estimated reflectance of the surface material may be different from the actual reflectance with 2 to 10% depending on reflectance and shape of the surface materials and geographical feature, slope and roughness.

TABLE VI. COMPARISON OF ESTIMATED REFLECTANCE OF THE MIXED PIXELS BASED ON LINEAR AND NONLINEAR MIXTURE MODELS AND THE PERCENT DIFFERENCE BETWEEN BOTH

| | Linear | Nonlinear | % Difference between both |
|------------------------|--------------|--------------|---------------------------|
| Site #1 (Band1, Band3) | 0.161, 0.451 | 0.168, 0.459 | 4.08, 1.83 |
| Site #2 (Band1, Band3) | 0.201, 0.314 | 0.221, 0.342 | 9.95, 8.92 |
| Site #3 (Band1, Band3) | 0.210, 0.302 | 0.217, 0.308 | 3.38, 2.08 |

D. Adjacency effect

Actual surface situations are different from the assumed surface situation of MCRTS. Although there are a variety of pixels with the different materials surrounding at the mixed pixel in concern, just two homogeneous surfaces with 25km by 50 km area is assumed in the MCRTS. The number of photons coming out from the top of the atmosphere through the IFOV (15m on the ground) is counted for calculation of TOA radiance of the mixed pixels that situates at the border between two surfaces.

In order to investigate the influences due to the surrounding pixels, a different reflectance ($\Gamma_A \pm 10\%$, $\Gamma_B \pm 10\%$) of neighboring pixels are considered. Namely, the rest of areas of "a" and "b", 24.925km by 50km in Figure 1 is filled up with $\pm 10\%$ different reflectance of materials for surface "A" and "B", respectively. TOA radiance of the mixed pixels is then affected by the surrounding pixels (it is called adjacency effect).

Adjacency effect of band1 is greater than band 3. The result of adjacency effect estimated with MCRTS for band 1 is shown in Table 7. The effect depends on reflectance, slope, and shape of ground materials of the neighboring pixels as well as optical depth of the atmosphere. As it is mentioned before, interaction between ground cover materials depends on the reflectance, shape of the materials and slope. Adjacency effect of site #2 is expected to be the largest followed by site #1 and #3. The results show almost same expected order except site #3. Contribution of reflectance to the adjacency effect seems to be greater than slope. It is found that the effect is within the range of a couple of percent.

TABLE VII. ADJACENCY EFFECT OF THE NEIGHBORING PIXELS WITH $\pm 10\%$ DIFFERENT REFLECTANCE TO THE TOA RADIANCE OF THE MIXED PIXELS ESTIMATED WITH MCS AT 550NM: TOP TWO COLUMN AND AT 810NM: BOTTOM TWO COLUMN (OPTICAL DEPTH OF MOLECULE AND AEROSOL ARE 0.35, 0.14, RESPECTIVELY.)

| Slope, Reflectance | Site #1: 24/28, 0.14/0.08 | | | Site #2: 30/26, 0.20/0.08 | | | Site #3: 20/0, 0.14/0.12 | | |
|--------------------|---------------------------|-------|--------|---------------------------|-------|-------|--------------------------|-------|--------|
| | -10% | 0% | +10% | -10% | 0% | +10% | -10% | 0% | +10% |
| Adjacency | 109.21 | 109.5 | 111.80 | 108.46 | 111.3 | 114.2 | 107.90 | 110.4 | 112.83 |
| % Ratio | -2.09 | 0 | +2.10 | -2.56 | 0 | +2.61 | -2.26 | 0 | +2.21 |
| Adjacency | 137.8 | 141.1 | 144.3 | 138.4 | 142.2 | 146.1 | 139.0 | 141.9 | 144.9 |
| % Ratio | -2.32 | 0 | +2.29 | -2.66 | 0 | +2.73 | -2.04 | 0 | +2.14 |

IV. CONCLUSION

It is found that the influence due to tree-tree interaction on the surface reflectance estimation depends on tree distance and ranges from 8 to 10%. Also it is found that the estimated surface reflectance based on the proposed nonlinear mixed pixel model is much closer to that from linear mixed pixel model. It may conclude that influence due to multiple reflections among ground cover targets has to be considered on the surface reflectance estimation.

Through the comparison between the estimated reflectance derived from the actual ASTER/VNIR of the mixed pixels and the estimated reflectance based on the linear and the proposed nonlinear mixture models shows the discrepancy ranges from about 2 to 10 %. Also it is found that the estimated reflectance based on the nonlinear model is much closer than that of the linear model.

Adjacency effect on TOA radiance of the mixed pixels is highly dependent on reflectance of materials followed by slope and shape of the materials. Adjacency effect from the surrounding pixels with 10% different reflectance is within 3% so that 2 to 10% of the difference between apparent and real reflectance exists with 3% of possible error. Real situation is more complicated and is not easy to simulate.

ACKNOWLEDGMENT

The author would like to thank Mr. Kohei Imaoka for his efforts through experiments and simulations.

REFERENCES

[1] Arai, K, Lecture Notes on Remote Sensing, Morikita-Shuppan, Co.Ltd., 2005

[2] C.C.Borel and S.A.Gerst, Nonlinear spectral mixing models for vegetative and soils surface, Remote Sensing of the Environment, 47, 2, 403-416, 1994.

[3] R.N.Clark and T.I.Roush, Reflectance spectroscopy: Quantitative analysis techniques for remote sensing applications, Journal of Geophysical Research, 89, B7, 6329-6340, 1984.

[4] B.Hapke, Bidirection reflectance spectroscopy, I. Theory, Journal of Geophysical Research, 86, 3039-3054, 1981.

[5] Mersenne Twister (MT), <http://www.math.sci.hiroshima-u.ac.jp/~m-mat/MT/mt.html>

[6] B.Nash and J.Conel, Spectral reflectance systematic for mixtures of powered hypersthene, labradorite and ilmenite, Journal of Geophysical Research, 79, 1615-1621, 1974.

[7] R.Singer, Near infrared spectral reflectance of mineral mixtures: Systematic combinations of pyroxenes olivine and iron oxides, Journal of Geophysical Research, 86, 7967-7982, 1974.

[8] R.Singer and T.B.McCord, Mars; Large scale mixing of bright and dark surface materials and implications for analysis of spectral reflectance, Proc., 10th Lunar and Planetary Sci., Conf., 1835-1848, 1979.

AUTHORS PROFILE

Kohei Arai, He received BS, MS and PhD degrees in 1972, 1974 and 1982, respectively. He was with The Institute for Industrial Science and Technology of the University of Tokyo from April 1974 to December 1978 also was with National Space Development Agency of Japan from January, 1979 to March, 1990. During from 1985 to 1987, he was with Canada Centre for Remote Sensing as a Post Doctoral Fellow of National Science and Engineering Research Council of Canada. He moved to Saga University as a Professor in Department of Information Science on April 1990. He was a councilor for the Aeronautics and Space related to the Technology Committee of the Ministry of Science and Technology during from 1998 to 2000. He was a councilor of Saga University for 2002 and 2003. He also was an executive councilor for the Remote Sensing Society of Japan for 2003 to 2005. He is an Adjunct Professor of University of Arizona, USA since 1998. He also is Vice Chairman of the Commission "A" of ICSU/COSPAR since 2008. He wrote 30 books and published 322 journal papers

Method for Psychological Status Monitoring with Line of Sight Vector Changes (Human Eye Movements) Detected with Wearing Glass

Kohei Arai¹

Graduate School of Science and Engineering
Saga University
Saga City, Japan

Kiyoshi Hasegawa²

² Hitachi Co. Ltd.
Tokyo, Japan

Abstract—Method for psychological status monitoring with line of sight vector changes (human eye movement) detected with wearing glass is proposed. Succored eye movement should be an indicator of humans' psychological status. Probability of succored eye movement, therefore, is measured. Through experiments with simple and complicated documents, relation between psychological status measured with eeg signals and the probability of succored eye movements is clarified. It is found that there is strong relation between both results in psychological status can be estimated with eye movement measurements.

Keywords—psychological status; eye movement; eye detection and tracking; eeg signal;

I. INTRODUCTION

The number of blink increases in accordance with angrily nevus, excitations while it decreases in accordance with concentration, cares. In accordance with Asher & Ort (1951), fixed eye status is affected by emotional words stimulating human brain with eye jerk movement in horizontal direction, frequent blink, and eye close [1]. Antrobus et al. (1964) said that eye movement when human actively think about something is much active than that when human think about something passively [2]. Stoy (1930) also said that eye movement when human look at spatial materials is much active than that when human look at non spatial materials [3]. Meanwhile, Greenberg (1970) said that optokinetic nystagmus increases when human calculation by heart for complicated calculations in comparison to that when human calculate by heart for simple calculations [4]. These studies are conducted with users who do not move at all. As mentioned above, there is strong relation between psychological status and eye movement. In particular, succored movement has a strong relation to psychological status.

Eye movements can be detected and tracked with camera images even if users are moving. By using glass mounting near infrared camera with near infrared light sources, acquired images do not affect by illumination condition changes and also it allows users' movements [5]-[10]. Therefore, eye movement detection and tracking can be done through users' movement results in estimation of psychological status monitoring during users' movement.

The proposed method and system allows such this functionality of psychological status monitoring under users'

movement conditions. Through experiments with simple and complicated documents, relation between psychological status measured with eeg signals and the probability of succored eye movements is clarified. It is found that there is strong relation between both results in psychological status can be estimated with eye movement measurements.

The following section describes the proposed method and system followed by experiments. Then final section describes conclusion with some discussions.

II. PROPOSED METHOD AND SYSTEM

A. System Architecture

The proposed system consists of the glass which mounts near infrared camera with near infrared LED: Light Emission Diodes which are aligned surrounding to the optical entrance of near infrared camera. Figure 1 shows outlook of the glass while major specification is shown in Table 1.

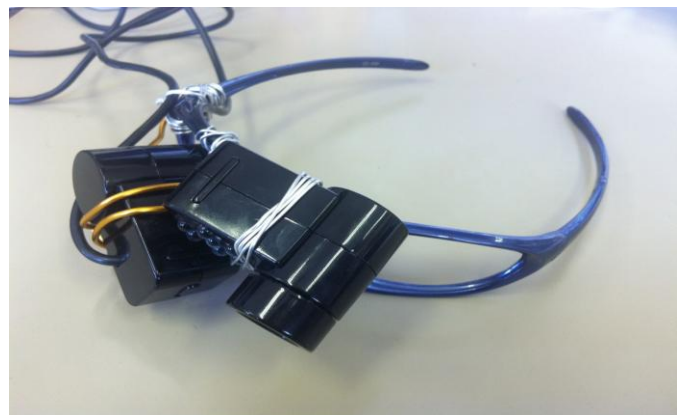


Fig. 1. Outlook of the glass mounting near infrared camera with near infrared LEDs

The glass is mounting two cameras, one is for acquiring human eye and the other camera is for acquiring the image at which user looks. As shown in Table1, camera has LED of light source so that eye movement can be detected and tracked without influence due to illumination condition changes. Also, the glass moves in accordance with head movements so that the proposed system allows users' movement.

TABLE I. SPECIFICATION OF NEAR INFRARED: NIR CAMERA

| | |
|---------------------|---------------------------------------|
| Pixel | 1.3 M |
| Resolution | 1280×1024 |
| Frame rate | 1280 x 1024: 7.5fps, 640 x 480: 30fps |
| Dimension | 52mm (W) × 65mm (D) × 70mm (H) |
| Weight | 85g |
| Operating condition | 0 - 40deg.C |
| Interface | SB 2.0 |
| IR Illumination | 7 IR LED |

III. EXPERIMENTS

B. Experimental Method

The experiments are conducted with eeg sensor. Eeg sensor of brain catcher manufactured by Noryoku Kaihatsu Co. Ltd. is used. Outlook of the eeg sensor is shown in Figure 2. Major specification of eeg sensor is shown in Table 2.



Fig. 2. Outlook of the eeg signal acquisition sensor of brain catcher manufactured by Noroku Kaihatsu Co. Ltd. is used.

TABLE II. SPECIFICATION OF EEG SENSOR

| | |
|--------------------|--------------------------|
| Frequency coverage | 4HZ~24HZ ±3dB for eeg |
| Frequency coverage | 150HZ~800HZ ±3dB for emg |
| Sampling frequency | 1024Hz |
| Quatization bit | 10 bit |
| Input impedance | 10MΩ |

C. Preliminary Experimental Results on Gaze Estimation Accuracy

System starts with find the location of pupil. After pupil location is found, next is converts into gaze angle. As we see in Figure 3, the single camera is used and the position is mounted on user's glass.

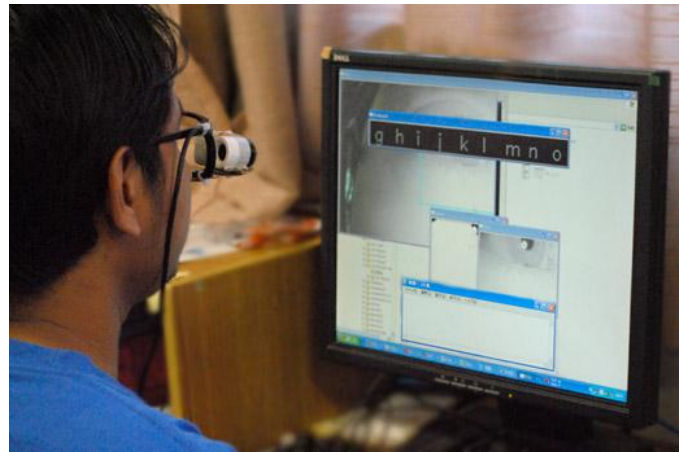


Fig. 3. Eye detection and tracking

It means that between camera and display is separated each others. Because of this, should has the connector that will connect between camera mounted on user's glass and display monitor in order to obtain that what user's look is same position with pointer in display. In order to connect them, the calibration is required. After user wearing the glass, user looks at four corners on display. By using the adjustment method, the user's gaze output will correlate with the pointer.

Gaze estimation accuracy is measured at the middle center to horizontally aligned five different locations with the different angles as shown in Figure 4. The experimental result shows the gaze estimation error at the center middle (No.1) shows zero while those for the angle ranges from -5 to 15 degrees is within 0.2 degree of angle estimation error as shown in Table 3.. Because the user looks at the center middle with 5 degree allowance results in 0.2 degree of gaze estimation accuracy.

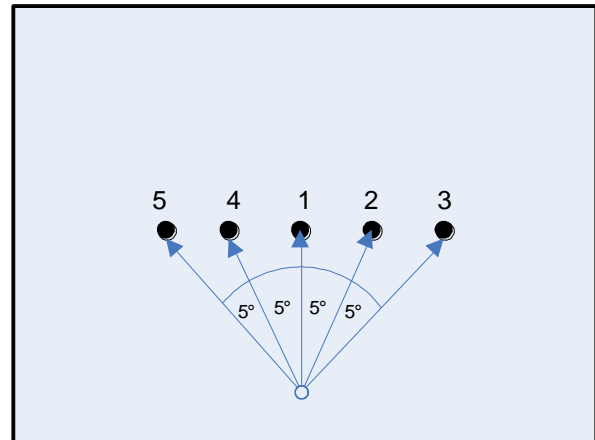


Fig. 4. Measuring accuracy

TABLE III. GAZE ESTIMATION ACCURACY AT THE DESIGNATED VIEWING ANGLES

| Point | 1 | 2 | 3 | 4 | 5 |
|---------------|---|-----|-----|-----|------|
| Error(degree) | 0 | 0.2 | 0.2 | 0.2 | 3.12 |

D. Documents Used for the Experiments

Two documents, relatively simple and comparatively complicated documents are prepared. Two documents are shown in Figure 5 (a) and (b). Four students read the two documents in almost same conditions. During students read two documents, eeg signals are acquired. The frequency components are analyzed with FFT: Fast Fourier Transformation. Then maximum frequency component is used for characterization of psychological status.

E. Preliminary Experimental Results of Maximum Frequency of eeg Signals

Eeg signals are acquired when a student is taking a rest and learn hard with e-learning contents. Maximum frequency of eeg signals are calculated at the same time. Figure 6 (a) shows an example of maximum frequency at when the student is taking a rest while Figure 6 (b) shows that at when the student is learning with e-learning contents, respectively. As shown in Figure 6, maximum frequency at when the student is learning is much higher than that at when the student is taking rest, obviously.

むかし、あるところに、おじいさんがひとりですんでいました。
あるひ、ひるごはんのあとにいぶくしている、つぼめが いちわ どまに おちてきました。
つぼめは、はねを バタバタさせて、まいあがろうとするのですが、すくにまた、どまに おちて、もがいています。

おじいさんが、どうしたのかとおもって みてみると、あしが おれていました。
「おお、かわいそうに。これでは、とぶことはできません。わしが なおしてやろうなあ」と、くすりをつけて、こえだを そえて ほうたいを まいて やりました。
おじいさんは、まいにち、つぼめを かいほうして やりました。

しばらくして つぼめのあしは、なおって、とべるようになりました。
おじいさんは、「よかった、よかった、もう だいじょうぶ!」と、いって はなして やりました。
つぼめは、おじいさんの いえのうえを、ぐるりと とんでから、とおくのそらへ とんでいきました。
「これから、きをつけて、げんきでくせよー。そうして、らいねんも また、こいよー」つぼめが みえなくなっても、おじいさんは、こえを かけつづけました。

それから、いちねん たちました。
おじいさんが、まえにわでいぶくしていると、つぼめが やってきました。
「お、きたかや。おまえは きょねん、たすけて やった やつか。よう きたなあ」と、はなしかけました。

つぼめは、しばらく おじいさんの あたまのうえを とびまわって いましたが、まっくらけな おおきな つぶを、ひとつぶ ポ テーンと おとして、とんでいってしまいました。

「なんだ これは! フンをおとしていったのかい」と、いいながら よくみると、おおきな すいかの たねでした。
「あれ あれ、すいかのたねを、おとしていったのか。そうか、おれに これをうえて、すいかが ならたら たべろということかな。きょねん、たすけて やったおかしに、すいかのたねを、もって来たというわけか」

おじいさんは、つぼめが もってきた すいかのたねを、はたけに まきました。
みずをやったり、こやしをやったり、だいに せわをしていると、やがて おおきな つるの ひびきて、みが ひとつ になりました。
おじいさんは、まいにちは たけにいて、すいかを なでて やりました。

すいかのみは、どんどん どんどん おおきくなって きました。
あるひ、おじいさんが、すいかを たたくと、ちょうど たべごろの おとが しました。
おじいさんは、おおきな すいかを うんとこしょ どんこいしょと、やつのことで、いえにも ちかえり ました。

おじいさんが、すいかを まつぶたつに わつたとたん、たねの ひとつぶ ひとつぶが、だいくさんや こびきさんになって、どつと でてきました。

(a) Relatively simple document

脳波 (のうは、Electroencephalogram : EEG) は、ヒト・動物の脳から生じる電気活動を、頭皮上、蝶形骨底、鼓膜、脳表、脳深部などに置いた電極で記録したものである。

英語の Electroencephalogram の忠実な訳語として、脳電図、EEG という呼び方もあり、中国語ではこちらの表現法を取っている。

本来は、脳波図と呼ぶべきであるが、一般的には「脳波」と簡略化して呼ばれることが多い。

脳波を測定、記録する装置を脳波計 (Electroencephalograph : EEG) と呼び、それを用いた脳波検査 (Electroencephalography : EEG) は、医療での臨床検査として、また医学、生理学、心理学、工学領域での研究方法として用いられる。

検査方法、検査機械、検査結果のどれも略語は EEG となるので、使い分けに注意が必要である。

個々の神経細胞の発火を観察する単一細胞電極とは異なり、電極近傍あるいは遠隔部の神経細胞集団の電気活動の総和を観察する (少数の例外を除く)。

近縁のものに、神経細胞の電気活動に伴って生じる磁場を観察する脳磁図 (のうじず、Magnetoencephalogram : MEG) がある。

直接記録する方法はしばしば臨床検査として用いられる。背景脳波 (基礎律動) や突発活動 (てんかん波形など) を観察する。

各種のてんかん、ナルコレプシー、変性疾患、代謝性疾患、神経系の感染症、脳器質的疾患、意識障害、睡眠障害、精神疾患などの診断の補助・状態把握などに用いられる。

波形の加工の方法として、主なものに加算平均法、双極子推定法、周波数解析、コヒーレンス法、主成分分析、独立成分分析などがあり、一部は臨床でも用いられている。

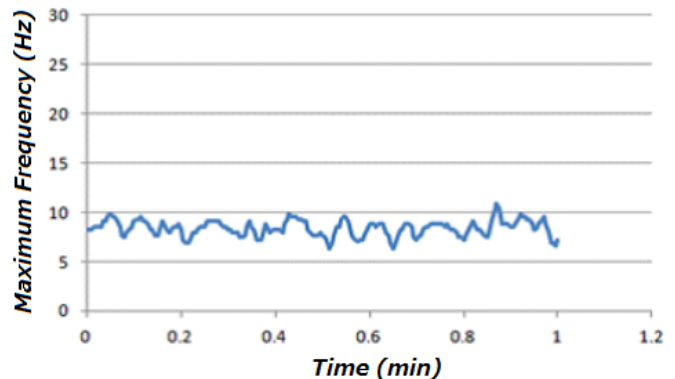
脳波を直接記録する方法はしばしば臨床検査として用いられる。背景脳波 (基礎律動) や突発活動 (てんかん波形など) を観察する。

各種のてんかん、ナルコレプシー、変性疾患、代謝性疾患、神経系の感染症、脳器質的疾患、意識障害、睡眠障害、精神疾患などの診断の補助・状態把握などに用いられる。

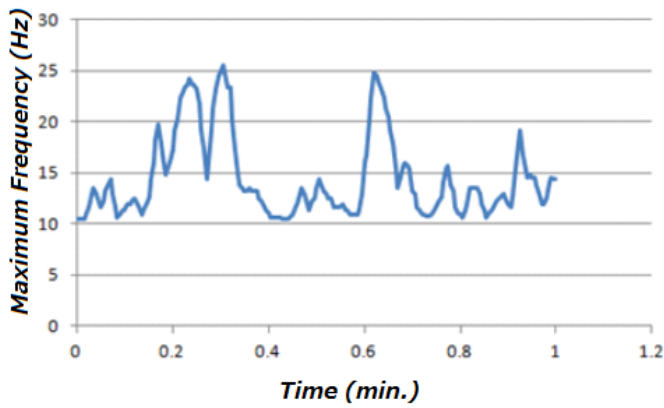
波形の加工の方法として、主なものに加算平均法、双極子推定法、周波数解析、コヒーレンス法、主成分分析、独立成分分析などがあり、一部は臨床でも用いられている。

(b) Comparatively complicated document

Fig. 5. Two documents used for the experiments



(a) Taking a rest



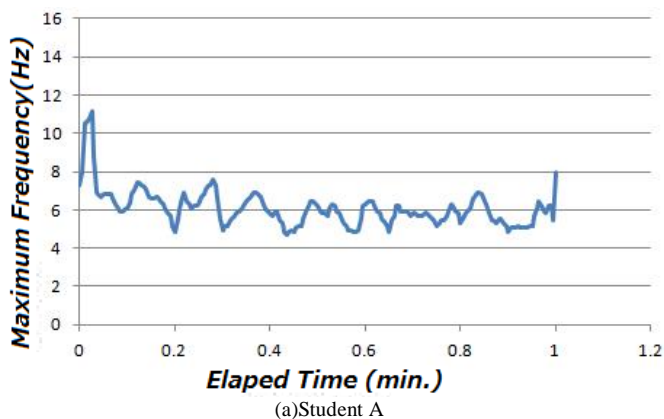
(b) Learning with e-learning contents.

Fig. 6. eeg derived maximum frequency comparison

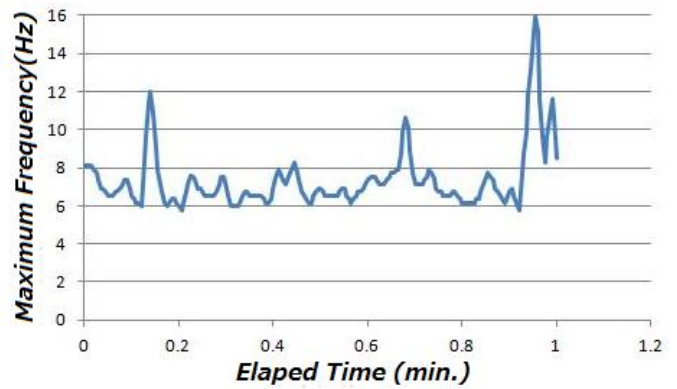
F. Experimental Results

Figure 7 shows eeg signals of the students A to D when they are reading the relatively simple document. Meanwhile, Figure 8 shows those for the students A to D when they read the comparatively complicated document. Each student shows a little bit different trend of the maximum frequency. Namely, each student feels difficultness or easiness of the document differently. The maximum frequency for the relatively simple document is below 10 Hz while that for the comparatively complicated document shows more than 10Hz in particular more than 15Hz for three students. Alpha frequency ranged from 8 to 13 Hz. Averaged maximum frequencies over the time for reading the relatively simple documents for the student A to D are 6, 7, 9, and 10, respectively. On the other hand, averaged maximum frequencies over the time for reading the relatively complicated documents for the student A to D are 23, 20, 15, and 14. Therefore, difference of maximum frequencies between relatively simple and comparatively complicated documents is significant.

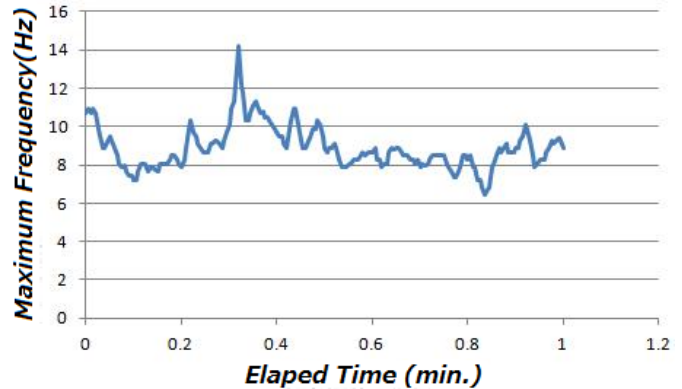
Therefore, most students read the relatively simple document in a relax situation while most students read the comparatively complicated document in a irritated situation because their maximum frequency component shows beta frequency dominantly.



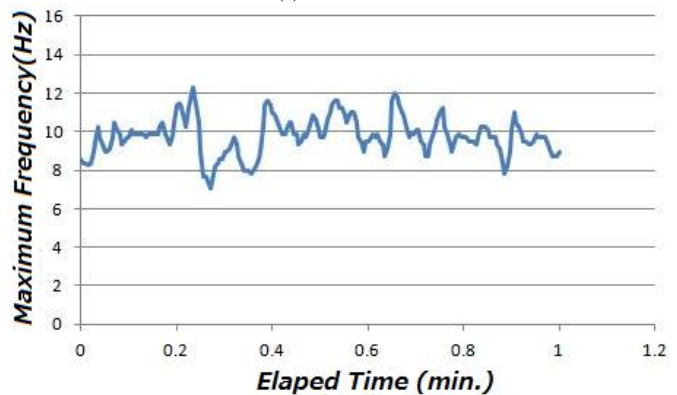
(a) Student A



(b) Student B

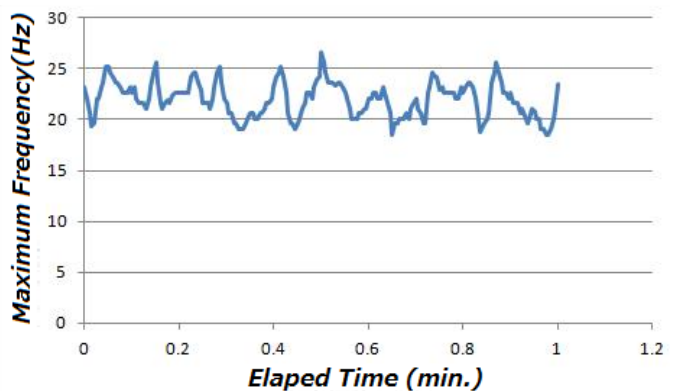


(c) Student C



(d) Student D

Fig. 7. Maximum frequency during the students read the relatively simple document



(a) Student A

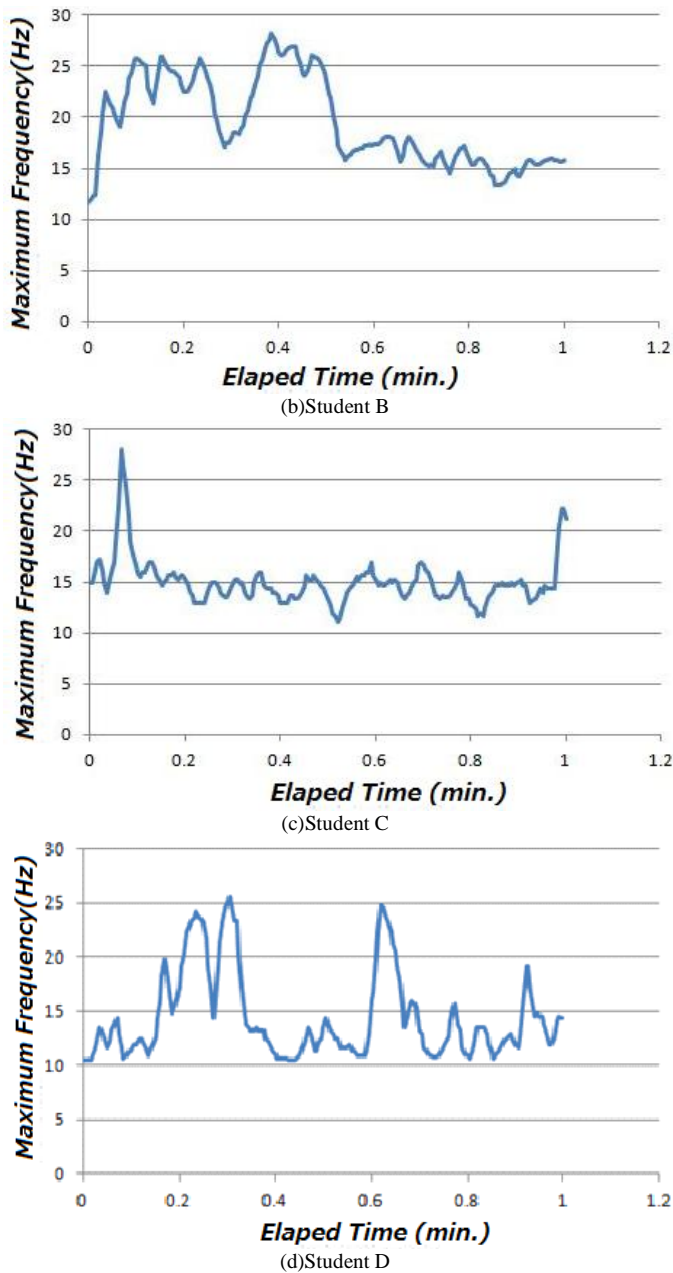


Fig. 8. Maximum frequency during the students read the relatively complicated document

Figure 9 shows the maximum frequency of eeg signal when the students read the two documents. Figure 10 shows the number of succored eye movement a second when the students are reading the two documents. Succored movements are detected with the acquired students' eye images through image analysis based on template matching. The number of succored movements for the relatively simple document is less than that for the comparatively complicated document, obviously. Furthermore, the difference of the number of succored movement between the two documents is dependent on each student.

Furthermore, Figure 11 shows the remarkable moments of the maximum frequency when the students are reading the

comparatively complicated document. In the figure, the first red circle is situated when the students read the word "Electroencephalogram" while the second red circle is situated when the students read the word of "ナルコレプシー" and the third red circle indicates at when the students read the word of "双極子推定法", respectively. These words are totally new for the students so that they had to read again the words.

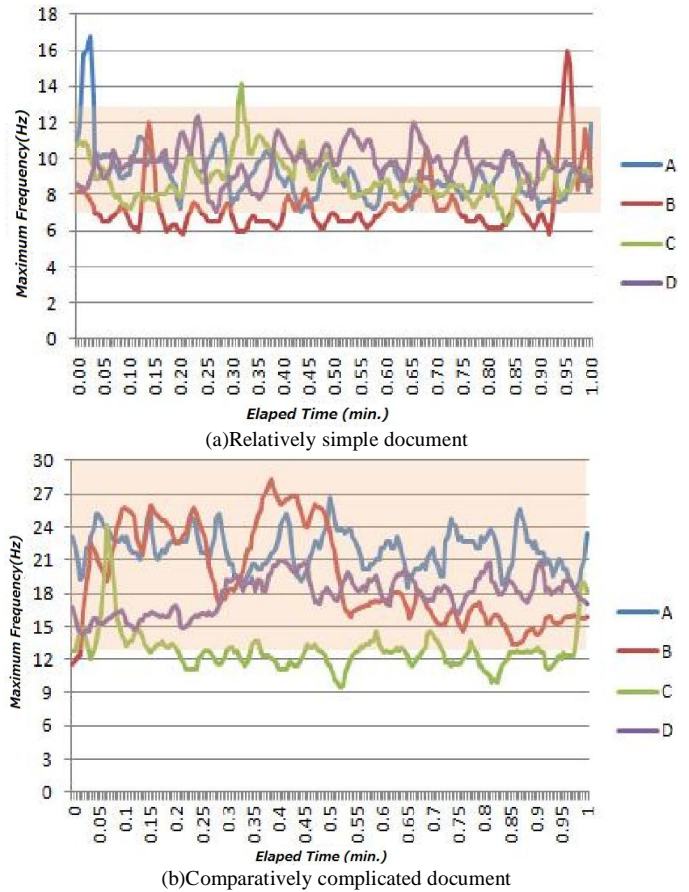


Fig. 9. Maximum frequency of eeg signal when the students read the two documents

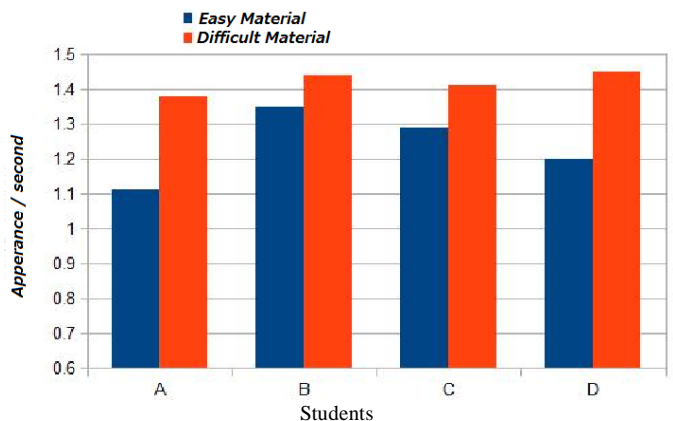


Fig. 10. The number of succored eye movement a second when the students are reading the two documents

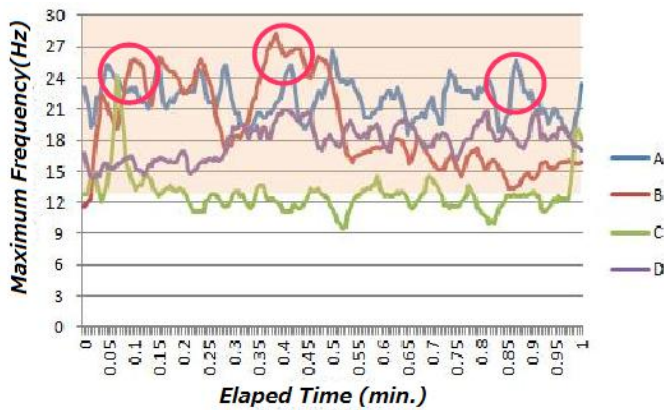


Fig. 11. The remarkable moments of the maximum frequency when the students are reading the comparatively complicated document.

The first red circle is situated when the students read the word “Electroencephalogram” while the second red circle is situated when the students read the word of “ナルコレプシー” and the third red circle indicates at when the students read the word of “双極子推定法”, respectively..

IV. CONCLUSION

Method for psychological status monitoring with line of sight vector changes (human eye movement) detected with wearing glass is proposed. Succored eye movement should be an indicator of humans’ psychological status. Probability of succored eye movement, therefore, is measured. Through experiments with simple and complicated documents, relation between psychological status measured with eeg signals and the probability of succored eye movements is clarified. It is found that there is strong relation between both results in

psychological status can be estimated with eye movement measurements.

ACKNOWLEDGMENT

The authors would like to thank Ms. Mayu Osumi for her effort to conduct the experiments together with the students who participated to the experiments.

REFERENCES

- [1] S. Brin and L. Page. The anatomy of a large-scale hypertextual Web search engine. *Computer Networks and ISDN Systems*, 30(1{7}):107{117, 1998.
- [2] Ruggieri, V., The running horse stops: the hypothetical role of the eyes in imagery of movement, *Perceptual and Motor Skills*, 89, 1088–1092 (1999).
- [3] Mariko Takeda, Effect of mental activity in problem solving on eye movement, *The Japanese Journal of Ergonomics*, 12, 175–181 (1976)
- [4] Asher, E. J. & Ort, R. S., Eye movement as a complex indicator, *J. Gen. Psychol.*, 45, 209–217 (1951).
- [5] Antrobus, J. S., Antrobus, J. S., & Singer, J. L., Eye movements accompanying daydreaming, visual imagery, thought suppression, *J. Abnorm. Soc. Psychol.*, 69, 244–252 (1964).

AUTHORS PROFILE

Kohei Aarai He received BS, MS and PhD degrees in 1972, 1974 and 1982, respectively. He was with The Institute for Industrial Science and Technology of the University of Tokyo from April 1974 to December 1978 and also was with National Space Development Agency of Japan from January, 1979 to March, 1990. During from 1985 to 1987, he was with Canada Centre for Remote Sensing as a Post Doctoral Fellow of National Science and Engineering Research Council of Canada. He moved to Saga University as a Professor in Department of Information Science on April 1990. He was a councilor for the Aeronautics and Space related to the Technology Committee of the Ministry of Science and Technology during from 1998 to 2000. He was a councilor of Saga University for 2002 and 2003. He also was an executive councilor for the Remote Sensing Society of Japan for 2003 to 2005. He is an Adjunct Professor of University of Arizona, USA since 1998. He also is Vice Chairman of the Commission-A of ICSU/COSPAR since 2008. He wrote 30 books and published 332 journal papers.

Mobile Devices Based 3D Image Display Depending on User's Actions and Movements

Kohei Arai¹, Herman Tolle¹

Graduate School of Science and Engineering
Saga University
Saga City, Japan

Akihiro Serita²

Serita Constructions Co. Ltd.
Takeo City, Japan

Abstract—Method and system for 3D image display onto mobile phone and/or tablet terminal is proposed. Displaying 3D images are changed in accordance with user's location and attitude as well as some motions. Also 3D images can be combined with real world images and virtual images. Through implementation and experiments with virtual images, all functionalities are verified and validated. One of applications of the proposed system is attempted for demonstration of virtual interior of the house in concern. User can take a look at the inside house in accordance with user's movement. Thus user can imagine how the interior of the house looks like.

Keywords—3D image representation; argumeted reality; virtual reality;

I. INTRODUCTION

There are strong demands of 3D image display onto mobile devices and or tablet terminals of which virtual 3D images are changed in accordance with users' movements. For instance, virtual interior (in house) 3D images are changed according to users' movement when users wear Head Mount Display: HMD on which the created 3D images are displayed. Then users can imagine interior images designed by architects.

OS of iPhone: iOS is well described [1], [2] together with 3D programming [3]. On the other hand, game and graphics programming under iOS and Android OS environment for OpenGL of computer graphics software is available [4]. There are a variety of software tools and library software for developing programs under Apple OS environment [5]. Also video programming can be done on iTune [6]. Motion detection and capturing can be done through sensor fusion on Android devices [7]. Thus mobile phone, tablet terminal based 3D image display depending on user's actions and movements can be created.

The following section describes the proposed method and system for displaying 3D images which depend on users' action and movement onto mobile devices and tablet terminals followed by implementation and experiments. Then conclusion is described with some discussions.

II. PROPOSED METHOD AND SYSTEM

A. Proposed System

Illustrative view of the proposed system is shown in Figure 1.

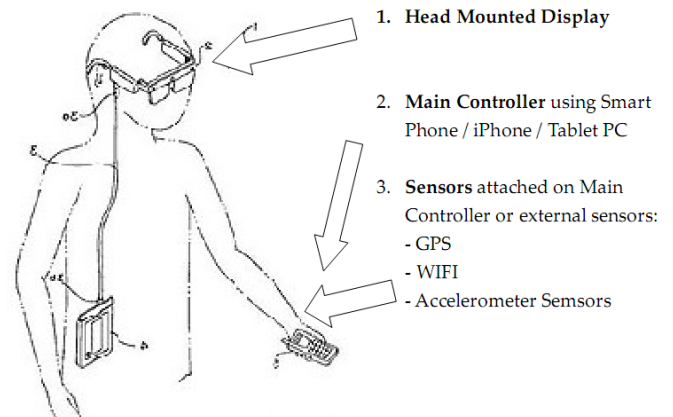


Fig. 1. Illustrative view of the proposed system

User wears Head Mount Display: HMD. User also has mobile device or tablet terminal which has GPS receiver, WiFi communication capability, and accelerometer together with gyro and magnetic compass. Therefore, users may move and may change their attitude together with some actions. Users can see 3D images displayed onto screen of mobile devices or tablet terminals as the users in the virtual studio which is shown in Figure 2. If users move in the virtual studio, then the displayed 3D image is changed in accordance with the movement. Also when users look to the right and left as well as up and down, then 3D image is changed according to the look angles defined in the Figure 3.

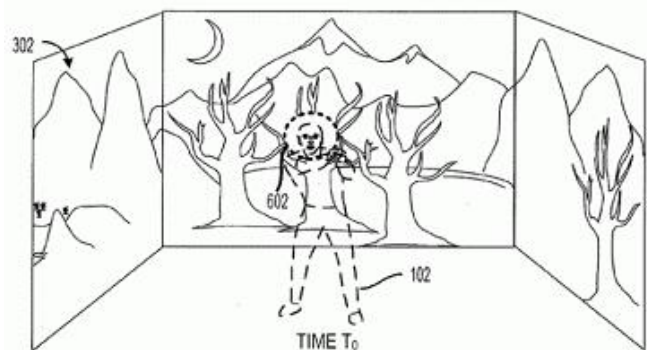


Fig. 2. Virtual studio

III. METHOD USED

A. Attitude Detection

Accelerometer data, usually, too rapidly changed. Therefore, some low pass filter is needed for detect relatively smoothly changed attitude as shown in Figure 5. If the iPhone and iPad is inclined 90 degrees, then x and y axis is exchanged as shown in Figure 6. If users change their attitude in pitching direction as shown in Figure 8, then heading angle can be estimated with accelerometer data.

Triple Axis Accelerometer (x, y, z) data can be transferred from iPhone to LIS302DL with communication through *Low Level Accelerometer API: LLA API*. These data should be filtered to remove shaking effect (using *low pass filter*).

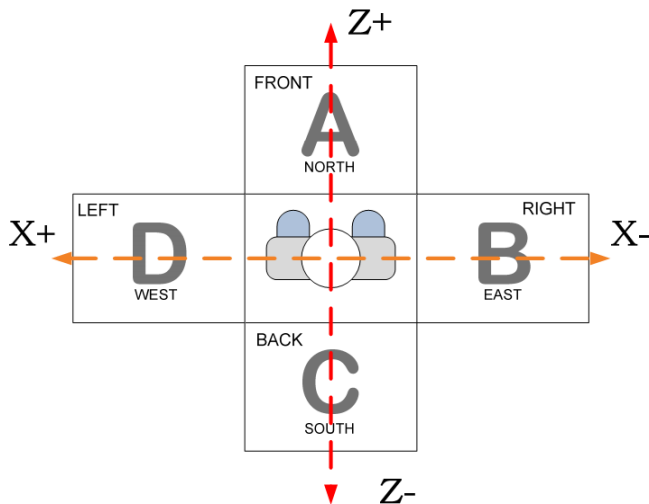


Fig. 3. Definition of user's location and looking angle

B. System Architecture

Proposed system architecture is shown in Figure 4.

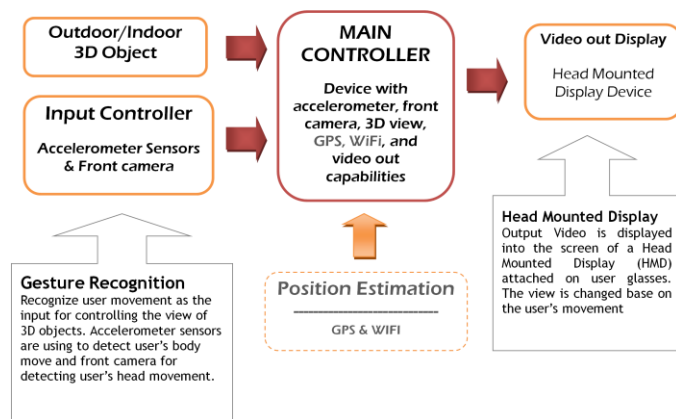
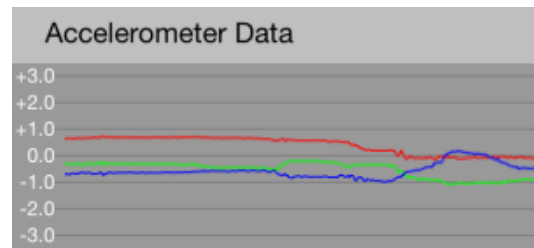


Fig. 4. Proposed system architecture

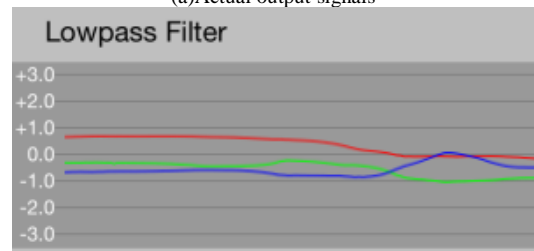
Users' action and movement can be detected with gesture recognition in the input controller which consists of accelerometer and gyro sensors. Recognize user movement as the input for controlling the view of 3D objects. Accelerometer sensors are using to detect user's body move and front camera for detecting user's head movement.

Indoor and outdoor 3D images can be created in accordance with the users' action and movements. These data are controlled by the main controller which includes front camera, GPS receiver, WiFi of equipments.

Main controller has video output capability. Therefore, created 3D images can be displayed onto mobile phones and or tablet terminals together with HMD. Output Video is displayed into the screen of a HMD attached on user glasses. The view is changed base on the user's movement.



(a)Actual output signals



(b)Filtered attitude signals

Fig. 5. Acquired and processed attitude data (Red: x, Green: y and Blue: z directions, respectively)

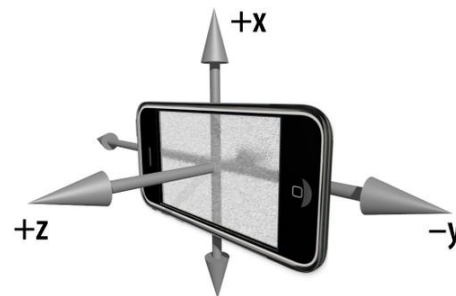


Fig. 6. Horizontally situated iPhone and iPad

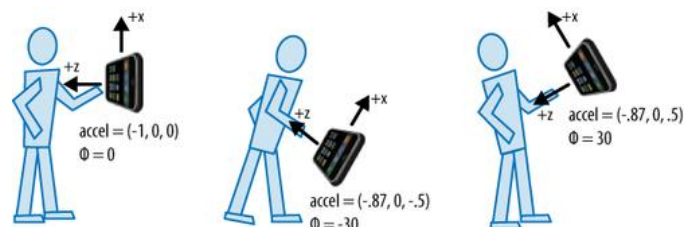


Fig. 7. Pitching motions of users' attitude changes

Body turn around, head look to the left-right can be detected with direction sensors (azimuth). Also head look down-up can be detected with direction of gravity (altitude).

Although direction of gravity did not tell the direction, direction can be determined by using Gyro Compass or GPS for outdoor case. For indoor case, we can use Compass (*magneticHeading*). Head movement (left-right) can be detected by using captured face image from *rear camera*, then using image processing for determine the movement.

B. Detection of Walking

The following three methods are attempted for detection of the linear movement:

- 1) Double integration of the acceleration to measure speed and then the distance.
- 2) Combination of Gyro Acceleration, Compass and Accelerometer to find Linear Movement
- 3) Using DeviceMotion Data (DeviceMotion is part of CoreMotion framework, a new framework on iOS as combination of Accelerometer & Gyr0)

There are four types of motion on DeviceMotion:

- 1) UserAcceleration
- 2) Attitude
- 3) RotationRate
- 4) Gravity

Each type of motion has different response for 3 different states (Stop, Walking, Rotating)

Using the response of **deviceMotion.rotationRate** then we develop our new method for user walking detection.

Walking can be detected by estimating cycle on accelerometer sensors signal. Figure 8 shows typical accelerometer output signals when users stay (Stable), move forward (Walking) and change their attitude in roll, pitch and yaw directions (Rotation). In the figure, left column shows the motion of users' acceleration while right column shows the motion of users' rotation rate (the first derivative). It is much easier to detect their motions by using rate data rather than the acceleration itself.

Rotation can be detected by using the motion of users' rotation rate in directions of roll, pitch and yaw angles. Rotation angles in direction of roll, pitch and yaw directions are estimated with the motion of users' acceleration data. Meanwhile, walking can be detected by using the motion of users' rotation rate. All of rotation rate in directions of roll, pitch and yaw directions is relatively small in comparison to that of the motion of users' rotation.

When users do not move, then accelerometer data shows stable while if users change their attitude in roll direction, then accelerometer shows relatively large changes in the corresponding direction. On the other hand, when users are walking, the accelerometer data shows small changes. Therefore, it is possible to detect users' walk.

C. Control Camera Position, Orientation of 3D Space in Computer Graphics

In order to create 3D Computer Graphics: CG images which depends on users' action and movement by frame by frame basis, users' position, action and face angle (head pose) has to be detected together with determination of camera position and looking angle, users' orientation of line of sight, and relation between camera and 3D object. Figure 9 shows the process flow of controlling camera position, orientation of 3D space in Computer Graphics: CG.

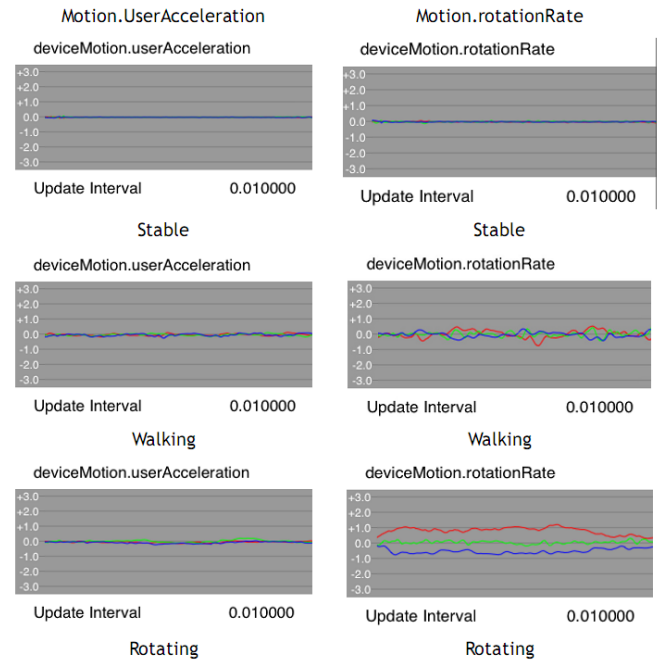


Fig. 8. Typical accelerometer output signals (Motion of users' acceleration (left hand side and motion, rotation rate (right hand side))

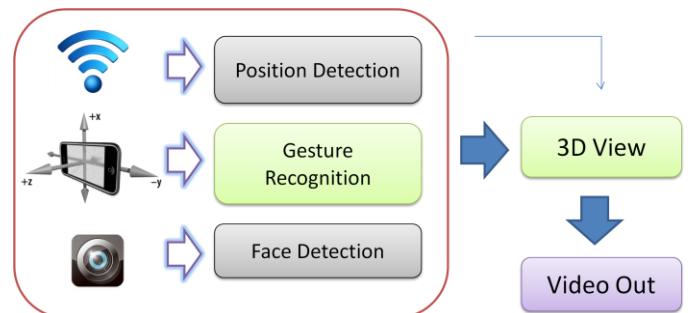


Fig. 9. Process flow of controlling camera position, orientation of 3D space in computer graphics

With the GPS receiver (Outdoor) and wireless LAN access point or WiFi access point (Indoor), users' location can be estimated. Using acquired users gesture with front camera mounted on mobile devices and/or tablet terminal, camera orientation in 3D space of CG can be estimated. Also users' head pose can be estimated by using the acquired image with the front camera.

IV. IMPEMETATIONS

A. Development Environment

Development environment is shown below,

- MacPro with OS X (Mountain Lion)
- Development Tools: Xcode 4.5.1
- Programming Language: Objective-C
- Device: iPhone 4s / iPad2 / iPad Mini
- Registered as iOS Developer University Program (Saga University, max for 200 developers)
- Scalar Head Mounted Display
- iWear iPhone Video Glasses

Development setup has to be done with the following procedure,

- Register as iOS Developer
- Register for iOS Developer University Program (free but limited for research purpose)
- Register the device for Development and Testing
- Get Certificate for the device and development permission
- Start development using Xcode

There are the following three modules for development,

- 3D object Scene View Controlling Module
 - Loading, rendering, displaying, changes view based on user input (touch screen or from sensors), Collision detection
- User Interface Controlling Module
 - Touch screen based controlling
 - Sensor based controlling
 - Walking, Turn Around, Look Up-Down, Shake
- Video Out System

In the 3D object Scene View Controlling Module, there are the following features,

- OpenGL ES based
- Standard file format for 3D object: **Wavefront** format (.obj, .mtl)
- Camera Frustum view based
- Controlling the motion with touch screen:
 - Rotate (Left / Right),
 - Look (Up / Down),
 - Step (Forward / Backward),
 - Collision Detection (Front / Back)

Body Movement recognizing module is based on the following methods,

- Internal Sensors: Accelerometer, Gyro, Magnetometer
- Pull Data access method
- Update Interval (Frequency): 24 Hertz (24 data in one second)
- Body movement method:
 - Look Up – Look Down → Altitude using Digital Compass
 - Turn Around (Left – Right) → Azimuth using Accelerometer
 - Walking (Step Forward – Step Backward) → Linear movement using MotionData.rotationRate
 - Small Jump (Shake) → Shake using Shake Event (Accelerometer)










Users' orientation can be estimated as follows,

- Pitch controlling using Digital Compass: magneticHeading vs true heading
- We use Core Location → locationManager:magneticHeading

B. Device Selection

Table 1 shows tradeoff table for possible devices for the proposed system.

TABLE I. TRADEOFF TABLE FOR POSSIBLE DEVICES FOR THE PROPOSED SYSTEM.

| Scenarios | 1 | 2 | 3 | 4 |
|------------------------|---|---|--|---|
| Controller: | PC or NOTEBOOK | iPhone/iPod | Android Tablet | Specific Android Tab |
| OS: | Windows OS | iOS, | Android OS | Android OS |
| Port: | VCA out | iPhone standard connector | Mini HDMI | Special TV Out |
| Programming: | General (C++, C#) | iPhone programming | Android Programming | Android Programming |
| Difficulties: | Moderate (**) | Difficult (****) | Difficult (****) | Difficult (****) |
| 3D Development: | Moderate (**) | Moderate (**) | Difficult (****) | Difficult (**) |
| Environment | PC based | MAC OS / iOS based | PC based | PC based |
| Sensors: | - | Accelerometer, Compass, GPS | Accelerometer, GPS | Accelerometer, GPS |
| Controller |  |  |  |  |
| Connector | VGA to RCA | iPhone TV Out | Mini HDMI to RCA | Specific TV Out Cable |
| |  |  |  |  |
| |  | | | |

Due to the fact that iPhone and iPad has a capability of gyro and magnetic compass and also has a capability to output 3D images to HMD easily, iPhone and iPad is used for the proposed system. Figure 10 shows the definition of coordinate system of the iPhone and iPad.

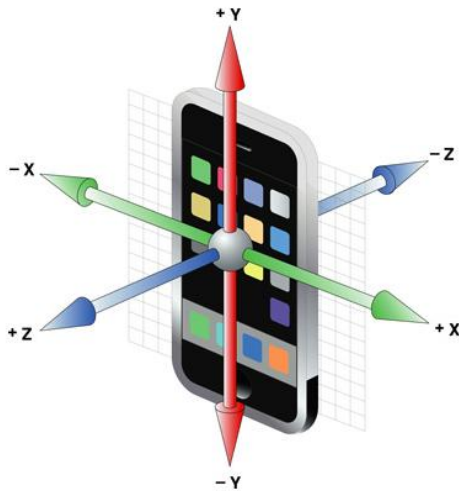


Fig. 10. Definition of coordinate system of iPhone and iPad.(Vertically situated case)

As is mentioned in the previous section, iPad is selected for the proposed system. The following HMD which is shown in Figure 11 can be attached to the iPad for displaying the created 3D images. Major specification of HMD is shown in Table 2.



Fig. 11. Outlook of the HMD used

TABLE II. MAJOR SPECIFICATION OF HMD USED

| | |
|------------------|------------------|
| Size | 154x21x40 |
| Display_Size | 60' |
| No.Pixels | 300x224 |
| Viewing_Angle | 32° |
| Video_Input | iPhone,iPod,iPad |
| Weight | 80g |
| Power_Cosumption | 3.7V,160mA |

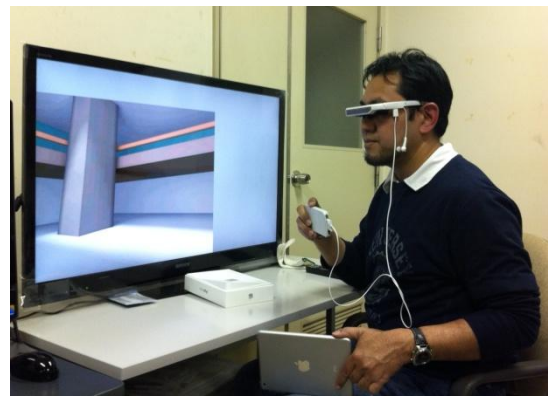


Fig. 12. Outlook of the proposed system

Figure 12 shows outlook of the proposed system. User wears the HMD which is attached to the iPhone in this case. In Figure 12, there is TV monitor for demonstration of the created 3D images by the iPhone.

C. Application Software

Two application software, with and without walking detection are created. With walking detection of application software allows display 3D images in accordance with users' action and movement, changing users' head pose and users' walking together with mobile devices orientations. Figure 13 shows the start display image onto mobile device.



Fig. 13. Start home display image onto mobile device

V. EXPERIEMNTS

A. Examples of 3D Displayed Images

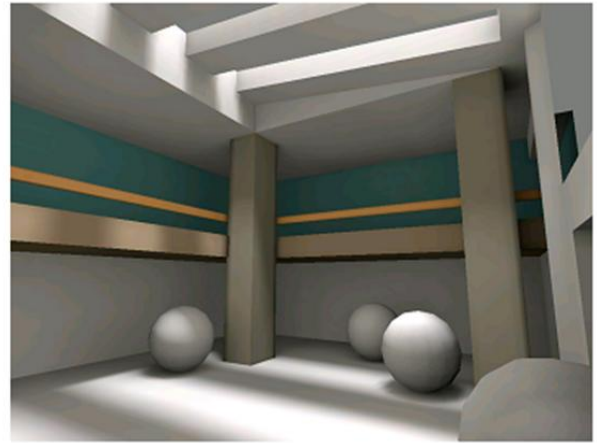
When user looks to the right direction, displayed image is changed to the right image. That is the same thing for left, up, and down directions. Also when he or she walks forward, then displayed 3D image is changed to the front image. This is the same thing for backward direction.

Figure 14 shows the displayed 3D image when user looks up and down, rotate in left and right directions, and step in forward and backward directions, respectively.



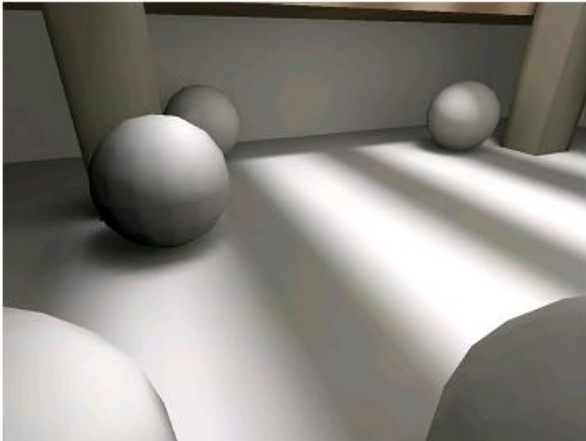
Look UP

(a)Look up



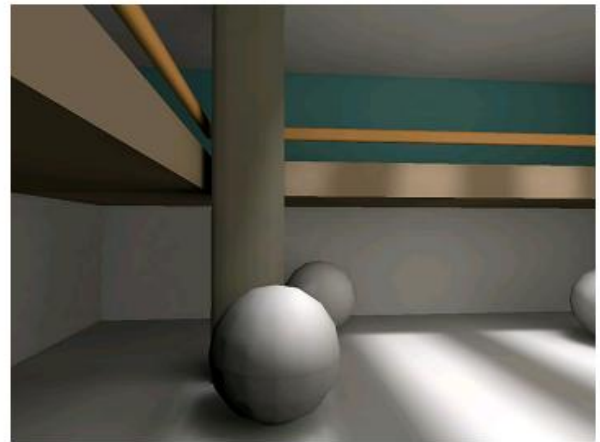
Rotate RIGHT

(d)Rotate right



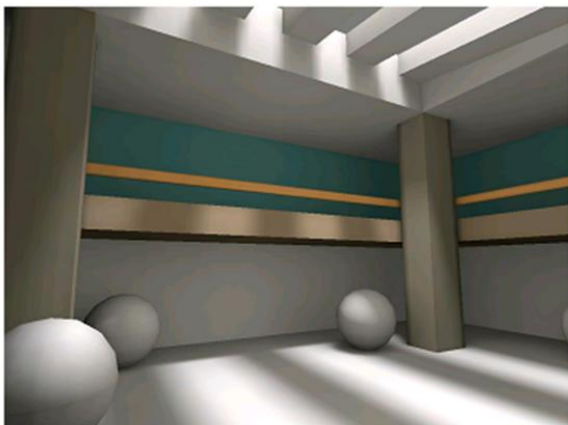
Look DOWN

(b)Look down



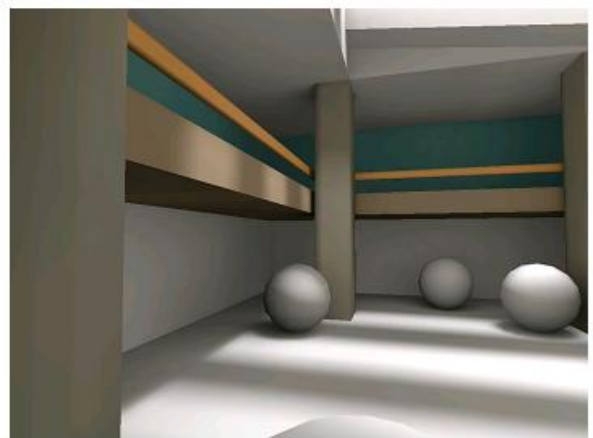
Step FORWARD

(e)Step forward



Rotate LEFT

(c)Rotate left



Step BACKWARD

(f)Step backward

Fig. 14. Displayed 3D images when user look up and down, rotate in left and right directions, and step in forward and backward directions

In these cases, three axis coordinate and roll, pitch, and yaw rotation axis are defined as shown in Figure 15.

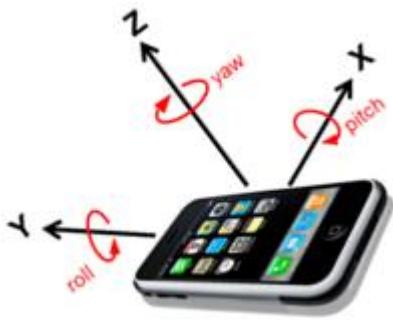


Fig. 15. Definitions of three axis coordinate and roll, pitch, and yaw rotation axis

In accordance with users' motion together with mobile phone movement, displayed 3D images are changed by frame by frame. Accelerometer data can be acquired 24 data a second. Taking every 6 data out of 24 data a second, users' attitude, roll, pitch, and yaw angle is estimated. Therefore, 4 times a second of attitude data are used for updating the 3D images which have to be created.

B. Example of 3D Display onto iPhone

Figure 16 shows the example of 3D image display onto iPhone.

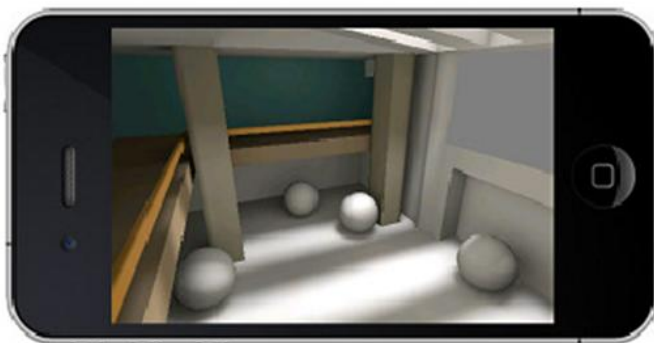
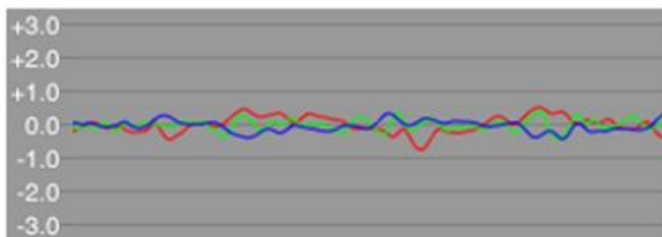


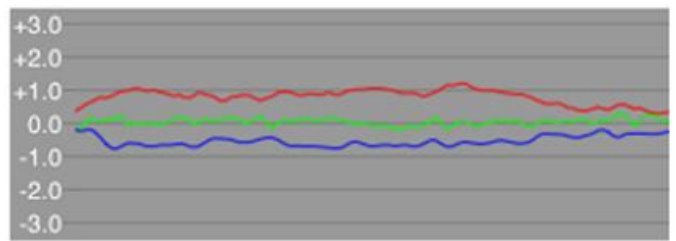
Fig. 16. Example of 3D image display onto mobile phone

C. Walking Detection

Figure 17(a) shows the motion of rotation rate when user walks while Figure 17 (b) shows that when user rotating in roll direction.



(a)Walking



(b)Rotation

Fig. 17. Motion of rotation rate

Figure 18 shows the acceleration and rotation rate when user walks. During walking, user acceleration in x, y, z directions is small. When user get close to the wall, 3D displayed image is close-up as shown in Figure 19.

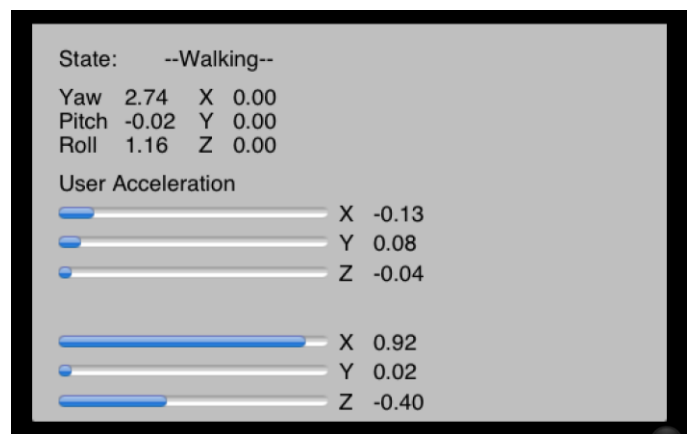
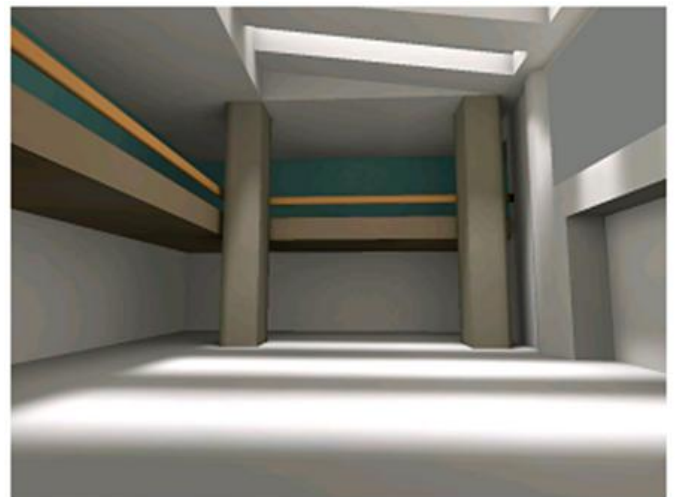
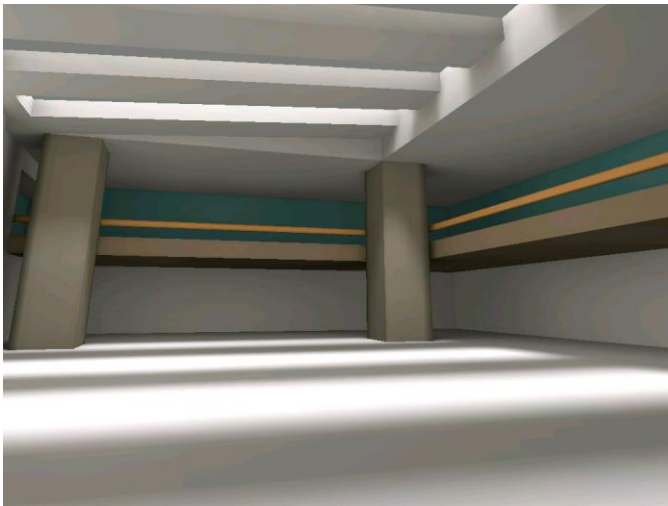


Fig. 18. Acceleration and rotation rate when user walks



(a)



(b)

Fig. 19. Example of 3D images during walking

D. Augmented Reality Application

One of Augmented Reality: AR applications are shown in Figure 20. The icon, description and character can be superimposed on real world images.



Fig. 20. Application of the proposed system to AR

VI. COMCLUSION

Method and system for 3D image display onto mobile phone and/or tablet terminal is proposed. Displaying 3D images are changed in accordance with user's location and attitude as well as some motions. Also 3D images can be combined with real world images and virtual images. Through implementation and experiments with virtual images, all functionalities are verified and validated. One of applications of the proposed system is attempted for demonstration of virtual interior of the house in concern. User can take a look at the inside house in accordance with user's movement. Thus user can imagine how the interior of the house looks like.

ACKNOWLEDGMENT

The authors would like to thank Arai's laboratory members for their useful comments and suggestions during this research works.

REFERENCES

- [1] Alasdair Allan, Basic Sensors in iOS, O'Reilly, 2011
- [2] David Mark et al., Beginning iOS 6 Development exploring the iOS SDK, Apres, 2012
- [3] Philip Rideout, iPhone 3D Programming, O'Reilly, 2010
- [4] Romain Marucchi-Foino, Game and Graphics Programming for iOS and Android with OpenGL ES 2.0, John Wiley & Sons, Inc, 2012
- [5] Apple Developer Resource, <http://developer.apple.com>
- [6] WWDC 2012 Session Videos, Developer on iTunes
- [7] Sensor Fusion on Android Devices: A Revolution in Motion Processing, YouTube Video: <http://www.youtube.com/watch?v=C7JQ7Rpnw2k>

AUTHORS PROFILE

Kohei Arai He received BS, MS and PhD degrees in 1972, 1974 and 1982, respectively. He was with The Institute for Industrial Science and Technology of the University of Tokyo from April 1974 to December 1978 and also was with National Space Development Agency of Japan from January, 1979 to March, 1990. During from 1985 to 1987, he was with Canada Centre for Remote Sensing as a Post Doctoral Fellow of National Science and Engineering Research Council of Canada. He moved to Saga University as a Professor in Department of Information Science on April 1990. He was a councilor for the Aeronautics and Space related to the Technology Committee of the Ministry of Science and Technology during from 1998 to 2000. He was a councilor of Saga University for 2002 and 2003. He also was an executive councilor for the Remote Sensing Society of Japan for 2003 to 2005. He is an Adjunct Professor of University of Arizona, USA since 1998. He also is Vice Chairman of the Commission-A of ICSU/COSPAR since 2008. He wrote 30 books and published 332 journal papers.

Relative Motion of Formation Flying with Elliptical Reference Orbit

Hany R Dwidar[†] and Ashraf H. Owis[†]

[†]Department of Astronomy, Space and Meteorology, Faculty of Science, Cairo University

Abstract—In this paper we present the optimal control of the relative motion of formation flying consisting of two spacecrafts. One of the spacecraft is considered as the chief, orbiting the Earth on a Highly Elliptical Orbit(HEO), and the other, orbiting the chief, is considered as the deputy. The Keplerian relative dynamics of the formation as well as the the second zonal hamonics of the Earth's gravitational field (J_2) are studied. To study these perturbative effect the linearized true anomaly varying Tschauner-Hempel equations are augmented to include the effect of J_2 . We solve the nonlinear feedback optimal control of the relative motion using the state dependent Riccati Equation(SDRE). The results are validated through a numerical example.

I. INTRODUCTION

The multi-spacecraft mission have proved powerful than the monolithic ones in the sense of reliability Reconfigurability, and redundancy. In addition to large apertures in the interferometric missions and therefore longer baseline. The new challenging technology require a high- Precision relative orbit control. Relative motion between a chief and a chaser spacecraft has been extensively studied over past several decades. The well-known Clohessy-Wiltshire(CW) equations[1] originally known as Hills equations[2] used to study the linearised equation of motion around the orbit of the chief satellite, which is circular and subject to the Keplerian motion only. Other models have been introduced in which the chief orbit is eccentric subject to the non-Keplerian perturbation forces [3], [4], [5], [6], [7], [8]. For near Earth space missions, the second zonal harmonic (J_2) perturbation is the dominant in for long term modelling context, and therefore has drawn considerable attention [9], [10], [11]. An analytic solution introduced [4]. A numerical solution based on the linear quadratic regulator (LQR), with limited thrust implemented, has been developed in [12]. The feedback optimal control of the relative motion of sun-facing formation flying using the generating function technique introduced by Scheeres 2006 to solve the Linear True Anomaly Variant Quadratic Regulator(LTAVQR) has been developed [16]. One of the most common strategies of controlling the relative position of a formation of satellite, is the chief and deputy strategy. In which, one of the spacecraft is considered as the chief, orbiting the Earth on a Highly Elliptical Orbit(HEO), and the other, orbiting the chief, is considered as the deputy. The reference orbit of the chief spacecraft is elliptic and the Tschauner-Hempel equations are used to formulated the dynamical model based on the gravitational filed of the Earth

up to the second zonal harmonics. We get closed loop feedback optimal control solution based on the State Dependent Riccati Equation(SDRE) that is able to accommodate some errors in the initial condition.

II. STATEMENT OF THE PROBLEM

Due to the limitation of the Cartesian coordinate system, we use the Local Vertical Local Horizontal (LVLH)coordinate system to overcome some drawbacks incurred by the Cartisan one such as, equation linearization and perturbation inclusion. We study the motion of two-spacecraft formation flying moving under the main gravitational field of the Earth and the second zonal harmonic. The chief spacecraft will move on an elliptic orbit described by the orbital elements($a, e, i, \Omega, \omega, \theta$) as shown in Figure 1 and the chaser one will be described with the chief's orbit as reference. The equation of motion can be written as[13], [14], [15]

$$\ddot{\vec{r}} = \vec{g}(\vec{r}) + \vec{J}(\vec{r}) \quad (1)$$

where \vec{g} , and \vec{J} are accelerations due to the spherical and oblate Earth.

We assume that the chief spacecraft is at reference orbit \vec{R}_{fc} and the chaser spacecraft at position vector \vec{R} . We can use equ(1) to write the accelerations of the two spacecrafts

$$\begin{aligned} \ddot{\vec{R}} &= \vec{g}(\vec{R}) + \vec{J}(\vec{R}) + \vec{a}(\vec{R}) \\ \ddot{\vec{R}}_{fc} &= \vec{g}(\vec{R}_{fc}) + \vec{J}(\vec{R}_{fc}) + \vec{a}(\vec{R}_{fc}) \end{aligned}$$

where we have (\vec{R}_{fc}) and (\vec{R}) are defined as follows

$$\begin{aligned} \vec{R}_{fc} &= R_{fc} \hat{i} && \text{(Non-inertial frame)} \\ \vec{R} &= (R_{fc} + x) \hat{i} + y \hat{j} + z \hat{k} && \text{(Non-inertial frame)} \end{aligned}$$

A. Equation of motion of the relative motion

To find the relative acceleration in the inertial frame $i \ddot{\rho}$ (the derivative in the inertial frame is identified by i) we compute

$$\ddot{\vec{R}} - \ddot{\vec{R}}_{fc} = \vec{g}(\vec{R}) - \vec{g}(\vec{R}_{fc}) + \vec{J}(\vec{R}) - \vec{J}(\vec{R}_{fc}) + \vec{a}(\vec{R}) - \vec{a}(\vec{R}_{fc}) \quad (2)$$

The relative acceleration in the non-inertial frame $\ddot{\rho} = \begin{bmatrix} \ddot{x} \\ \ddot{y} \\ \ddot{z} \end{bmatrix}$ is given by

$$\ddot{\rho} = \ddot{i}\rho - 2\dot{\theta} \times \dot{\rho} - \dot{\theta} \times (\theta \times \rho) - \ddot{\theta} \times \rho \quad (3)$$

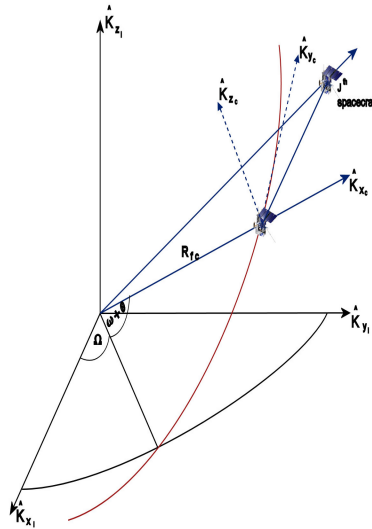


Figure 1.

Where $\dot{\theta}$, $\ddot{\theta}$ correspond to the angular velocity and acceleration of this orbiting reference frame.

$$\begin{aligned} \dot{\theta} &= \dot{\theta} \hat{k} \\ |\vec{R}_{fc}| &= \frac{a(1-e^2)}{1+e \cos f} \\ \dot{\theta} &= \frac{n(1+e \cos \theta)^2}{(1-e^2)^{3/2}} \end{aligned}$$

The relation between time and true anomaly is given by

$$t - t_p = \frac{1}{n} \left[2 \arctan \left(\sqrt{\frac{1-e}{1+e}} \tan \frac{\theta}{2} \right) - \frac{e\sqrt{1-e^2} \sin \theta}{1+e \cos \theta} \right]$$

Where $n = (\mu/a^3)^{1/2}$ is the mean motion of the reference orbit.

If we use θ as the free variable, the equation of motion can be transformed using the relationships

$$(\dot{\cdot})^\bullet = (\dot{\cdot})' \dot{\theta}, \quad (\ddot{\cdot})^{\bullet\bullet} = (\ddot{\cdot})'' \dot{\theta}^2 + \dot{\theta} \dot{\theta}' (\dot{\cdot})'$$

Using the above equation we get

$$\frac{d}{dt} \begin{bmatrix} \dot{x} \\ \dot{y} \\ \dot{z} \end{bmatrix} = \begin{bmatrix} x'' \dot{\theta}^2 + \dot{\theta} \dot{\theta}' x' \\ y'' \dot{\theta}^2 + \dot{\theta} \dot{\theta}' y' \\ z'' \dot{\theta}^2 + \dot{\theta} \dot{\theta}' z' \end{bmatrix} \quad (4)$$

From equ (4) we can write the state equation of system in terms of (θ) as the free variables as follows

$$\frac{d}{d\theta} \begin{bmatrix} x \\ y \\ z \\ x' \\ y' \\ z' \end{bmatrix} = \begin{bmatrix} x' \\ y' \\ z' \\ \frac{\dot{x} - \dot{\theta} \dot{\theta}' x'}{\dot{\theta}^2} \\ \frac{\dot{y} - \dot{\theta} \dot{\theta}' y'}{\dot{\theta}^2} \\ \frac{\dot{z} - \dot{\theta} \dot{\theta}' z'}{\dot{\theta}^2} \end{bmatrix} \quad (5)$$

Where $\dot{\theta}' = \frac{-2n(1+e \cos \theta)e \sin \theta}{(1-e^2)^{3/2}}$

B. The gravitational acceleration

To find the gravitational acceleration due to the spherical Earth and the second zonal harmonics (J_2) term we should write the gravitational potential in the following augmented form

$$U(r) = \frac{\mu}{r} - \frac{3\mu J_2 R_\oplus^2 z^2}{2r^5} + \frac{\mu J_2 R_\oplus^2}{2r^3} \quad (6)$$

and hence the acceleration resulting from this potential will be

$$\begin{aligned} \vec{r} &= -\frac{\mu}{r^3} \vec{r} + \frac{15\mu J_2 R_\oplus^2 z^2}{2r^6} \vec{r} - \frac{3\mu J_2 R_\oplus^2}{2r^4} \vec{r} - \frac{3\mu J_2 R_\oplus^2 z^2}{r^5} \hat{K} \\ &= \vec{g}(\vec{r}) + \vec{J}(\vec{r}) \end{aligned} \quad (7)$$

where \vec{g} and \vec{J} are the the accelerations of the spherical and oblate Earth respectively and \hat{K} is unit vector in the inertial ECI frame.

The last term can be written in the orbiting non-inertial frame as follows

$$-\frac{3\mu J_2 R_\oplus^2}{r^4} \begin{pmatrix} \sin(\Omega) \sin^2(i) \\ -\cos(\Omega) \sin^2(i) \\ \cos(i) \sin(i) \end{pmatrix} \quad (8)$$

Within the assumption that $|\vec{\rho}| \ll |\vec{R}_{fc}|$ We can write

$$\vec{g}(\vec{R}) - \vec{g}(\vec{R}_{fc}) = \frac{-\mu}{|\vec{R}_{fc}|^3} (-2x\hat{i} + y\hat{j} + z\hat{k}) \quad (9)$$

Also we have

$$\vec{J}(\vec{R}) - \vec{J}(\vec{R}_{fc}) = 6 \frac{\mu J_2 R_\oplus^2}{R_{fc}^5} A(\theta) \begin{bmatrix} x \\ y \\ z \end{bmatrix} \quad (10)$$

where $A(\theta) =$

$$\begin{bmatrix} 1 - 3(\sin i \sin(\theta + \omega))^2 & \sin 2(\theta + \omega) \sin^2 i & \sin 2i \sin(\theta + \omega) \\ \sin 2(\theta + \omega) \sin^2 i & -\frac{1}{4} - \frac{1}{2} \sin^2 i + \frac{7}{4} (\sin i \sin(\theta + \omega))^2 & -\frac{1}{4} \sin 2i \cos(\theta + \omega) \\ \sin 2i \sin(\theta + \omega) & -\frac{1}{4} \sin 2i \cos(\theta + \omega) & -\frac{3}{4} + \frac{1}{2} \sin^2 i + \frac{5}{4} (\sin i \sin(\theta + \omega))^2 \end{bmatrix}$$

Plugging eqs 9, and 10 into equ.3 and then substituting into equ.5 we get the state equation of the system as

$$X' = A(\theta)X + B(\theta)U \quad (11)$$

where $X = [x, y, z, x', y', z']$ is the state vector and $U = [u_x, u_y, u_z]$ is the control vector

$$A(\theta) = \begin{bmatrix} a_{11} & a_{12} & a_{13} & a_{14} & a_{15} & a_{16} \\ a_{21} & a_{22} & a_{23} & a_{24} & a_{25} & a_{26} \\ a_{31} & a_{32} & a_{33} & a_{34} & a_{35} & a_{36} \\ a_{41} & a_{42} & a_{43} & a_{44} & a_{45} & a_{46} \\ a_{51} & a_{52} & a_{53} & a_{54} & a_{55} & a_{56} \\ a_{61} & a_{62} & a_{63} & a_{64} & a_{65} & a_{66} \end{bmatrix}$$

$$B(\theta) = \frac{(1 - e^2)^3}{(1 + e \cos \theta)^4 n^2} \begin{bmatrix} 0 & 0 & 0 \\ 0 & 0 & 0 \\ 0 & 0 & 0 \\ 1 & 0 & 0 \\ 0 & 1 & 0 \\ 0 & 0 & 1 \end{bmatrix}$$

where

$$\begin{aligned}
 a_{14} &= 1, & a_{11} &= a_{12} = a_{13} = a_{15} = a_{16} = 0, \\
 a_{21} &= a_{22} = a_{23} = a_{24} = a_{26} = 0, & a_{25} &= 1, \\
 a_{34} &= a_{31} = a_{35} = a_{32} = a_{33} = 0, & a_{36} &= 1, \\
 a_{41} &= \frac{3 + e \sin \theta}{1 + e \cos \theta} + \frac{6J_2R_\oplus^2}{a^2(1 - e^2)^2} (1 - 3(\sin i \sin(\theta + \omega))^2)(1 + e \cos \theta), \\
 a_{42} &= -\frac{2e \sin \theta}{1 + e \cos \theta} + \frac{6J_2R_\oplus^2}{a^2(1 - e^2)^2} (\sin 2(\theta + \omega) \sin^2 i)(1 + e \cos \theta), \\
 a_{43} &= \frac{6J_2R_\oplus^2}{a^2(1 - e^2)^2} \sin 2i \sin((\theta + \omega)(1 + e \cos \theta), \\
 a_{44} &= \frac{2e \sin \theta}{1 + e \cos \theta}, \\
 a_{45} &= 2, \\
 a_{46} &= 0, \\
 \\
 a_{51} &= \frac{2e \sin \theta}{1 + e \cos \theta} + \frac{6J_2R_\oplus^2}{a^2(1 - e^2)^2} \sin 2(\theta + \omega) \sin^2 i(1 + e \cos \theta), \\
 a_{52} &= \frac{e \cos \theta}{1 + e \cos \theta} + \frac{3J_2R_\oplus^2}{a^2(1 - e^2)^2} \left(-\frac{1}{2} - \sin^2 i + \frac{7}{2}(\sin i \sin(\theta + \omega))^2\right)(1 + e \cos \theta), \\
 a_{53} &= -\frac{3J_2R_\oplus^2}{2a^2(1 - e^2)^2} (\sin 2i \cos((\theta + \omega))(1 + e \cos \theta), \\
 a_{54} &= -2, \\
 a_{55} &= \frac{2e \sin \theta}{1 + e \cos \theta}, \\
 a_{56} &= 0, \\
 \\
 a_{64} &= a_{65} = 0, \\
 a_{61} &= \frac{6J_2R_\oplus^2}{a^2(1 - e^2)^2} \sin 2i \sin((\theta + \omega)(1 + e \cos \theta), \\
 a_{62} &= -\frac{3J_2R_\oplus^2}{2a^2(1 - e^2)^2} \sin 2i \cos(\theta + \omega)(1 + e \cos \theta), \\
 a_{63} &= \frac{-1}{1 + e \cos \theta} \\
 &\quad + \frac{3J_2R_\oplus^2}{2a^2(1 - e^2)^2} (-3 + 2 \sin^2 i + 5(\sin i \sin(\theta + \omega))^2)(1 + e \cos \theta), \\
 a_{66} &= \frac{2e \sin \theta}{1 + e \cos \theta},
 \end{aligned}$$

III. STATE DEPENDENT RICCATI EQUATION

Consider the consider the State Dependent Linear Quadratic Regulator written as follows:

$$\dot{\mathbf{x}} = \mathbf{A}(\mathbf{x})\mathbf{x}(t) + \mathbf{B}(\mathbf{x})\mathbf{u}(t), \quad \mathbf{x}(t_0) = \mathbf{x}_0 \in \mathbb{R}^n$$

where $\mathbf{x}(t) \in \mathbb{R}^n$ is the state vector and $\mathbf{u}(t) \in \mathbb{R}^m$ is the control vector.

The optimization problem is to find the control \mathbf{u}^* that minimizes the cost function :

$$J_{LQR} = \frac{1}{2} \int_{t_0}^{t_f} (\mathbf{x}^T \mathbf{Q} \mathbf{x} + \mathbf{u}^T \mathbf{R} \mathbf{u}) dt \quad (12)$$

where \mathbf{Q} and \mathbf{R} are the weight matrices.

State Dependent Riccati Equation The feedback optimal solution of the above problem \mathbf{u}^* is given by

$$\mathbf{u}^*(\mathbf{x}) = -\mathbf{R}^{-1}(\mathbf{x})\mathbf{B}^T(\mathbf{x})\mathbf{P}(\mathbf{x})\mathbf{x} \quad (13)$$

Where $\mathbf{P}(\mathbf{x})$ is obtained by solving the SDRE State Dependent Riccati equation:

$$\dot{\mathbf{P}}(\mathbf{x}) + \mathbf{A}^T(\mathbf{x})\mathbf{P}(\mathbf{x}) + \mathbf{P}(\mathbf{x})\mathbf{A}(\mathbf{x}) + \mathbf{Q}(\mathbf{x}) - \mathbf{P}(\mathbf{x})\mathbf{B}(\mathbf{x})\mathbf{R}^{-1}(\mathbf{x})\mathbf{B}^T(\mathbf{x})\mathbf{P}(\mathbf{x}) = 0 \quad (14)$$

We note that the Riccati matrix, $\mathbf{P}(\mathbf{x})$ depends on the choice of $\mathbf{A}(\mathbf{x})$, and since $\mathbf{A}(\mathbf{x})$ is not unique we have multiple optimal solutions.

IV. FACTORED CONTROLLABILITY

For the factored system equ.(11) the controllability is established by verifying that the controllability matrix

$$\mathbf{M}_{cl} = [\mathbf{B} \ \mathbf{AB} \ \mathbf{A}^2\mathbf{B} \ \mathbf{A}^3\mathbf{B}]$$

has a rank equals to $n = 6 \ \forall x$ in the domain.

Since \mathbf{A} and \mathbf{B} have nonvanishing rows the controllability matrix \mathbf{M}_{cl} for the System equ.(11) is of rank 6.

V. NUMERICAL EXAMPLE

The elements of the reference satellite are

| | | |
|---------------------------------------|---|-----------------------|
| eccentricity | = | 0.6 |
| Semi-major axis | = | 60 *10 ⁶ m |
| inclination | = | PI/3.0 rad |
| argument of perigee | = | 0 rad |
| right ascension of the ascending node | = | 0.69813 rad |

and the intial condition are

$$\begin{aligned} \theta_0 &= -0.1 \text{ rad} \\ X_0 &= [150, 1, 1, 0, 0, 0] \end{aligned}$$

and the final condition are

$$\begin{aligned} \theta_f &= 0.1 \text{ rad} \\ X_f &= [150, 1, 1, 0, 0, 0] \end{aligned}$$

$$Q(t) = \begin{bmatrix} 1 & 0 & 0 & 0 & 0 & 0 \\ 0 & 1 & 0 & 0 & 0 & 0 \\ 0 & 0 & 1 & 0 & 0 & 0 \\ 0 & 0 & 0 & 1 & 0 & 0 \\ 0 & 0 & 0 & 0 & 1 & 0 \\ 0 & 0 & 0 & 0 & 0 & 1 \end{bmatrix} \quad R(t) = 10^{12} * \begin{bmatrix} 1 & 0 & 0 \\ 0 & 1 & 0 \\ 0 & 0 & 1 \end{bmatrix}$$

$$Q_f(t) = \begin{bmatrix} 0 & 0 & 0 & 0 & 0 & 0 \\ 0 & 0 & 0 & 0 & 0 & 0 \\ 0 & 0 & 0 & 0 & 0 & 0 \\ 0 & 0 & 0 & 0 & 0 & 0 \\ 0 & 0 & 0 & 0 & 0 & 0 \\ 0 & 0 & 0 & 0 & 0 & 0 \end{bmatrix}$$

VI. CONCLUSIONS

- The feedback optimal control of relative motion of formation flying problem is solved by linearizing the original nonlinear dynamics.
- The time varying linearized problem has been solved using the State Dependent Riccati Equation technique.
- The method can be used for arbitrary boundary condition.
- The result is valid for any short time span formation flying rendezvous maneuver.

ACKNOWLEDGEMENTS

This project was supported financially by the Science and Technology Development Fund (STDF), Egypt, Grant No 666

REFERENCES

- [1] Clohessy, W.H., Wiltshire, R.S., *Terminal Guidance System for Satellite Rendezvous*, Journal of the Aerospace Sciences, Vol. 27, No. 9, 1960, pp. 653-658.
- [2] Hill, G., *Researches in Lunar Theory*, American Journal of Mathematics, Vol. 1, 1878, pp.5-26
- [3] Wiesel, W.E., *Relative Satellite Motion About an Oblate Planet*, Journal of Guidance, Control, and Dynamics, Vol. 25, No. 4, 2002, pp. 776-785.
- [4] Melton, R., *Time-Explicit Representation of Relative Motion Between Elliptical Orbits*, Journal of Guidance, Control, and Dynamics, Vol. 23, No. 4, 2000, pp. 604-610.
- [5] Tschauner, J., Hempel, P., *Rendezvous Zu Einem In Elliptischer Bahn Umlaufenden Ziel*, Astronautica Acta, Vol. 11, No. 2, 1965, pp. 104-109
- [6] Inalhan, G., Tillerson, M. and How, J. P. *Relative Dynamics and Control of Spacecraft Formation in Eccentric Orbits*, Journal of Guidance Control and Dynamics Vol. 25, No. 61, PP. 48-59
- [7] Gurfil, P., *Relative Motion Between Elliptic Orbits Generalized Boundedness Conditions and Optimal Formation keeping*, Journal of Guidance, Control, and Dynamic Vol. 28, No. 4, 2005, pp. 761 -767
- [8] Palmer, P.L., Imre, E., *Relative Motion Between Satellites on Neighboring Keplerian Orbits*, Journal of Guidance, Control, and Dynamics, Vol. 30, No. 2, 2007, pp. 521-528.
- [9] Schweighart, S. A., Sedwick, and R. J., *High-Fidelity Linearized J_2 Model for Satellite Formation Flight*, Journal of Guidance Control and Dynamics Vol. 25, No. 6, PP. 1173-1180
- [10] Schaub, H., and Alfriend, K. T., J. *J_2 Invariant Orbits for Spacecraft Formations*, Celestial Mechanics and Dynamical Astronomy, Vol. 79, 2001, pp. 77 -95.
- [11] Vadali, S.R, Sengupta, P., Yan, H., Alfriend, K.T., *Fundamental Frequencies of Satellite Relative Motion and Control of Formations*, Journal of Guidance, Control, and Dynamics, Vol. 31, No. 5, 2008, pp. 1239-1248
- [12] Lantoine, G., Epenoy, R., *A Quadratically-Constrained Linear Quadratic Regulator Approach for Finite-Thrust Orbital Rendezvous*, Journal of Guidance, Control and Dynamics, Vol. 35, No. 6, 2012, pp. 1787-1797
- [13] Capo-Lugo, P.A., and Baniun, P.M., *Active control Schemes to Satisfy Separation Distance Constraints*, Journal of Guidance Control and Dynamics Vol. 30, No. 4, PP. 1152-1155
- [14] Theron, A., Jouhaud, F. and Chretien, J.-P., *Modelisation du Mouvement Orbital Relatif entre Deux Satellites*, Note interne 1/08282, ONERA, January 2004.
- [15] Perea, L., D'AmicoS., and Elosegui, P., *Relative Orbit Control of a Virtual Telescope in an Eccentric Orbit*, 21st International Symposium on Space Flight Dynamics, 28 Sep. -2 Oct. 2009, Toulouse, France (2009).
- [16] Owis, A. and Dwidar, H. , *Feedback Optimal Control of Relative Motion for Elliptical Reference Orbit of Sun-Facing Formation Flying*, New Trends in Astrodynamics and Applications VI New York University, New York City June 6-8, 2011

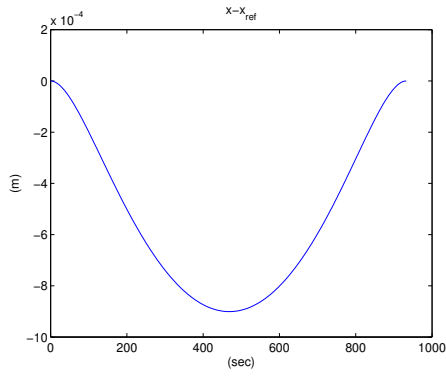


Figure 2.

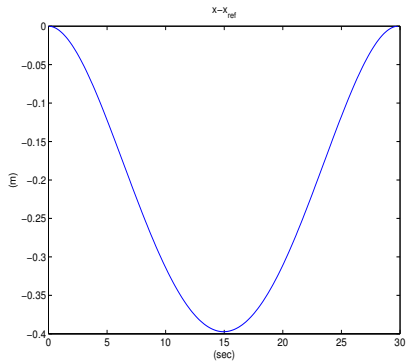


Figure 3.

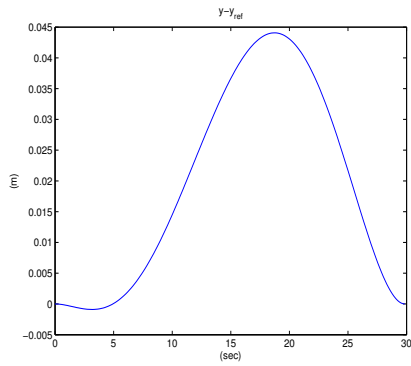


Figure 4.

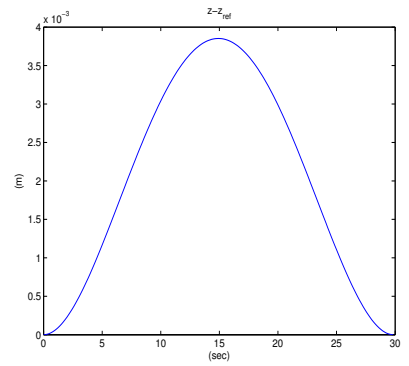


Figure 5.

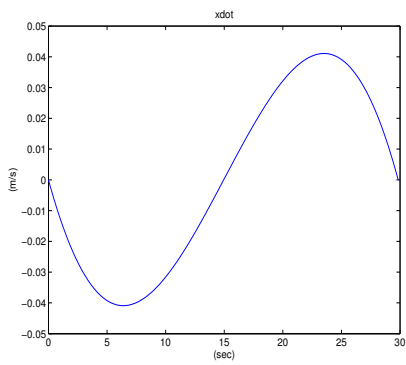


Figure 6.

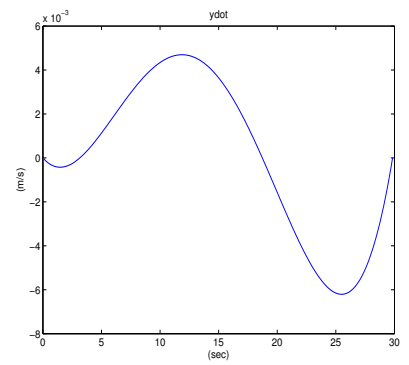


Figure 7.

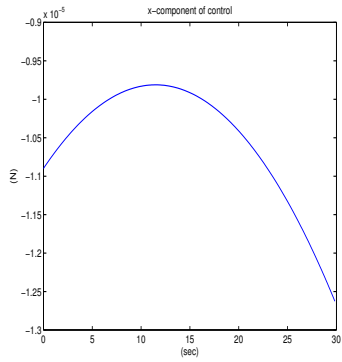


Figure 8.

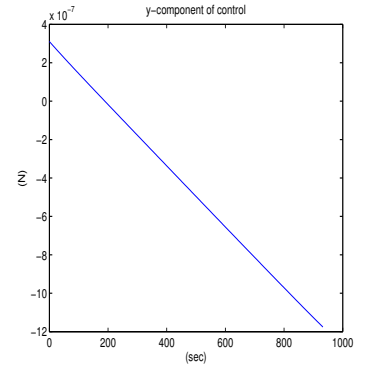


Figure 9.

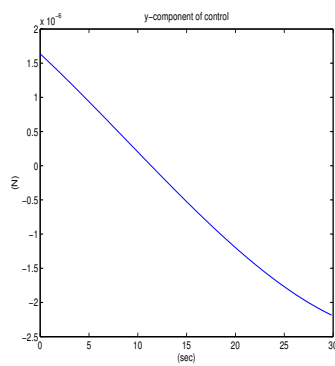


Figure 10.